

POLITECNICO DI TORINO

Corso di Laurea Magistrale in Ingegneria Biomedica



**Politecnico
di Torino**

Tesi di Laurea Magistrale

**Multifunctional magnetic nanoparticles for the
treatment of tumors**

Relatori

prof.ssa Enrica Verné

prof.ssa Marta Miola

Candidata

Giuliana D'Alterio

Anno Accademico 2021-2022

Table of Contents

Introduction	1
Chapter 1.....	3
Multifunctional nanoparticles	3
1.1 Magnetic NPs	4
1.1.1 Magnetic properties: Bulk vs MNPs.....	5
1.1.2 Synthesis and surface functionalization.....	8
1.1.3 Applications in biomedicine	12
1.2 Plasmonic and Au NPs.....	15
1.2.1 Plasmonic properties.....	16
1.2.2 Synthesis methos	17
1.2.3 Applications in biomedicine	18
1.3 Magneto-plasmonic NPs	20
Chapter 2	23
Green synthesis.....	23
2.1 Plants.....	24
2.2 Micro-organisms	25
2.2.1 Algae extracts	26
2.2.2 Bacteria	26
2.2.3 Fungi, actinomycetes and yeasts.....	27
2.3 Curcumin.....	28
2.3.1 Curcumin chemical properties	29
2.3.2 Curcumin reactivity	30
2.3.3 Curcumin-conjugated nanoparticles	33
Chapter 3	39
Advanced cancer treatment	39

3.1 Nanoparticles and curcumin in tumor treatments	40
3.2 Curcumin-based nanosystems	41
3.3 Magnetic NPs	43
3.3.1 MNPs applications for tumor treatments	45
3.3.2 Curcumin-magnetite NPs applications for tumor treatments	47
3.4 Gold NPs	51
3.4.1 Gold NPs applications for tumor treatments	52
3.4.2 Curcumin-gold NPs applications for tumor treatments	53
3.5 Magnetic-plasmonic NPs	55
3.5.1 Synthesis	55
3.5.2 Applications in biomedicine	56
Chapter 4	58
Materials and methods	58
4.1 Synthesis and functionalization methods	58
4.1.1 Magnetite nanoparticles	58
4.1.2 Gold nanoparticles	63
4.1.3 Gold-magnetite nanoconjugates	64
4.2 Characterization techniques	66
4.2.1 Ultraviolet-visible Spectroscopy	67
4.2.2 Fourier Transform Infrared Spectroscopy	67
4.2.3 Energy Dispersive Spectroscopy	68
4.2.4 Dynamic Light Scattering	68
4.2.5 Vibrating sample magnetometer	69
4.2.6 Laser	69
Chapter 5	71
Results and discussion	71
5.1 Magnetite nanoparticles	71

5.2 Gold nanoparticles	77
5.3 Gold-magnetite nanoparticles.....	78
5.3.1 First synthesis method	78
5.3.2 Second synthesis method	79
Chapter 6	94
Conclusions	94
References	97

Introduction

Cancer is one of the biggest challenges in the medical field and the need to develop advanced technologies and innovative strategies to treat tumors arises from the high rate of incidence and mortality of this pathology. The conventional therapies, such as surgery, chemotherapeutic treatment and radiotherapy, since they act on both cancer cells and healthy ones, result in several side effects in patients. The use of nanoparticles has been recently introduced for tumor diagnosis and treatment because of their distinctive properties and sizes, allowing them to transport drugs to the tumoral site, to be used as heat mediator for hyperthermia treatment and to be used as contrast agent for imaging applications. In particular, the interest of researchers focused on the design and development of multifunctional nanoparticles having the great potential to combine two or more functionalities in order to overcome the limitations of single particles.

For the development of nanoparticles, various synthesis methods have been investigated which, however, often involve complicated and expensive procedures, including high temperature, energy consumption and toxic precursors, resulting in high risks for human health and the environment. For this reason, new ecological synthesis methods for obtaining nanoparticles gained a great amount of attention by the researchers. These kinds of synthesis methods use materials coming from biological routes such as plants and microorganisms as reducing and stabilizing agents for metallic species.

The goal of this thesis is to synthesize and characterize eco-friendly multifunctional nanosystems using curcumin as a bioactive molecule for their potential application in tumor diagnosis and treatment.

Magnetite and gold nanoparticles have been chosen for obtaining multifunctional nanoconjugates because of the possibility to combine magnetic and plasmonic properties in one nanocomposite. Magnetite nanoparticles with a superparamagnetic behavior can be remotely controlled by applying an alternating magnetic field, making them highly suitable for therapeutic applications. They are also characterized by low toxicity and represent very efficient contrast agents for magnetic resonance imaging. As for the choice of gold nanoparticles, their main property involves surface plasmon resonance

phenomena which allow the absorption of light and the generation of heat, mostly used in photothermal and photodynamic therapy. They are also easy to synthesize and possess high biocompatibility.

Curcumin is used as a reducing agent during the synthesis process of gold nanoparticles and as conjugating agent for obtaining the magnetite-plasmonic nanostructures. Curcumin represents a phenolic phytochemical compound widely used in Asian cuisine and also in medicine because of its antioxidant and antitumor properties. The main limitation of curcumin in biomedical applications is related to its chemical instability and low bioavailability that can be overcome by using nanostructures as curcumin carriers.

The first two chapters of this thesis will contain a summary on magnetite and gold nanoparticles properties and their applications are reported, followed by a study on the different green synthesis methods. The third chapter will contain an overview on the use of nanoparticles for the diagnosis and treatment of different tumors.

Finally, the last chapters are based on the experimental work, where two different synthesis methods have been explored in order to obtain the gold-magnetite heterodimers, using curcumin as a reducing agent. The different strategies of synthesis and characterization methods used for analysing the nanostructures are reported and discussed.

Chapter 1

Multifunctional nanoparticles

Nanomaterials and nanotechnology-based devices are widely used in the pharmaceutical industry, medicine, electronics, robotics and tissue engineering. Nanoparticles (NPs) has been used as delivery systems for small molecules, DNA, RNA and proteins but also to deliver drugs to target tissues. Their size (diameters ranging from 1 to 100 nm) is comparable with the dimensions of objects such as viruses, making them suitable for applications in life sciences. Nanoparticles have indeed the ability to attach to biological entities without modifying their function and their high surface-area-to-volume ratio permits strong bonds with surfactant molecules [2]. Considering the nature of the raw material and the shape, a huge variety of nanoparticles exist: they can be made by both organic materials (such as liposomes, dendrimers, carbon nanotubes) and inorganic materials (such as quantum dots, magnetic NPs, gold NPs) [3]. Their specific properties (chemical and physical) are different from the same material in the bulk form. In the nano form, a material possesses interesting optical, magnetic, and electrical properties which cannot be found in their bulk form. This phenomenon can be described as the “quantum size effect” [1].

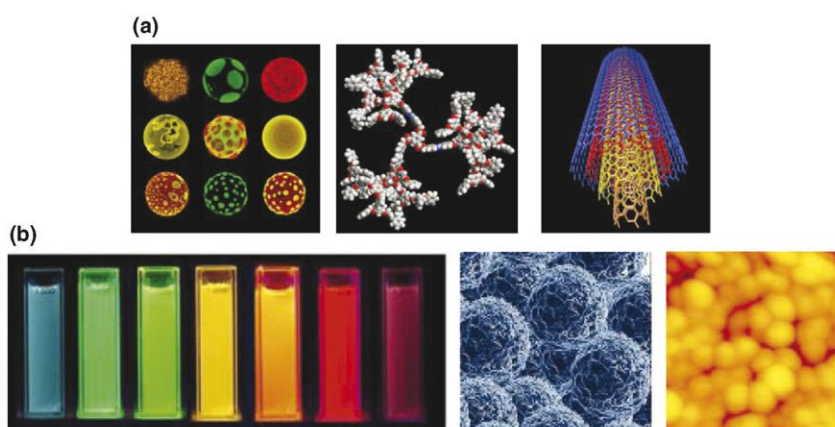


Figure 1. Example of nanoparticles (a) Organic nanoparticles (b) inorganic nanoparticles [3]

Nanomedicine can be defined as an application of nanotechnology for improved diagnosis, treatment and prevention from disease [17]. In particular, among all NPs, the metallic nanomaterials are considered the most promising because of their remarkable antibacterial properties [35]. An emerging field of medicine is the theranostic one: this

term derives from the combination of two words, therapeutics and diagnosis, where drugs and techniques are combined in order to simultaneously diagnose and treat medical conditions. The nowadays challenge is to design multifunctional theranostic nanoparticles capable to perform at the same time the diagnosis and treatment of a specific disease [13].

1.1 Magnetic NPs

Iron oxide nanoparticle (IONP)-based technologies are found to be of great interest catalysing rapid developments in nanotechnology. IONPs are classified into different phases as shown in the table 1:

Table 1. IONPs classification

IONPs	properties	references
<i>Magnetite</i> (Fe_3O_4)	<ul style="list-style-type: none"> ▪ centered cubic spinel structure ▪ <i>n</i>- and <i>p</i>-type semiconductor ▪ ferromagnetism at room temperature ▪ the lowest resistivity ▪ small bandgap (0.1 eV) 	[4][14]
<i>Hematite</i> ($\alpha\text{-Fe}_2\text{O}_3$)	<ul style="list-style-type: none"> ▪ the most stable iron oxide ▪ <i>n</i>-type semiconductor under ambient conditions ▪ weakly ferromagnetic or antiferromagnetic ▪ starting material for the synthesis of magnetite and maghemite 	[4]
<i>Maghemite</i> ($\gamma\text{-Fe}_2\text{O}_3$)	<ul style="list-style-type: none"> ▪ cubic structure ▪ <i>n</i>-type semiconductor ▪ ferromagnetism at room temperature ▪ bandgap of 2.0 eV ▪ ferrimagnetic 	[4]
<i>Wustite</i> (FeO)	<ul style="list-style-type: none"> ▪ antiferromagnetic 	[4]

Among IONPs, mainly Fe_3O_4 and $\gamma\text{-Fe}_2\text{O}_3$ are extensively studied since its biocompatibility and biodegradability have already proven in bio labelling and bio separation [1]. Magnetite is a common magnetic iron oxide with a cubic inverse spinel structure [5].

Magnetic nanoparticles (MNPs) have shown promising performance in different sectors such as the electronic, chemical and industrial ones and, in particular, in the medical field due to their unique features such as excellent magnetic properties, chemical stability, biocompatibility, targeting ability and biological degradability [14][18]. Indeed, MNPs can be visualized by magnetic resonance imaging (MRI), heated to provide hyperthermia for cancer treatment, guided to target sites by applying an external magnetic field and coated with different shells for active targeting. Ferrous or ferric oxide is the main constituent of magnetic NPs. In its most basic form, a biomedical MNP comprises an inorganic nanoparticle core and a biocompatible surface coating that provides stability under physiological conditions [13].

1.1.1 Magnetic properties: Bulk vs MNPs

Nanosized particles have specific physical and chemical properties which differ from the bulk counterparts. Bulk magnetic materials are composed by multiple magnetic domains in which the magnetization is in a uniform direction. They exhibit a permanent magnetization in the absence of a magnetic field under specific conditions (ferromagnetism). In the bulk form property is attributed to the average of all the quantum forces that affect all the atoms. In the nanoscale, there is an impact of specific individual atoms or molecules because each MNP can be considered a single magnetic domain. Depending on the orientation of the magnetic dipoles that constitute the materials when subjected to an external magnetic field, different magnetic states occur such as: [14]

- *Diamagnetism*, characterized by dipoles oriented in the opposite direction with respected the external magnetic field;
- *Paramagnetism*, where the magnetic moments are randomly aligned and the overall structure has zero net magnetization; the moments align when exposed to an external magnetic field producing a small net crystal magnetization in the same direction;
- *Ferromagnetism*, where the individual moments have parallel alignment in absence of external magnetic field making them able to generate a spontaneous magnetization;
- *Antiferromagnetism*, which magnetic dipoles are oriented antiparallel, cancelling each other and obtaining no magnetization;

- *Ferrimagnetism*, where the individual moments have antiparallel alignment but with different magnetization values in the two orientations, resulting into a spontaneous magnetization.

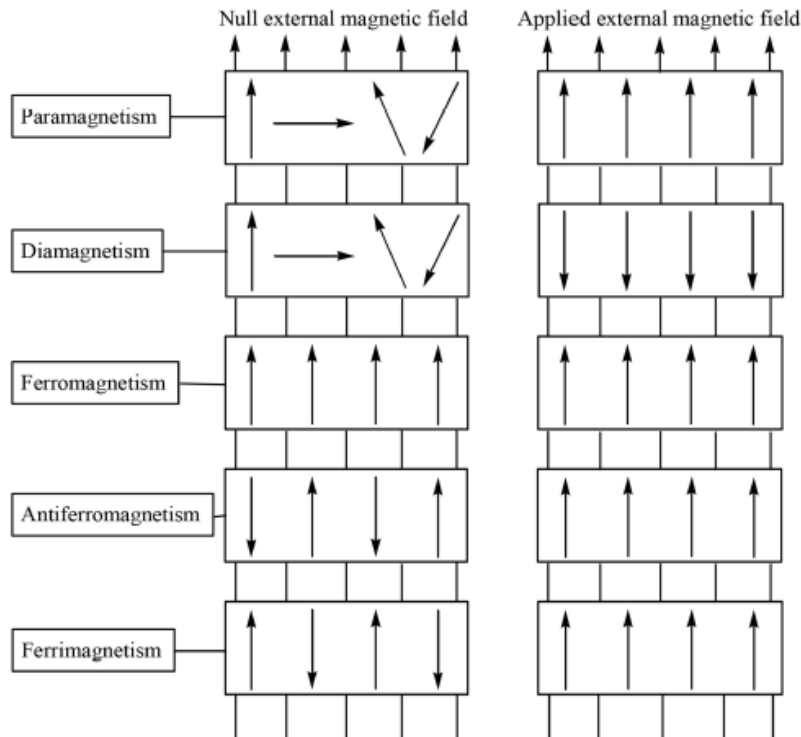


Figure 2. Magnetism in the presence and absence of an external magnetic field [15]

The response type to the magnetic field (including ferromagnetic, paramagnetic, antiferromagnetic and ferrimagnetic) together with the magnetization, that can be measured from hysteresis loops (M-H), are the main magnetic properties useful for the characterization of IONPs. Considering the hysteresis loops, some important magnetic parameters can be obtained such as: the *saturation magnetization* (M_s), the maximum magnetization value achieved when the applied magnetic field induce the alignment of magnetic dipoles in the same direction of the magnetic field itself; the *remanence magnetization* (M_r), the magnetization value after the removal of the applied magnetic field; the *coercivity* (H_c), the magnitude of the field that is necessary to apply in order to bring the material magnetization to zero [4].

Magnetic activity strongly depends on material size and temperature and on the applied magnetic field, in fact magnetite nanoparticles (MNPs) exhibit superparamagnetism while bulk magnetite has a ferrimagnetic behaviour. By decreasing NPs size, their

superparamagnetic behaviour will be enhanced while ferromagnetic behaviour is reduced [1][4][5]. Magnetic Fe₃O₄ nanoparticles are superparamagnetic below the size of 20 nm, it means MNPs do not retain any magnetism after removal of the magnetic field and the M-H curve should show no hysteresis (figure 3); this is a very important property for biomedical applications that concur to avoid coagulation and the possibility of agglomeration in vivo [14].

In order to understand the superparamagnetism, it is possible to consider the behaviour of well-isolated single domain particle. The magnetic anisotropy energy per particle is the energy responsible for holding the magnetic moments along a certain direction and it can be expressed as follows:

$$E(\theta) = K_{eff}V\sin^2\theta$$

where V is the volume of the particle, K_{eff} in the anisotropy constant and θ is the angle between magnetization and easy axis. $K_{eff}V$ is the energy barrier separating the two equivalent directions of magnetization. When the particles size decreases, the thermal energy, k_{BT} , exceeds the energy barrier $K_{eff}V$ and magnetization is easily flipped. For $k_{BT} > K_{eff}V$ the system behaves like a paramagnet and, instead of atomic magnetic moments, there is now a giant moment inside each particle. This system is named a superparamagnet [17].

Superparamagnetism displayed by iron oxide magnetic nanoparticles makes ferromagnets useful for application in biomedical sciences, in fact, they can be directed to active site by controlling with external AC magnetic field [15].

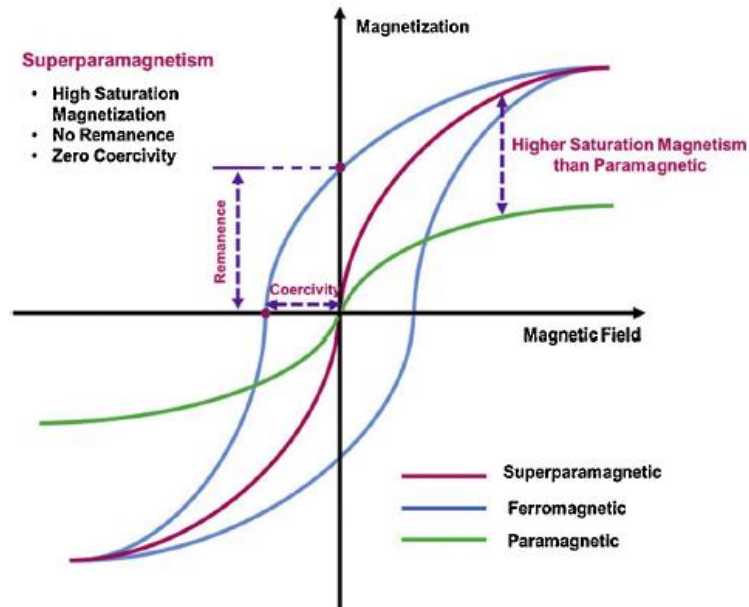


Figure 3. Magnetization characteristics of ferromagnetic materials [14]

1.1.2 Synthesis and surface functionalization [1],[2],[4],[6]-[12],[15]

The main advantages of MNPs over other nanoparticles are their cost effectiveness, simple production and reproducibility. The most common structure for biomedical applications is the “core-shell” structure, characterised by an iron oxide core and a shell composed by small silane linker, polymer, lipid etc., which possess good biocompatibility. The main goal is to obtain controlled nanoparticles in terms of size, shape, purity, crystallinity, and morphology in desired solvents.

Synthesis methods

Different methods have been investigated in literature to develop MNPs. They can be divided in four main categories: (1) Precipitation from solution; (2) Gas phase synthesis; (3) Solid phase synthesis; (4) Combustion synthesis.

Starting from the precipitation from solution methods, the co-precipitation is the most suitable method to prepare IONPs from the solutions of aqueous salt. It consists of mixing ferric and ferrous ions in a 1:2 molar ration in very basic solutions at room temperature or at elevated temperature. Expected pH levels for the complete precipitation are between 8 and 14. By regulating the pH and ionic strength of the medium in which the precipitation occurs, it is possible to control the means size of the particles: indeed, by increasing the

pH and ionic strength, the MNPs size decreases. Moreover, in the co-precipitation the quality of the MNPs is successfully reproducible.

Microemulsion is another common method to synthesize nanoparticles, where microemulsions are clear, stable, and isotropic liquid mixtures of oil, water and amphiphilic molecule known as surfactant, which reduces the interfacial tension. The two main types of microemulsions are direct (oil dispersed in water) and reverse (water dispersed in oil). With the use of simple equipment, microemulsion technique allows to synthesize a great variety of nanomaterials with excellent control over size, shape and composition.

Thermal decomposition method allows to overcome the limitation of co-precipitation where the size and size distribution of the synthesized particles are hardly controlled. The thermal decomposition strategies can be divided into hot-injection approaches, where the precursors are injected into a hot reaction mixture, and convectional reaction strategies, where a reaction mixture is prepared at room temperature and then heated. However, safety issues are associated at higher temperature and pressure of organic liquids and vapor phases used during the reactions conducted in the absence of air.

Hydrothermal (or solvothermal) synthesis is one of the most successful methods to prepare magnetic nanoparticles and ultrafine powders. The crystals of nanoparticles are grown by heterogenous reaction under high temperature and high pressure conditions. Precursors' concentration controls the size and size distribution, in fact, by increasing the precursors concentration and keeping constant the rest of the variables, the obtained particles are generally spherical.

Considering the gas phase synthesis, the spray and laser pyrolysis, sonochemical and arc discharge have been shown to be excellent methods for the direct synthesis of well-defined MNPs under controlled conditions.

A summary comparison of the different synthesis is reported in the Table 2.

Table 2. Summary comparison of different MNPs synthesis methods [4][12]

Method	Solvent	Size range (nm)	T (°C)	Morphology	Remark	Yield
Co-precipitation	Water	15-200	20-90	Spherical	NPs shape and size hardly controlled	High/scalable
Microemulsion	Organic	4-12	20-50	Spherical or cubic	NPs shape and size easily controlled	Low
Thermal decomposition	Organic compounds	500-550	100-320	Spherical	NPs size and distribution easily controlled High temperature safety issues	High/scalable
Hydrothermal synthesis	Water-ethanol	520	220	Spherical	Very simple synthesis High temperature	High/scalable
Spray pyrolysis	Organic	6-60	5-60	Spherical but aggregated	Aggregated particles	High/scalable
Laser pyrolysis	Organic	2-7	5-30	Spherical	Non-aggregated and thin sized NPs	High/scalable
Sonochemical	Water	25	10-30	Spherical and rod shaped	High mono-dispersive NPs	Medium
Arc discharge	Organic	15	5-30	Spherical	NPs shape easily controlled	Medium

Surface modification

Superparamagnetic iron oxide NPs (SPIONs) have a large surface-to volume ratio and it causes a tendency to aggregation. Moreover, they have high chemical activity and are easily oxidized in air causing a loss of magnetism and dispersibility. Surface modification

is an important step since the shielding shell does not simply prevent the SPIONs from degradation, improve biocompatibility, reduce toxicity and ensure non-immunogenicity obtaining “stealth” particles, but also provide the additional functionalization with other components such as functional groups, various drugs or specific binding sites. Moreover, the hydrophobic interactions between particles cause agglomerations and formations of large clusters, resulting in increased particle size. Finally, for many biomedical applications, SPIONs need to be functionalized in order to conjugate with biological entities such as DNA, antibodies, and enzymes.

The main surface modification strategies can be divided in two groups: coating with organic shells, as well as by the polymers and surfactant, or coating with inorganic components.

SPIONs with any organic material coating, such as dextran, starch, poly(ethylene glycol)(PEG), polyethylenimine (PEI), etc., are mainly used for magnetic recording, MRI, and in the biological field for specific drug targeting, magnetic cell separation, etc, while SPIONs inorganic material coatings, such as silica, Au, metal oxides, etc, not only provide stability to the NPs in solution but are also used for biological labelling, catalysis, optical bioimaging, and so on. In particular, the *silica coating* can enhance the dispersion in solution and increase the stability of SPIONs, while the abundant silanol groups on the silica layer and the hydrophilic surface of silica-coated nanoparticles can be used to provide surface NPs with various functional groups.

Surface modification

Another important step is the SPIONs functionalization by bioactive molecules. According to the type of biomolecule, different kind of functionalization can be considered: a first example is molecules with hydrophobic groups and a weak attraction for solvent, such as fatty acid like oleic acid and linoleic acid, or alkyl phenol; this functionalization allows NPs to repulse themselves, thanks to the presence of hydrophobic groups on their surface, improving their stability in solution. Another type of functionalization is based on the use of water-soluble molecules containing hydrophobic groups such as the ammonium salt, amino acids, citric acids, etc. In this case, the hydrophilic groups on the surface of functionalized SPIONs are strongly attracted by the solvent environment and an electrostatic repulsion between NPs is created, improving again their stability in the solution. Aminosilane like the 3-aminopropyltriethoxysilane

(APTES) have been used for performing the salinization, another NPs functionalization, which provides amino groups on NPs surface, allowing the connection of SPIONs with other metals, polymers and biomolecules.

Another functionalization strategy is based on the use of inorganic materials including silica, metal, metal oxides, etc. The combination of *metallic NPs* (e.g., Au, Ag, Cu, Pd, etc) and SPIONs have been investigated by several researchers due to their combined physiochemical properties and potential properties in biotechnology and biomedicine. These structures indeed can be modified with different functional groups or moieties on the surface of SPIONs to improve stability and biocompatibility. The most efficient functionalization method is the sequential growth of metallic components onto the surface of the NPs core in a one-pot reaction. Bi-functional nanoparticles which are composed of SPIONs and metallic nanoparticles not only can be used as optical labels in bioimaging, diagnosis and therapy, but also allow some biomolecules to be tagged and separated, together with targeted drug delivery and magnetic resonance imaging under the induction of an external magnetic field.

1.1.3 Applications in biomedicine

Magnetic IONPs with a long blood retention time, biodegradability and low toxicity have emerged as one of the primary nanomaterials for biomedical applications *in vitro* and *in vivo*. Considering their unique physical, thermal, and mechanical properties, magnetic NPs represent excellent platforms for biomedical research for both diagnostic and therapeutic purposes such as [4][5]:

- magnetically controllable drug delivery systems
- contrast agents for medical diagnostics
- mediators of hyperthermia cancer treatments
- magnetic thermoablation treatments
- gene delivery
- magnetofection

The effectiveness of the MNPs for these applications depends on: (a) high magnetic saturation; (b) size of particles (in the range between 6-15 nm); (c) superparamagnetic behaviour; (d) biocompatibility and interactive functions at the surface [5][19][20].

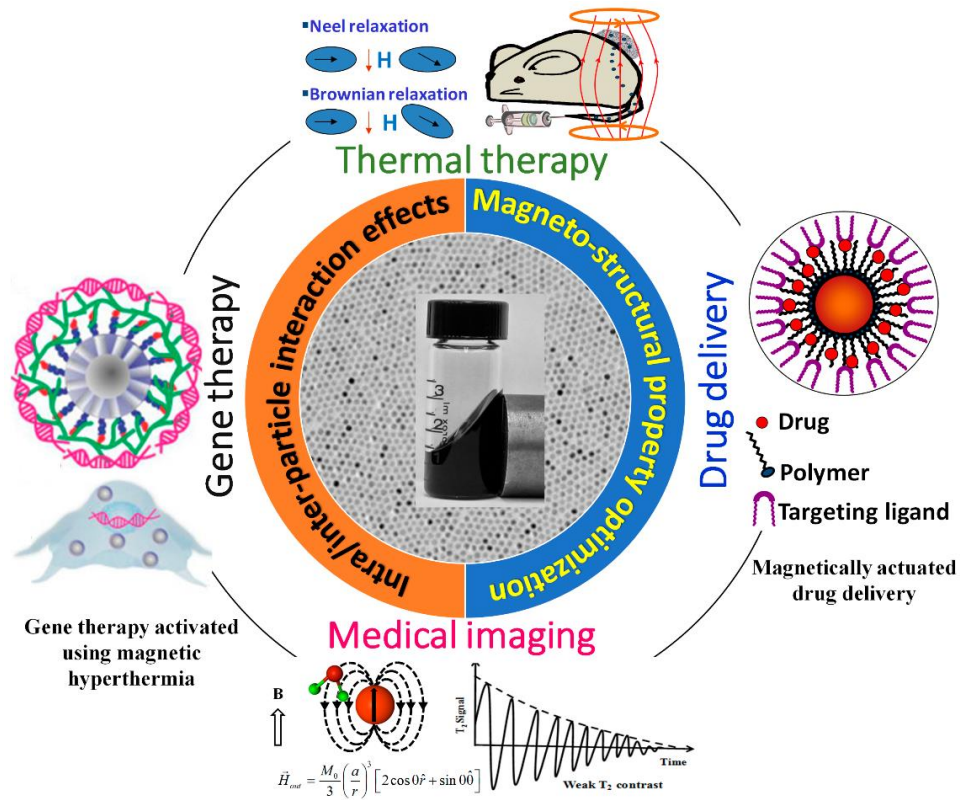


Figure 4. MNPs applications in biomedicine [16]

Drug delivery

MNPs are the most efficient delivery system for all types of hydrophilic and hydrophobic drug molecules because of their following properties: (1) high chemical stability; (2) biocompatibility; (3) higher colloidal stability; (4) retained superparamagnetic properties; (5) reduce drug waste; (6) reduce adverse reaction of drugs; (7) sustained delivery to desired targeted organ and (8) low cost [12]. The main goal of targeted drug delivery is to concentrate the drugs in the tissues of interest while reducing the relative concentration of medication in the remaining tissues by applying an external magnetic field. For these applications, the size, the charge and the surface chemistry of the magnetic particles are particularly important because they strongly affect both the blood circulation time as well as bioavailability of the particles within the body. For example, larger particles with diameters greater than 200 nm are removed by the cells of the phagocyte system, resulting in a decreased blood circulation time, while smaller particles with diameters inferior to 10 nm are rapidly removed through renal clearance [5]. Particles ranging from 10 to 100 nm demonstrate the most prolonged blood circulation time and are optimal for

intravenous injection. Moreover, below-20 nm IONPs are super-paramagnetic in nature and ideal for biomedical application since they can be manipulated by external magnetic fields [1].

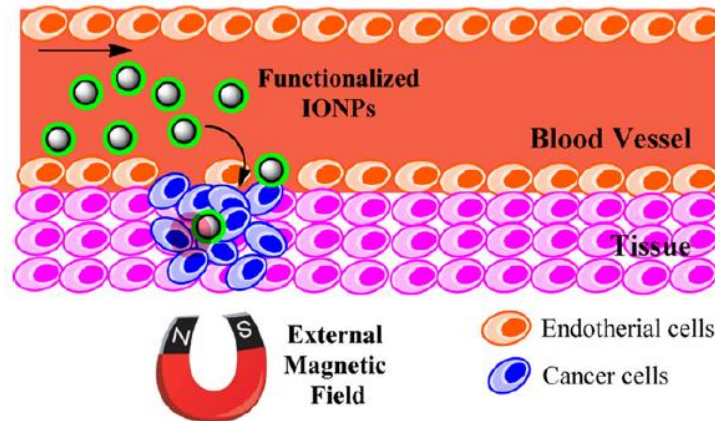


Figure 5. Schematic representation of magnetic nanoparticle-based drug delivery system: the magnetic carriers concentrate at the targeted site using an external magnetic field and, once they are at the specific site, drugs are released from the magnetic carrier [4]

Medical imaging

Magnetic resonance imaging (MRI) is a powerful imaging tool due to its non-invasive nature, high spatial resolution and tomographic capabilities. This technique is really useful for observing the differentiation between pathogenic and healthy tissues [1][13]. It is based on the response produced by the spin of proton with the application of magnetic field: the two relaxation processes, transverse relaxation (T₂-decay) and longitudinal relaxation (T₁-recovery), are used to produce the MR image [12]. For MRI purposes iron oxide cores are commonly used as T₂ contrast agent.

Magnetic hyperthermia

According to The European Society for Hyperthermic Oncology (ESHO), hyperthermia is defined as non-invasive therapy which uses the generation of a higher temperature at a tumor-involved region of the body. Hyperthermia treatment temperatures range between 40–45 °C. Moreover, cancer cells are more sensitive to the temperature because of the low concentration of oxygen and the low pH in the tumor tissue [1][12][13]. In magnetic hyperthermia, when SPIONs are subject to a high frequency alternating magnetic field, they are able to generate heat through Néelian and Brownian relaxation loss: the Néelian relaxation is related to the heat generated by the rotation of single magnetic moments

within the particles, while the Brownian one is related to the heat generated by the physical rotation of particles when an external magnetic field is applied. When SPIONs are injected into the body, they tend to accumulate into the tumoral tissue due to its unorganized vasculature; it results in an effective increase of temperature into the unhealthy tissue with respect to the surrounding healthy one. The amount of heat produced depends on the magnetic properties of the material, the strength of the magnetic field, the frequency of oscillation and the cooling capacity of the blood flow in the tumor site [5]. The main parameter that determines how effectively NPs generate heat to the tissue during magnetic hyperthermia treatment is the specific adsorption rate (SAR). SAR is the rate at which electromagnetic energy (E_{em}) is absorbed by a unit mass of a biological material (m) when exposed to a radio frequency (RF) electromagnetic field [4].

It can be expressed as follows:

$$SAR = \frac{d}{dt} \left(\frac{E_{em}}{dm} \right)$$

An enhancement of hyperthermia research is the use of tumor-targeted MNPs with additional potential of drug payload [13].

Gene therapy and magnetofection

This therapy introduces exogenous DNA into a patient in order to treat a genetic disease. The new DNA contains a functioning gene to correct the effects of a disease-causing mutations. It has a wide range of applications, including genetic disorders, cardiovascular diseases, cancers or neuro-degenerative diseases. Magnetofection is a technique based on the association of MNPs with nonviral or viral vectors to optimize gene delivery in the presence of magnetic field [14].

1.2 Plasmonic and Au NPs

Plasmonic nanoparticles, including gold, silver and platinum particles, are discrete metallic particles that have unique optical properties due to their size and shape. Among plasmonic NPs, gold nanoparticles (AuNPs) have tremendous potential for bionanotechnology-based applications [21].

1.2.1 Plasmonic properties

The physical, chemical and optical properties of metals depend on the spatial motion of the constituent electrons. The metallic materials with dimensions smaller than the wavelength of incident light (i.e., 1-100 nm) have new properties that are quite different from those of the bulk material because of the spatial restrictions of electronic motion.

Localized Surface Plasmon Resonance (LSPR)

Under the stimulation of light, the free electrons are excited and the displacement of the electron cloud produces oscillations on the particle surface, termed localized surface plasmon (LSP). When the frequency of the incident light matches (resonance) with the LSP oscillation frequency of the plasmonic metal nanoparticles, the plasmonic NPs strongly absorb the light and this generates highly amplified and localized electric field in the proximity of the particle surface. This resonant condition of LSP at a particular frequency of light is called the LSP resonance (LSPR) [21][23]. Excited LSPs follow two different decay process, absorption and scattering, which reflects the observed colour of the colloidal metal nanoparticle solution. Some of the absorbed light decays by emitting photons at the same frequency as the incident light (*scattering*), while some decays by converting into hot electrons (*absorption*) [23].

After absorbing photons, AuNPs convert the light energy of the electrons into kinetic energy and part of it is transformed into vibration energy. The vibration energy is finally expressed in the form of heat and this represents the so-called “photothermal effect” [22].

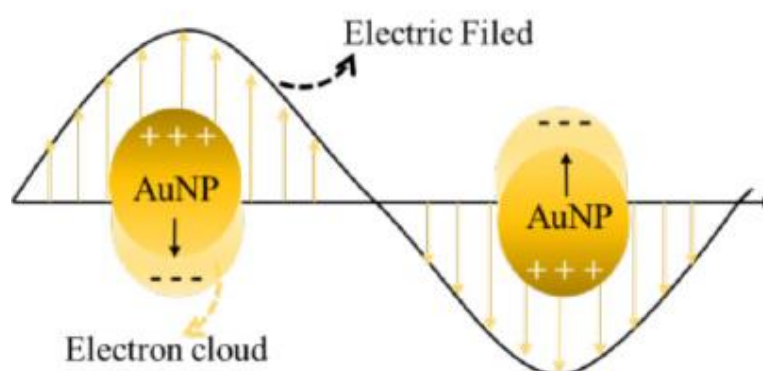


Figure 6. Localized surface plasmon resonance (LSPR) of AuNPs [22]

LSPR of AuNPs is highly dependent on the factors that affects the electrons density on the particle surface such as size, shape, composition and microenvironment [22]. These factors affect the absorption and scattering properties of plasmonic nanoparticles.

The peak intensity of the LSPR band increases by increasing the size of the nanoparticles [23]. In the case of nanospheres, Au NPs exhibit a LSPR band in the spectral range going from the visible to the near infrared (520-550 nm).

When LSPR occurs, the photothermal conversion efficiency, photochemistry conversion and light energy absorption of the AuNPs are strongly enhanced. These properties can be used for the photothermal therapy (PTT), photodynamic therapy (PDT) and colorimetric assays in tumor diagnosis [22].

1.2.2 Synthesis methods

Among the plasmonic NPs, gold nanoparticles (AuNPs) have been found to have a great potential in the biomedical field thanks to their nontoxicity and unique optical, physicochemical and biological properties [21]. The current studies reported in nanotechnology enables the successful synthesis of AuNPs with an average particle size lower than 10 nm, experimentally determined by Diffraction Light Scattering (DLS) means. Different syntheses have been found in literature to obtain AuNPs such as [21]:

- Conventional chemical synthesis
- Polymer-mediated synthesis
- UV-induced photochemical synthesis
- Ultrasound-assisted synthesis
- Laser ablation synthesis
- Microbial mediated synthesis
- Extracellular and intracellular synthesis
- Plant mediated synthesis.

Among the conventional chemical synthesis, the *chemical reduction* method is the most used to produce AuNPs; it is based on two main steps: (1) the use of reduction agents such as citric acids and borohydride which provide electrons to reduce gold ions, and (2) the use of stabilization agents such as polymers and trisodium citrate dihydrate, which role is to stabilize nanoparticles avoiding aggregation thanks to repulsive forces. The ratio

between the reducing agent and the stabilizing agent significantly influences the size of the obtained nanoparticles [21][24].

Polymer-mediated synthesis allows to better control the size and shape of nano-gold since, as various research studies have shown, the interaction of gold nanoparticles with polymers strongly impact the size, stability and distribution of particles.

Other kinds of synthesis exploit UV radiation with different wavelengths, ultrasound wave generator and pulsed laser to reduce gold ions, while more recent studies have been focused on the research of cost effective and eco-friendly synthesis of AuNPs by using microbes, plant and fruit extracts instead of hazardous chemicals and toxic derivatives [24].

1.2.3 Applications in biomedicine

Plasmonic nanoparticles have gained great consideration in biomedical field thanks to their size-dependent properties and behaviour. Indeed, their size is responsible for their bioavailability, bioaccumulation, and toxicity in a biological system [21].

Some examples of the use of gold nanoparticles in medical applications are:

- Drug delivery
- Photothermal therapy
- Photodynamic therapy
- Sensing

Delivery system

One of the greatest challenges in anti-tumor targeted drug delivery system is to develop personalized, tunable and suitable carrier platforms in order to obtain a controllable and targeted drug release. The gold nanoparticle surface charge plays a critical role during the fabrication of nanosystems for controlled and targeted drug therapy. Previous research studied have revealed, indeed, that the toxicity level assigned to AuNPs is strongly related to the particle surface charge: positively charged gold nanoparticles cause cell death at a lower concentration, while the neutrally charged particles determine cellular death at significantly higher concentration [21]. Moreover, the large ratio of surface area-volume of Au NPs enables their surface to be coated with hundreds of molecules such as therapeutic, diagnostic and targeting agents but also ligands and antibodies [24].

Photothermal therapy (PTT)

The photothermal conversion has a promising prospect in *photothermal therapy (PTT)* since the temperature inside the nanoparticles, raised by light-absorption, is effectively transferred to the medium surrounding the nanoparticles [22][23]. This treatment modality, indeed, explores the local increase of temperature causing mechanical and/or chemical changes in cells or larger structures, including cancer tumors. The plasmonic NPs are exploited to specifically deliver heat to selected locations, defining the so-called PPTT. Among the different noble metals, gold is the most suitable material for nanoparticles because of its chemical/biological stability, low cytotoxicity, LSPR tunability and high light absorption efficiency [25].

After the accumulation at targeted tumors, LSPs are coherently excited by laser irradiation and their rapid relaxation produces a localized thermal effect, which induces death of nanoparticle-targeted cells and reduces the damage on the surrounding healthy tissue. NIR light (650-900 nm) has been widely used in biomedical applications because it can penetrate deep into the tissues because of the low absorption and scattering exhibited by biological tissues as water, blood and fat [23][25]. However, radiation in the visible light region can also be used for in vitro studies and for superficial tumors as skin tumors. PTT is a minimally invasive technique to treat tumors and has great potential to overcome or improve currently used therapies in oncology. It exhibits, indeed, spatiotemporal selectivity, high sensitivity, side effect reduction, cost effectiveness and it represents a fast and effective treatment. Moreover, synergetic therapies with different therapeutic methods such as photodynamic therapy (PDR), radiotherapy and chemotherapy have been investigated in order to enhance the therapeutic efficacy of PTT [23].

Photodynamic therapy (PDT)

Among the different therapeutic modalities, PDT is mainly related to the optical properties of gold NPs and it represents a clinical treatment based on the activation of photosensitizers (PSs), which are light-absorbing molecules. Light irradiation at a specific wavelength causes the PSs to generate reactive oxygen species (ROS) which are toxic to the targeted disease cells. Rose bengal and phthalocyanine are some examples of PSs however, those are generally limited in medical applications because of their photo-induced degradation and enzymatic degradation, while AuNPs are promising PSs for PDT

thanks to their excellent photostability and superior resistance to photo-induced degradation and enzymatic degradation [23][26].

1.3 Magneto-plasmonic NPs

Multifunctional nanoparticles have gained wide attention during the last years because of their potential: combining two or more functionalities, they can indeed overcome some of the limitations of conventional applications using single nanoparticles. The following work focuses on gold-magnetite NPs that synergistically show excellent magnetic and plasmonic characteristics in a unique platform and represent a great resource for biomedical applications such as magnetic hyperthermia, photothermal therapy, drug delivery and imaging. Various multifunctional nanostructures have been developed since it is possible to optimize their physical and chemical properties by changing their morphology and surface functionalization. The most employed method for the synthesis of these multifunctional nanostructure is the chemical decomposition where seeds are directly deposited on a preformed core with a consequent controlled growth of the seeds. According to their structure, it is possible to divide magnetic-plasmonic heterodimers in two categories: (1) Fe_3O_4 -Au Nanostructures (*FANSs*) and (2) Au- Fe_3O_4 Nanostructures (*AFNSs*).

The first one is characterized by a Fe_3O_4 single core or multicores and an Au surface coating, where gold acts as a shell; depending on the shape of Au shell, different FANSs can be obtained such as (Figure 7):

- Core-satellites structure (a)
- Spherical core-shell structure (b)
- Non-spherical core-shell structure (c)
- Hollow structure (d).

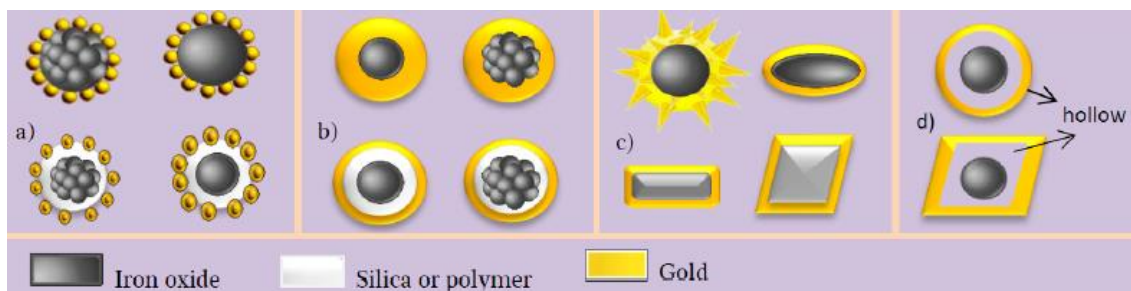


Figure 7. Main structures of FANSs [102]

The second category is characterized by a single Au core or multicores, surrounded by a Fe_3O_4 coating. The main classes of AFNSs are (Figure 8):

- Dumbbells structure (a)
- Core-satellites structure (a)
- Spherical core-shell structure (b)
- Non-spherical core-shell (c)

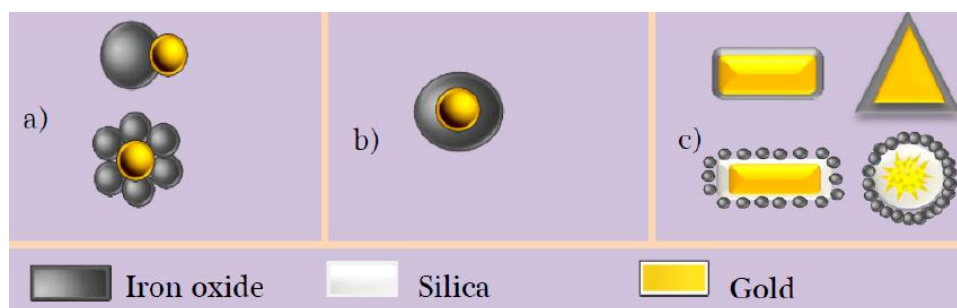


Figure 8. Main structures of AFNSs [102]

However, in most cases the magnetic-plasmonic nanostructures consist of magnetic hosts and plasmonic guests, where magnetic nanoparticles are usually first pre-synthesized via common methods and then they are employed as host seed for chemical deposition of the gold component.

The main advantage is the possibility to combine magnetic and plasmonic properties in one nanocomposite in order to obtain new multifunctional nanomaterials with unique multimodal properties. In particular, the main plasmonic nanoparticles properties involve surface plasmon resonance phenomena which allow to achieve the intensive selective absorption or scattering of light that is mostly used in biosensing, diagnostic and photothermal and photodynamic therapy; while the magnetic nanoparticles, thanks to their properties, can be delivered to the desired area by applying an external magnetic field and by targeted functionalisation and NPs can be hold there until the treatment is

complete. In this way, magneto-plasmonic nanoparticles show a great potential for the drug delivery applications [3][27][28][102].

Chapter 2

Green biosynthesis

Nanoparticles have recently gained a lot of attentions in science and industry since they can be successfully used in various fields thanks to their unique features. A lot of synthesis methods have been reported for producing nanoparticles with desired properties, however, their production involves complicated and expensive procedures, including very high temperature, energy consumption and toxic precursors which lead to the formation of pollutant coproducts. In order to overcome the problems caused by conventional approaches, different researchers have been studying new ecological synthesis methods for obtaining NPs using materials coming from biological routes, such as [29][47]:

- Plants
- Micro-organisms
- Natural polymers

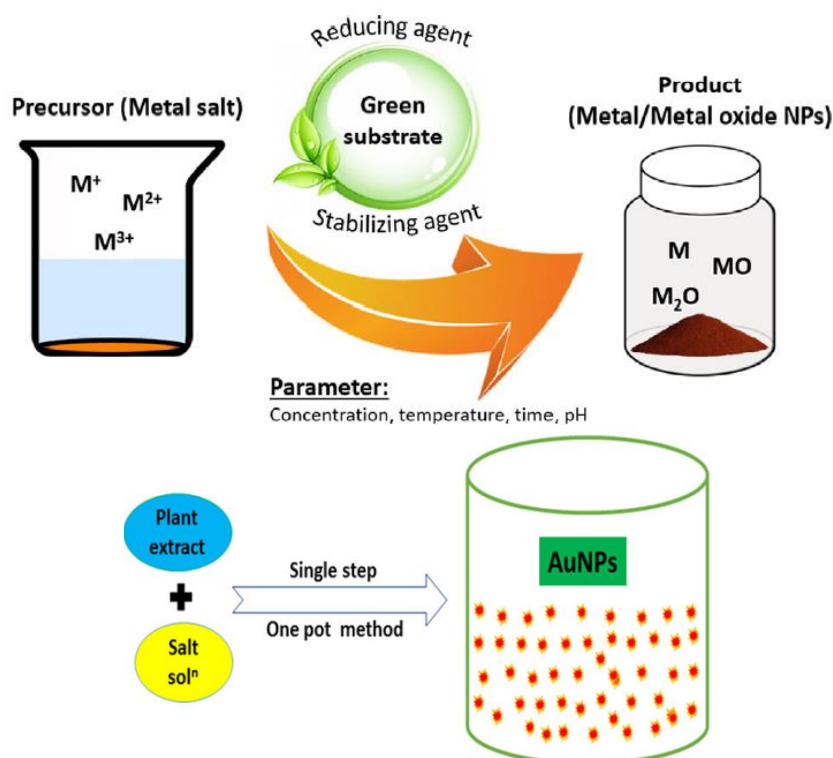


Figure 9. Nanoparticles biosynthesis process: Metal oxide NPs [30] and Gold NPs [35]

These green methods are not only simple, but also economic, less waste production, environmentally friendly, and they reduce the toxicity potential of the nanoparticles. However, this synthesis not always led to the formation of NPs with good properties for use in biological applications [30][48]. Green biosynthesis employs the bottom-up approach where the main reaction occurring is the reduction/oxidation. The green chemical reduction method involves two essential steps: (1) the use of a reducing agent, that allows the transformation of the metallic species from its bulk composition to its electric state, and (2) the stabilizing agent [48]. The materials needed are metal salt as precursor and green substrate, as shown in figure 9: the plant phytochemicals with antioxidant or reducing properties are usually responsible for the reduction of salts into their respective NPs, so the metal atoms assemble to form clusters and then eventually nanoparticles [4]. In fact, the dissolved metal ions are reduced into nano metals thanks to the biochemical processes in biological agents [35]. Biomolecules, such as protein, phenol, flavonoids, etc. present for example in the plant extract, play an important role in the reduction of metals ions and capping of the NPs. By modifying the concentration of metal salt, the concentration of green extracts, the time and temperature for reaction and the pH of the solution, it is possible to obtain properties that are needed for respective applications [30].

In the following chapter some green routes for nanoparticles synthesis are presented, focusing in particular on the use of curcumin and its properties and applications in biomedical field.

2.1 Plants

Among all the different green synthesis, biosynthesis using plant extracts is the most popular since they can act as both reducing and stabilizing agents in the nanoparticles synthesis [30]. The polyphenols are abundant in plants extracts and, together with other active biomolecules, are responsible of NPs formation by bio-reduction of metal ions. Polyphenols are characterised by aromatic rings that bind hydroxyl groups (OH) that make them soluble in water and they are useful in both reduction and stabilization of metallic NPs [36]. The plant-mediated synthesis of metallic nanomaterials is carried out by using various parts of plants including tissue, extracts, and other parts of the living plants, which contain reducing agents such as citric acid, ascorbic acid, enzymes like

dehydrogenases [15]. In order to obtain extract, the different plant parts are washed with distilled water, chopped in small pieces and boiled into an universal solvent [35]. The main advantages of green biosynthesis using plant extract are that it can be obtained easily, large scale production, cost effective and environmental benign, while the main disadvantages are, for example, the decreased rate of synthesis and the difficulty in controlling the size, shape, and crystallinity of NPs. Moreover, not all the plants are suitable for the synthesis of nanoparticles [4][15][30].

Carob leaf extract has been employed as a rapid, non-toxic, facile and green resource for preparation of iron oxide magnetic nanoparticles in a single step reaction at low temperature using Fe(III):Fe(II) and sodium hydroxide solutions. Protein within the extract act as capping agent due to their carboxylic groups. The average diameter of the obtained monodispersed nanoparticles is of 4-8 nm [15]. *Ngernpimai et al.* used the *Aloe vera* for obtaining Fe₃O₄ NPs. The spherical nanoparticles were then passed through the serial centrifugation steps and their size decrease with increasing degree of centrifugation. Moreover, by controlling the reaction time and temperature, a smaller size and irregular shape of NPs were produced [33][34].

For gold nanoparticles synthesis, different ratio of gold salt and plant extract are simply mixed at room temperature. There is no need to add external stabilizing/capping agents since the phytochemicals acts as both reducing and stabilizing agents. *Nagajyothi et al.* used *Lonicera japonica* which amide, alkane, amino and alcohol present in this flower extract were involved in the bioreduction of chloroauric acid to synthesize gold NPs [35].

2.2 Micro-organisms

Micro-organisms secrete biomolecules such as enzymes, proteins, sugars, etc., that can be used for the synthesis of NPs by reduction/oxidation of metallic ions. The biosynthesis can be either extracellular or intracellular and the size and morphology of the synthesized nanoparticles are influenced by the biochemical processing activities of micro-organisms. The main microbial methods for the synthesis of inorganic nanoparticles are mediated by: actinomycetes, algae, bacteria, fungi, viruses, yeasts [35].

2.2.1 Algae extracts

Algae, which is also known as seaweed or in general as marine plant, can be used for the synthesis of metallic nanoparticles. The phytochemicals that are present in the algae, indeed, can act as metal-reducing agents and capping agents to provide a robust coating on the metal NPs in a single step [30]. As example, *Mahdavi et al.* used the *Sargassum muticum*, a brown seaweed, for the synthesis of Fe₃O₄ NPs. The procedure was simple and consisted in mixing FeCl₃ solution to the brown seaweed extract and, through a reduction process, the metallic nanoparticles were immediately produced with a cubic shape and particles size of 18 ± 4 nm. In this process, the main components present in seaweed, such as sulphate, hydroxyl and aldehyde group, led to the reduction of Fe³⁺ and stabilized the nanoparticles [30].

2.2.2 Bacteria

In bacteria, the reduction on metallic ions can occur intracellularly or extracellularly and the presence of different types of biomolecules with carboxylic and amine groups prevents the agglomeration of nanoparticles. In the traditional biosynthesis for magnetic IONPs, magnetotactic bacteria and iron reducing bacteria are the most used but recently new types of bacteria have been employed [4]. *Bharde et al.* have reported that the bacterium *Actinobacter* sp. reacting with a ferric chloride precursor was capable of synthesizing maghemite NPs under aerobic conditions. This procedure offered a significant advance with respect the magnetotactic and iron reducing bacteria since the reaction occurred under aerobic conditions [31]. *Sundaram et al.* reported the ability of *Bacillus subtilis* strains isolated from rhizosphere soil to produce IONPs. This synthesis allows to obtain stabilized Fe₃O₄ NPs and shows the applicability of the isolated *Bacillus subtilis* strain for the bulk synthesis of IONPs [32].

The thermophilic bacteria can be very useful for the extracellular synthesis of both gold and silver NPs [36]. A highly efficient bacterium *Stenotrophomonas maltophilia* has been studied for the synthesis of gold nanoparticles of desired size and shape. The results showed that the isolated strains of the bacterium present a specific NADPH-dependent enzyme that is capable to reduce Au³⁺ to Au⁰ through an electron shuttling mechanism [35]. Moreover, *Staphylococcus aureus* bacterium was used for the synthesis of silver nanoparticles (Ag NPs) obtaining spherical shape NPs with sizes between 2 and 100 nm.

2.2.3 Fungi, actinomycetes and yeasts

Fungi have been exploited for the biogenesis of the gold nanoparticles because of the large quantities of enzymes that they secrete. In particular, gold ions were absorbed by them and that lead to the formation of the gold nanoparticles. Moreover, filamentous fungi have unique advantages with respect other microorganisms such as high metal tolerance and the capability of bioaccumulation. Nanoparticles with a better size and polydispersity can be obtained by using *actinomycetes* thanks to their capability to be easily modified genetically. Only few yeast strains have been used for gold NPs synthesis such as the *Hansenula anomala* which has the ability to donate electrons: the reductants are extracted from the yeast, and they are used as reagents for the synthesis of gold nanoparticles [37].

Table 3. Summary of different NPs biosynthesis methods using different green bioreductants.

Type	Name	NPs	Information	Ref.
Plant extract	<i>Aloe Vera</i>	Fe ₃ O ₄	Spherical NPs with a dimension range of 93-227 nm. By modifying the parameters during the reaction, smaller and irregular agglomerated NPs are obtained.	[30] [33] [34]
Plant extract	<i>Carob leaf extract</i>	Fe ₃ O ₄	Single step synthesis at low temperature. The obtained NPs are monodispersed with an average diameter of 4-8 nm.	[15]
Algae extract	<i>Sargassum muticum</i>	Fe ₃ O ₄	Metallic NPs are immediately obtained by mixing the brown seaweed solution and the FeCl ₃ solution with a cubic shape and a dimension of 18 ± 4 nm.	[30]
Flower extract	<i>Lonicera japonica</i>	Au	Gold nanoparticles with antimicrobial activity are obtained in one single step reactions where amide, alkane, amino and alcohol present in the flower extract were involved in the stabilization and bio reduction.	[35]
Bacteria	<i>Actinobacter</i> sp.	Fe ₂ O ₃	Maghemite NPs synthesis under aerobic conditions using the	[31]

			bacterium reacting with a ferric chloride precursor.	
Bacteria	<i>Bacillus subtilis</i>	Fe ₃ O ₄	The strains of the bacterium have been used for the bulk synthesis of stabilized IONPs.	[32]
Bacteria	<i>Stenotrophomonas maltophilia</i>	Au	Gold nanoparticles synthesis is performed by the bacterium through an enzymatic reduction of gold ions.	[35]
Bacteria	<i>Staphylococcus aureus</i>	Ag	It is used as reducing agent and lead to the production of spherical silver nanoparticles of 2-100 nm.	[35]
Yeast	<i>Hansenula anomala</i>	Au	The reductants are extracted from the yeast and used as a reagent during the synthesis of gold nanoparticles.	[37]

2.3 Curcumin

Curcumin is a yellow polyphenolic phytochemical compound commonly used as natural colouring agent in Asian cuisine, traditional cosmetics, and medicine [40]. It shows heptadienone linkage between two methoxy phenyl rings and it is derived from *Curcuma longa* (turmeric) that represents a plant that has been widely used in cuisine as a spice and also for curing the diseases (Figure 10) [39].

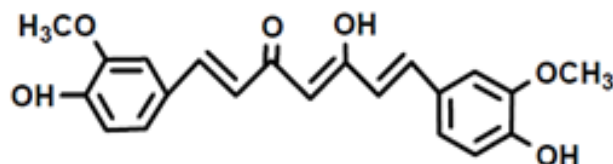


Figure 10. Curcumin molecule [39]

Curcumin was isolated for the first time by Vogel in 1842 from turmeric by solvent extraction followed by column chromatography. In the 14th century, curcumin was

introduced to the western world, and it is now studied for its multiple therapeutic effects such as antioxidant, antitumoral, antibacterial activity, antifungal, anti-inflammatory, anti-viral, etc. and for its profound biological activities [29][38][40]. Different studies reported that the curcumin at an optimized dose has low toxicity, and it is safe up to 8g per day, which makes it highly suitable for clinical applications [38][42]. Curcumin has shown remarkable anticancer activities by affecting diverse molecular targets. It is also a promising agent for the treatment of neurological disorders such as Alzheimer's disease and Parkinson's disease thanks to its anti-inflammatory activity [41][42][45]. Despite its benefits, the use of turmeric is limited due to its low solubility in water, which makes it hardly accessible for cells, its weak absorption, a rapid metabolism, a rapid systemic elimination, and a limited blood-brain barrier (BBB) permeability [29][44]. However, several curcumin carriers have been synthesized as a drug delivery system using biocompatible organic substances like liposomes, viruses, biopolymers, cellulose, etc., in order to improve curcumin water solubility, its bioavailability and its therapy efficacy. Liposomes are the most popular carriers used in drug delivery, but they suffer from fast elimination from the blood circulation, physical and chemical instability, aggregation, fusion, and degradation. Magnetic nanoparticles are another example of curcumin carrier [42].

2.3.1 Curcumin chemical properties

Curcumin is a symmetric molecule composed by two aromatic rings with o-methoxy phenolic groups which are connected by a seven carbon linker containing α,β -unsaturated β -diketone moiety that give rise to the keto-enol tautomerism of curcumin (Figure 11).

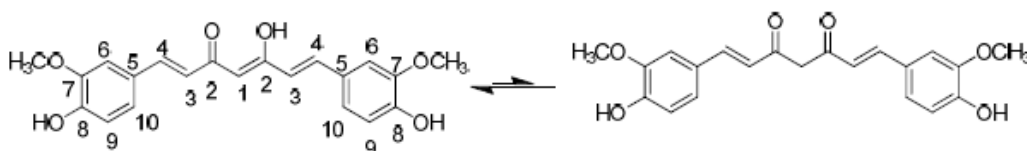


Figure 11. Keto-enol form of curcumin [46]

The keto and enol conformations are in equilibrium due to the intramolecular hydrogen atoms transfer at the β -diketone chain [39][44]. It has a molecular weight of 368.38 g/mole and a melting point of 183 °C [38]. Its IUPAC name is (1E,6E)-1,7-bis(4-hydroxy-3-methoxyphenyl)-1,6-heptadiene-3,5-dione, with chemical formula $C_{21}H_{20}O_6$ [39].

Curcumin is a hydrophobic molecule, soluble in polar solvents like oil, acetone, ethanol, methanol etc., and it is highly susceptible for pH change in water: at acidic and neutral pH, curcumin is insoluble in water with a pale yellow solution colour, while it is soluble at alkaline pH since the acidic phenol group in curcumin donates its hydrogen, forming the phenolate ion enabling curcumin to dissolve into water, where the solution colour turns dark orange [38][39][48]. Stability of curcumin is very important to maintain its physiological activities; it is stable below pH 7.0 but, by increasing the pH values, curcumin easily degrades within 30 min to Trans-6-(40-hydroxy-30-methoxyphenyl)-2,4-dioxo-5-hexanal, ferulic acid, feruloylmethane and vanillin: ferulic acid and feruloylmethane are formed initially, while the degradation products formed by hydrolysis of feruloylmethane are vanillin and acetone. Under acid conditions, the degradation of curcumin is much slower [38][41]. Curcumin is also sensitive to light indeed, in the presence of light, the degradation is much higher: for example, curcumin at pH 1.2 is highly stable in the absence of light as compared to pH 1.2 in the presence of light [38]. The physicochemical properties and antioxidant activities of curcumin depend on the amount of keto-enol-enolate of the heptadienone moiety in equilibrium. In acidic and neutral conditions (i.e., pH 3-7), curcumin mostly exhibit the keto form, acting as a proton donor. In keto form, indeed, the heptadienone linkage contains a highly activated carbon atom with two labile hydrogens that became the site of reaction. In the enolate form, the phenolic part of curcumin represents the reaction site and act as an electron donor [41].

2.3.2 Curcumin reactivity

Scientific research has shown the diverse pharmacological effects of curcumin and its ability to act as a chemo preventive agent as well as a therapeutic agent against several chronic diseases like inflammation, cancer, cardiovascular disease [39]. In order to understand the biological activity of curcumin, important chemical reactions associated to it have been considered such as the hydrogen donation reactions leading to oxidation of curcumin and its chemical reactivity with reactive oxygen species (ROS), enzymatic reactions and formation of nanoconjugates [39]. Moreover, the nucleophilic addition reactions, occurring between the unsaturated ketone of curcumin molecule as an acceptor and anions of -OH, -SH, -SeH as donors, has been reported to be very important to explain the biological chemistry of curcumin in living cells; this reaction in fact is the mainly

responsible for the inhibition of the thioredoxin reductase (an enzyme involved in maintaining the cellular redox homeostasis) by curcumin [39].

Antioxidant activity

The antioxidant activity of curcumin is believed to derive from its phenol moiety, and it is helpful in protecting normal cells from free radical-induced damage since it is an excellent scavenger of most ROS [39][41]. In the brain, curcumin is able to stabilize antioxidant enzymes and protect for radical-induced DNA damages in neuronal cells [44]. Different studies have shown that free radical oxidants participate in hydrogen abstraction and in electron transfer reaction; indeed, during free radical reaction, all three active sites of curcumin can undergo oxidation by electron transfer and hydrogen abstraction (Figure 12); the most easily abstractable hydrogen is from the phenol-OH group, leading to the formation of phenoxy radicals. Moreover, curcumin has a metal chelating ability that allows the formation of complexes with metals like Cu^{2+} , Mn^{2+} , which act as metal-based antioxidants [39].

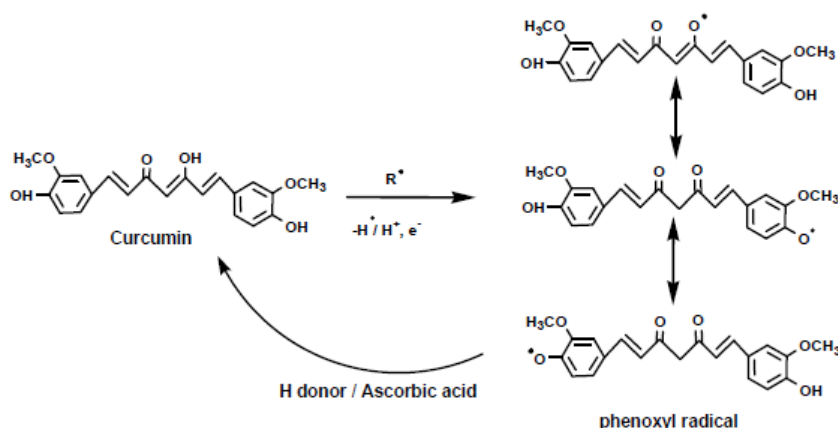


Figure 12. Three active sites of curcumin undergoing oxidation [39]

Antibacterial and anti-inflammatory activity

Curcumin is also known to have direct antibacterial activity against different kind of bacteria. The phototoxicity of curcumin in bacterial systems has been studied and the results have shown that curcumin exhibited negligible effect against bacteria in the absence of light. *Tønnesen et al.* demonstrated that, under visible light, curcumin possesses phototoxic effects on some bacteria like *Salmonella typhimurium* and *E. coli* [41][43][46].

Thanks to its anti-inflammatory activity, curcumin shows great promise for the treatment of various pro-inflammatory chronic illness such as Alzheimer's disease, multiple sclerosis, cancer, etc. even if its oral administration shows a rapid metabolism and elimination due mainly to its poor solubility [39].

Curcumin-metal ion interactions

Curcumin shows a metal chelating ability through the β -diketo group thanks to the presence of OH groups and one CH_2 group [39][44]. Indeed, curcumin forms stable complexes with most of the metal ions; the structure and physical properties of these entities depend on the nature of the metal ion and on the stoichiometry of the reaction condition. In general, the curcumin:metal stoichiometry is 2:1 (Figure 13). Metal salts and stoichiometric amount of curcumin are mixed in suitable solvents for few hours in order to obtain the curcumin-metal complexes. The enolic proton is replaced by the metal ion while the o-methoxy phenolic moiety remains intact [39]. Curcumin can chelate transition metals (Fe^{3+} , Mn^{2+} , Ni^{2+} , Cu^{2+} , Zn^{2+} , Pb^{2+} , Cd^{2+} , Ru^{3+} , Re^{3+} , etc.), and non-transition metal ions (Al^{3+} , Ga^{3+} , Sm^{3+} , Eu^{3+} , Dy^{3+} , Y^{3+} , Se^{2+} , etc.) [46].

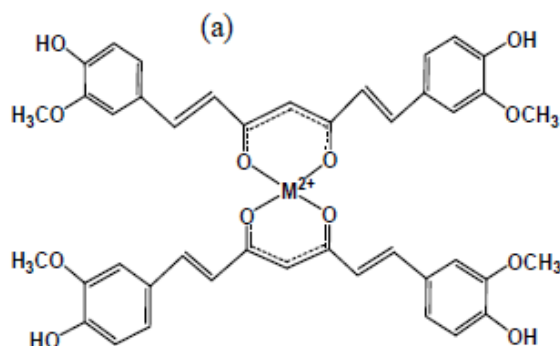


Figure 13. Structure of 2:1 curcumin-metal complex [39]

Curcumin-metal complexes are very important in the treatment of Alzheimer's disease with 1:1 Al^{3+} -curcumin complex since, thanks to its lipophilic nature, curcumin can cross the blood brain barrier and chelate metal ions that are toxic to the neurons [39][41]. These complexes found other applications in anti-cancer, gastroprotective and antidepressant treatments. In particular, curcumin-metal systems are being explored as better anti-tumor agents than curcumin itself [39].

2.3.3 Curcumin-conjugated nanoparticles

In recent years, the challenges of increasing the curcumin bioavailability culminated with the development of nanoparticles. The conjugation or loading of curcumin onto different platforms in order to increase its therapeutic effects is a topic of high interest [49]. Consequently, curcumin in nanoparticle formation has been introduced as a principal reducing agent and stabilizing compound; curcumin provide, indeed, the reduction of the metal from M^{*+} to M^0 and the stabilization of the obtained NPs. This combination of green synthesis and curcumin to produce nanoparticles led to the reduction of toxic waste. Different kind of NPs has been synthesized through the green chemical reduction using curcumin such as gold nanoparticles (Au NPs), silver nanoparticles (Ag NPs), iron nanoparticles (Fe NPs), etc. Their size and shape strongly depend on the amount of curcumin added during the synthesis [48]. The main aim of this work is the synthesis and characterization of multifunctional nanostructures composed by magnetite and gold nanoparticles using curcumin as bioactive agent. In this section, different synthesis routes present in the literature will be shown.

Curcumin-metal nanoparticles

Conjugates of curcumin and metal oxide nanoparticles have promising potential in nanomedicine as drug delivery system and MRI contrasting agent. Curcumin bound to novel metal and oxide nanoparticles have been studied also to improve the anti-cancer activity of curcumin: indeed, due to their selective accumulations and ability to cause hyperthermia, MNP-curcumin are attracting the attention of many researchers for application in cancer therapy [39].

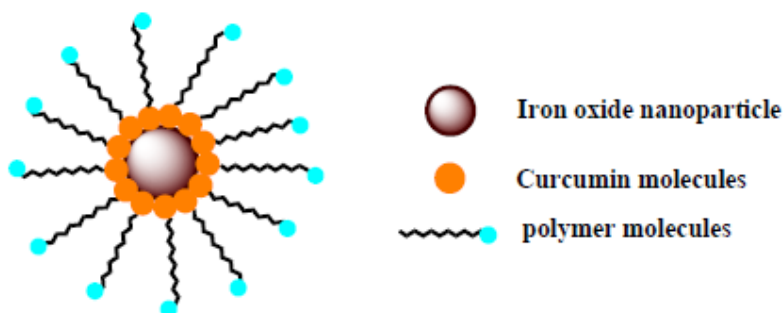


Figure 14. Curcumin functionalized IONPs stabilized by polymer [39]

Usually, magnetic nanoparticles are synthesized and then coated with biopolymers in order to *load hydrophobic curcumin* (Figure 14): *Yellapu et al.* prepared curcumin-loaded MNPs modified with cyclodextrin and reported inhibitions effect in ovaria, breast, and prostate cancer cells [53], while *Ashkbar et al.* synthesized silica-coated Fe_3O_4 magnetic nanoparticles loaded with curcumin as a natural photosensitizer for the treatment of breast cancer using simultaneously PDT and PTT [54]. Magnetic-curcumin nanoparticles can be also used in neurodegenerative disorders under the influence of an external magnetic field. *Kwok Kin Cheng et al.* encapsulated curcumin in the structure of the magnetic nanoparticles coated with polyethylene glycol (PEG) and poly-lactic (PLA) for detecting amyloid plaques in Alzheimer's disease [57], while *Mancarella et al.* synthesized the curcumin loaded magnetic nanoparticles coated with dextran (DXS) and poly-lysine (PLL) for curcumin delivery to cancer cells [58]. Moreover, *Rahimnia et al.* investigated the loading and conjugation of curcumin on oleic acid (OA) and citric acid (CA) functionalized iron oxide NPs for diagnostic purposes [49]. Finally, *Nosrati et al* prepared serum albumin-coated magnetic nanoparticles as curcumin carriers.

Novel magnetite NPs are obtained by co-precipitation in the presence of turmeric (*Curcuma longa*) extract (Figure 15): *Bhandari et al.* reported a simple coating of Fe_3O_4 NPs using *curcumin as stabilizing agent*; these NPs were found to be useful as antioxidant agent [59]. *Temelie et al.* described the turmeric-assisted NPs synthesis as an ecological method for the synthesis of NPs which can be used to increase the bioavailability of the substance [29].

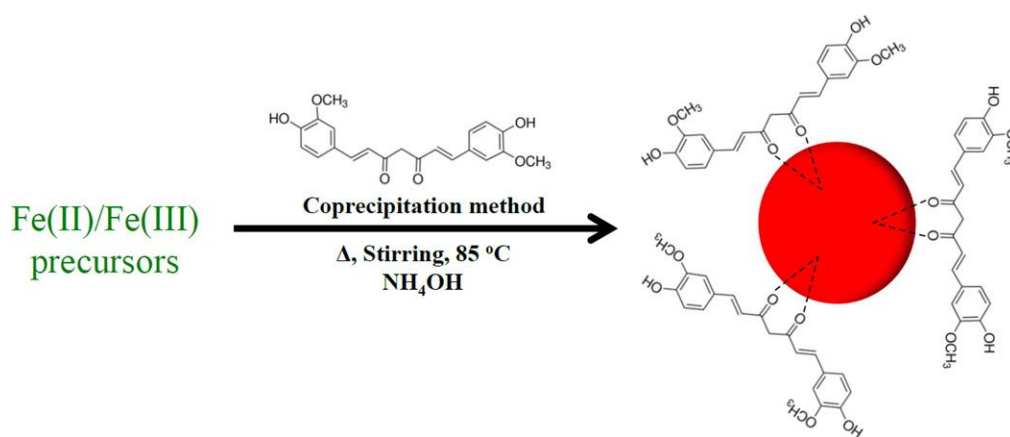


Figure 15. Single step curcumin coated magnetic Fe_3O_4 [59]

Some of the curcumin-metal nanoconjugates present in literature have been summarised in the following table 4:

Table 4. Curcumin-metal nanoparticles examples

Synthesis method	Solution	Coating	Cur-loading	T	pH	Ref.
Co-precipitation	Aqueous	-	Keto-enolic functionality of Cur molecule	T _{room}	-	[29]
Co-precipitation	Aqueous	OA or CA	Hydrogen bond or -COOH functional groups	-	12-13	[49]
Co-precipitation	Aqueous	β-cyclodextrin + Pluronic F68 polymer	Diffusion and retention in hydrophobic cavity	-	-	[53]
Co-precipitation	Aqueous	Silica	covalent bond between silicon-oxygen and curcumin diketo moiety	25°C	7.4	[54]
Co-precipitation	Aqueous	BSA (bovine serum albumin)	-	T _{room}	11	[56]
Co-precipitation (reverse)	DMF (dimethyl fumarate)	PEG-PLA (stabilizer)	Adsorption	T _{room}	5.5	[57]

Co-precipitation	Ethanol	PLL-DXS	Adsorption	30°C	-	[58]
Co-precipitation	DMSO (dimethyl sulfoxide)	-	Keto-enolic functionality of Cur molecule (acting also as stabilizer)	85°C	-	[59]

Curcumin-gold nanoparticles

Curcumin-gold composites find application in biology and medicine for drug delivery, diagnosis, and cancer treatment thanks to their hemocompatibility and non-toxicity [39]. Gold nanoparticle-based curcumin formulations have been successfully synthesized and reported in recent studies: their synthesis consist of mixing alkaline curcumin solution to gold salts, where the ionized curcumin acts both as a reducing and capping agent. Both the phenolic-OH and enolic-OH donate hydrogen for reduction of Au^{3+} ions to Au^0 (Figure 16) [39]. For curcumin-gold NPs synthesis, chemical reduction is the main method employed and curcumin, according to different cases, can be dissolved in aqueous or organic solvent.

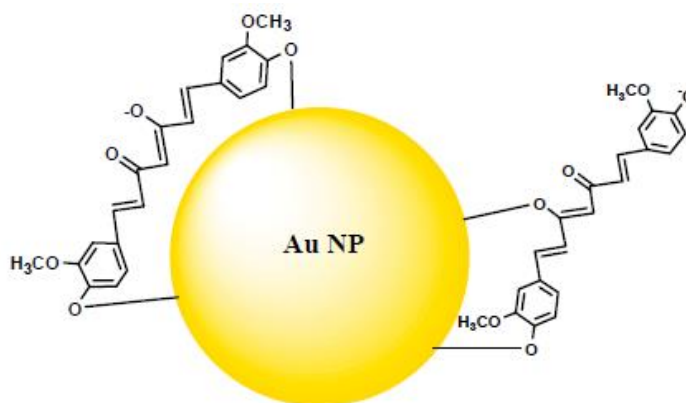


Figure 16. Gold nanoparticles capping by curcumin molecules [39]

Sreelakshmi et al. synthesized gold NPs using curcumin only as a reducing and stabilizing agent mixed with gold chloride (HAuCl_4) in basic media at 90 °C. They confirmed the formation of Au NPs after 15 minutes of adding curcumin, with a changing in colour

solution from yellow to light violet. By changing the concentration of H₂AuCl₄, different NPs sizes were achieved [50]. Similarly, Singh *et al* produced gold NPs using curcumin only at 90°C. The high temperature of the reaction allowed to better control the nucleation and growth of the Au NPs in order to achieve better size distribution of the nanoparticles [61].

Other researchers like Prabhu *et al.* used curcumin as reducing agent for the biosynthesis of gold NPs obtaining highly stable isotropic and monodisperse nanoparticles [51], while Abdulwahab *et al.* monitored the synthesis of gold NPs using curcumin as a reducing agent and by adding H₂AuCl₄ dropwise at pH 9.3 [52].

Sindhu *et al.* produced Au NPs using curcumin only at pH 9.2; the synthesis was carried out for three consecutive days in order to make all curcumin react and maximize the reduction. The obtained NPs had an increased stability of 6 months, and they were efficacy to be used in cell culture study [60].

Some of the curcumin-gold nanoconjugates present in literature have been summarised in the following table 5:

Table 5. Curcumin-gold nanoparticles examples

Synthesis method	Solution	Curcumin role	T	pH	Ref.
Chemical reduction	Aqueous	Reducing and stabilizing agent (through the chelation of metal with 1,3-diketone functionality of the Curcumin)	90°C	11	[50]
Chemical reduction	Aqueous	Reducing agent	100°C	6.68	[51]
Chemical reduction	Aqueous for H ₂ AuCl ₄ , organic (DMSO) for Cur	Reducing (Cur-3 formation after the H- atoms dissociation from the -OH group of the enolic Cur, O ⁻ electrons reduce gold ions) and stabilizing agent	-	9.3	[52]

Chemical reduction	Aqueous for H _{Au} Cl ₄ , organic (DMSO) for Cur	Reducing (-OH groups of curcumin reduce gold ions) and stabilizing agent (the unaltered aromatic rings and heptadiene chain of curcumin coat and stabilize Au NPs)	T _{room}	8-11	[60]
Chemical reduction	Aqueous	Reducing (electron transfer from Cur to gold ions) and stabilizing agent	90°C	5.67 (final)	[61]

Chapter 3

Advanced cancer treatments

In 2008, according to the GLOBOCAN, a predictable 12.7 million fresh cases of cancer and 7.6 million cancer losses occur. The majority of universally identified cancers are breast cancer (1.38 million, 10.9% of the total), colorectal cancers (1.23 million, 9.7%) and lung cancer (1.61 million, 12.7% of the total). The main widespread reasons of fatality due to cancer are lung (1.38 million, 18.2% of the total), liver (0.69 million, 9.2%) and stomach cancer (0.74 million, 9.7%) (Fig. 17) [12]. This data shows that, despite intensive research efforts over past few decades, cancer remains one of the leading causes of death in the world [17].

The goal of this work is to synthesize and characterize multifunctional systems composed by magnetite NPs, gold NPs and curcumin for their application in tumor diagnosis and treatment. In the following chapter, some previous research present in literature employing multifunctional NPs and curcumin for tumor treatments are presented.

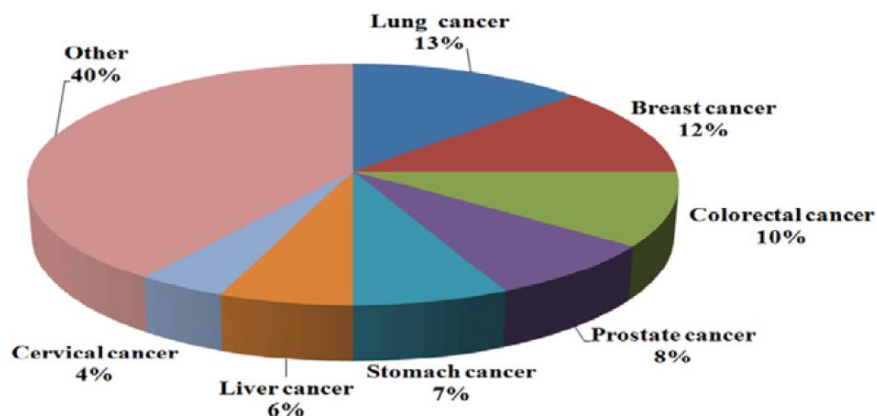


Figure 17. Most common cancer worldwide [12]

In the present scenario, there are three basic treatments that are used for cancer therapy: (1) radiotherapy, (2) chemotherapy, and (3) surgery. These methods present some specific side effects: indeed, an effective cancerous device should have the ability to eliminate or reduce tumor without damaging the healthy tissue; moreover, not often the traditional methods can be applied for the treatment of metastatic cancer.

3.1 Nanoparticles and curcumin in tumor treatments

Cancer is one of the biggest challenges and the main goal is not only to improve the therapeutic outcome, but also to improve the methods of treatment and to reduce the adverse effects. *Nanoparticles* has recently been introduced for tumor diagnosis and therapy because of their distinctive properties and sizes (approximately 1 to 100 nm) that allow them to transport the desired therapeutic to its target or as contrast agent for imaging applications [65]. Delivery of nanomedicines to solid tumors depends on the abnormal tumor microenvironment, characterized by the *enhanced permeability and retention* (EPR) effect, and on the physicochemical properties of the nanoparticles.

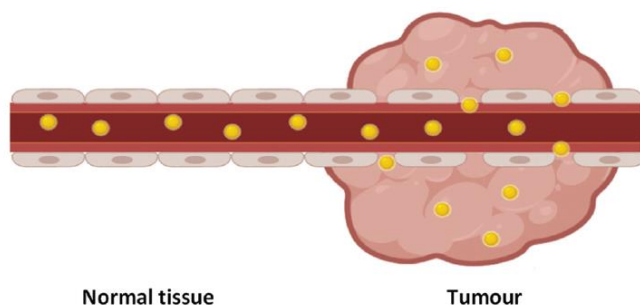


Figure 18. The passive targeting of NPs toward tumors through the EPR effect [65]

In particular, the EPR effect is based on the hyperpermeability of the tumor vessels, which allows particles to enter the tumor interstitial and, because of the absence of functional lymphatics in the tumor interiors, NPs can remain there for a long time. This mechanism is at the base of the NPs passive targeting (Figure 18) [64]. However, as the interest in personalised medicine has grown in recent years, the focus has turned towards the active targeting, which involves the attachment of a targeting moiety, that is specific toward a desired surface receptor, onto the nanoparticles surface. For cancer treatment, the targeting moiety that is usually used recognises a receptor that is overexpressed by tumor cells [65]. Nanoparticles have been mainly utilized in the design of anticancer therapies for carrying drugs into specific targets, containing molecules able to respond to endogenous and/or exogenous stimuli [55].

3.2 Curcumin-based nanosystems

One of the major risk factors for cancer is the inflammation: this represents the first response of the immune system to irritation or infection by microorganisms. Different treatments have been used to slow or limit the process of tissue damage that occurs in the inflammatory area such as non-steroidal anti-inflammatory drugs. However, their adverse effects, such as the severe complications of chemotherapy drugs, have intensified the explorations of natural anti-inflammatory agents with fewer side effects like *curcumin*, which is capable to inhibit cancerous cells proliferation [45][81]. Clinical trials have shown that curcumin is very promising for medication of pro-inflammatory chronic illness such as cancer because of its chemopreventive, antiproliferative, antiangiogenic and antimetastatic capabilities. In particular, the proapoptotic and antiangiogenic actions are mainly regulated by different cell signaling pathways, such as W_{nt}/β -catenin, PI3K/Akt, JAK/STAT, MAPK, p53, and NF- κ B [55]. Moreover, curcumin can affect cells signaling pathways to negatively affect cancer cells: indeed, it inhibits VEGF and suppresses VEGF receptor-2, fibroblast growth factor 2, matrix metalloproteinases 2 and 9, etc. [42].

Table 6. Effects of curcumin on cancerous processes observed on clinical trials [55]

Tumor type	Curcumin effect	Ref.
Breast	<ul style="list-style-type: none"> Improves physical performance 	[67]
	<ul style="list-style-type: none"> ↓ CEA (carcinoembryonic antigen) ↓ VEGF levels and antiangiogenic effect No change in CA15.3 (cancer antigen 15.3) 	[68]
Skin	<ul style="list-style-type: none"> Histologic improvements of precancerous lesions 	[66]
Lung	<ul style="list-style-type: none"> Improves the antitumor immunity 	[74]
Colorectal	<ul style="list-style-type: none"> ↓ 40% ACF (colorectal aberrant crypt foci) 	[70]
	<ul style="list-style-type: none"> ↓ M1G levels (DNA adduct 3-(2-deoxy-β-dierythro-pentafuranosyl)pyrimido[1,2-α]purin-10(3H)-one) ↓ 57-62% of inducible PGE2 (prostaglandin E2) 	[69]

	<ul style="list-style-type: none"> No change is COX-2 protein levels (enzyme cyclooxygenase-2) 	[71]
Pancreas	<ul style="list-style-type: none"> 1/25 patients: tumor regression (73%) ↓ COX-2 ↓ NF-κB (nuclear factor kappa B) ↓ pSTAT3 (phosphorylated signal transducer and activator of transcription 3) 	[72]
Multiple myeloma	<ul style="list-style-type: none"> ↓ COX-2 ↓ NF-κB ↓ pSTAT3 ↓ paraprotein levels 	[75] [76]
Prostate	<ul style="list-style-type: none"> Suppress PSA production (prostate specific antigen) 	[73]

Nanotechnology can improve the effect of conventional chemotherapeutic, for this reason, in order to maximize the beneficial health effects of curcumin, various approaches have been used to develop a drug delivery system of curcumin by using nanoparticles [55].

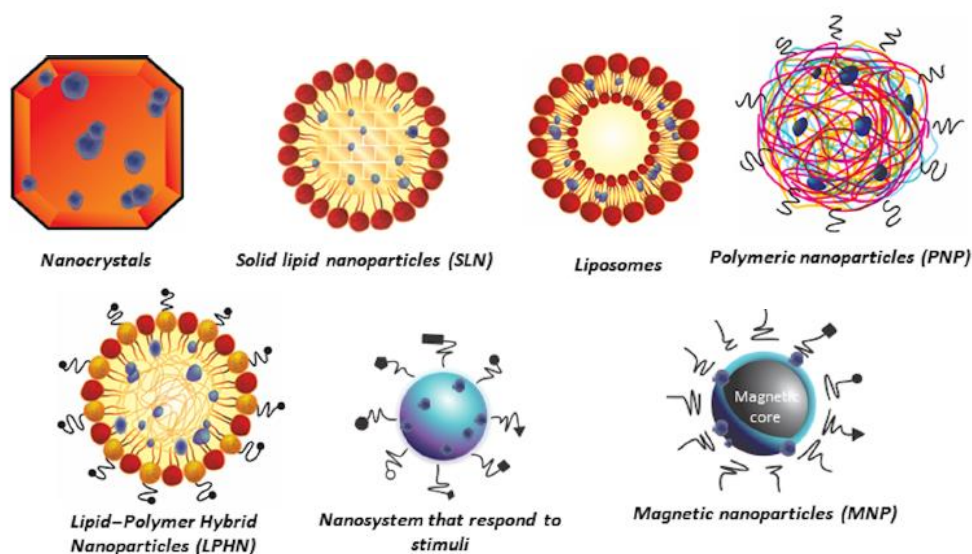


Figure 19. Curcumin-based nanosystems [55]

There are different kinds of nanosystems that can contain curcumin by themselves or in addition to another molecule, such as (Figure 19) [55]:

- a) **Nanocrystals**, crystalline materials containing the drug at the nanoscale with a size of 10-1000 nm;
- b) **Nanosuspension**, a colloidal dispersion of pure particles of a drug stabilized by surfactants;
- c) **Solid lipid NPs (SLN)**, containing crystalized solid lipid droplets with the drug of interest loaded into the solid lipid phase;
- d) **Liposomes**, self-assembled vesicles with at least one phospholipid bilayer with a size of 50-450 nm;
- e) **Polymeric NPs (PNP)**, solid colloids with the drug loaded in the polymeric matrix and with a size of up to 1000 nm;
- f) **Lipid-polymer hybrid NPs (LPHN)**, constituted by lipophilic and hydrophilic polymers with a high encapsulation efficacy and well-defined release kinetics;
- g) **Magnetic NPs (MNP)**, containing molecules capable to respond to magnetic fields.

The nanoparticles' size influences directly curcumin biodistribution, so the optimization of their size is necessary to obtain an increased organ concentration [55]. Furthermore, studies in literature have shown that these wide variety of NPs for curcumin delivery significantly reduced the tumor volume/weight, inhibited cancer cell proliferation, and increased tumor apoptosis and necrosis; moreover, they also allowed an increase in the toxicity of curcumin on the cancer cells without increasing its toxicity on the normal cells [80][81].

3.3 Magnetic NPs

MNPs are found to be of great interest for their potential as delivery system of therapeutic moiety to target tissue, such as tumors, where the compound of interest can be released. Moreover, magnetic nanoparticles can be used as contrast agent for magnetic resonance (MRI) and heat mediators for cancer therapy (hyperthermia) [12][55].

Delivery system for cancer therapy

MNPs represent the most efficient delivery system capable to act as carriers for all types of hydrophilic and hydrophobic drug molecules: this is possible thanks to their properties such as (a) high chemical stability, (b) biocompatibility, (c) higher colloidal stability, (d) retained superparamagnetic properties, (e) reduced adverse reaction of drugs, (f) sustained delivery to desired targeted site, and (g) low cost [12]. Some of the main advantages of nanosized drug administration are the improved pharmacokinetic profile, the higher selectivity towards tumor cells, and the increased cellular internalization [55]. Magnetic nanoparticles have been used to improve curcumin anticancer activity; this is a dual effect nanosystem capable to respond to external stimuli (alternating magnetic field) in addition to internal ones [55].

Hyperthermia for cancer therapy

Hyperthermia is a treatment that selectively destroys the tumor cell by increasing the tumor temperature to 42°C-45°C and it can be used in a synergistic way with other treatment such as radiotherapy or chemotherapy [12]. Compared with normal tissue blood vessels, tumor vascular variety has a lot of holes in the pipe wall, so the tumor tissue cooling ability is worse than normal tissue and the heat produced is more likely to accumulate within the tumor rather than normal tissues. Moreover, tumor cells are less heat-resistant than normal cells because of their low concentration of oxygen along with low pH [12][22]. MNPs are employed to generate heat in the tumor tissue: an alternating current magnetic field of sufficient strength and frequency is applied, causing the particles to heat: this is called internal hyperthermia since the heat is applied from inside the body [17]. The heat produced by MNPs depends on the combination of particles diameter and size distribution and on the amplitude and frequency of the alternating magnetic field. The use of magnetic mediators for cancer hyperthermia therapy appears to be very promising because of their temperature homogeneity and their magnetic properties: indeed, MNPs can be used for purposes prior to heating distribution in tissues such as for drug delivery or MRI. Despite the increasing number of researches in this field, the clinical implications of MNPs for cancer hyperthermia treatment has not been established yet; this is mainly due to the poor site specificity and low controlled heat distribution within the tumor related to the current techniques. To date, MNPs have been mostly used in pre-clinical trials because they show low toxicity, and their metabolic pathway is

known [17]. The nowadays main challenge is to design stealth NPs with grafting on the surface ligands able to facilitate their specific internalization in tumor cells.

Magnetic Resonance Imaging for cancer diagnosis

MRI is based on the response that is produced by the spin of protons after the application of magnetic field. By applying the magnetic field, indeed, all protons are aligned and when a radio frequency pulse is applied, the associated protons are disturbed and then relaxed to original state. To produce the MR image, two self-determining relaxation processes are utilized: transverse relaxation (T2-decay) and longitudinal relaxation (T1-recovery). MNPs are T2 contrast agents. Moreover, thanks to their shape and greater surface area, along with increased blood half-life, they enhance the relaxivity for MRI [12].

3.3.1 MNPs applications for tumor treatments

Brain Tumor

Abakumov et al. [63] synthesize MNPs as magnetic resonance imaging (MRI) agents for *in vivo* visualization of gliomas. Gliomas represent the 80% of all malignant brain tumors and are characterized by fast progression; due to current diagnosis limitation, surgery is often performed in advanced stage of disease when the tumor has already extended into the surrounding tissues. Nowadays, MRI is one of the leading methods for diagnosis of brain tumors. High-grade gliomas lead to the secretion of pro-angiogenic factors, such as the vascular endothelial growth factor (VEGF), resulting in a growth of blood vessels within the tumor. Moreover, the progression of the tumor is associated with the increased leakiness and permeability of the blood-brain barrier (BBB). These elements together facilitate the penetration of nanoparticles into interstitial space resulting in a successful penetration and retention of nanoparticles, which have been modified with antibodies against tumor-specific or endothelium-specific antigens. The core is made of ferric oxide (Fe_3O_4), prepared by thermal decomposition method and then coated with bovine serum albumin (BSA), which has been covalently conjugated with monoclonal antibodies against vascular endothelial growth factor (mAbVEGF). The obtained nanoparticles size is of 53 ± 9 nm and the result showed that:

- (a) they are stable and non-toxic to various cells with concentration range up to 2.5 mg/mL
- (b) the VEGF targeted MNPs efficiently bound to the VEGF-positive glioma C6 cells *in vitro*
- (c) they are successful contrast agents

Lung cancer

Lung cancer is the main cause of cancer patient death in the world, and it can be divided into small cell carcinoma (10-15%) and non-small cell carcinoma (85-90%). Despite significant progress has been made in the diagnosis and treatment of this type of cancer, the prognosis results to be still unsatisfactory.

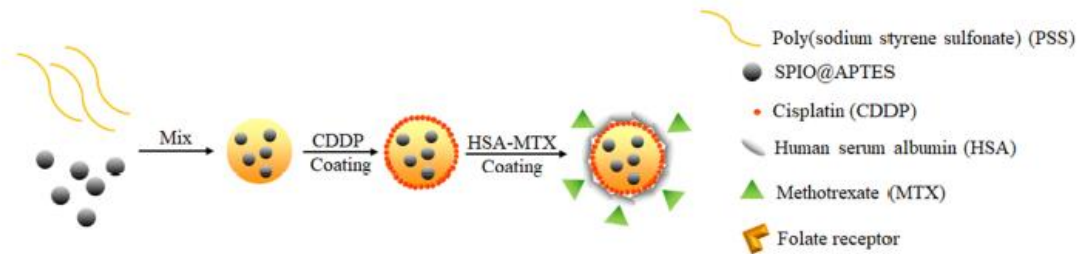


Figure 20. SPIO@PSS/CDDP/HSA-MTX NPS for lung cancer treatment

Yang *et al.* [62] developed a magnetite-based nanomedicine that serves a dual purpose in hyperthermia and chemotherapy for lung cancer treatment with the aim to overcome the problems of traditional chemotherapy. The complex is made of superparamagnetic iron oxide (SPIO) and poly(sodium styrene sulfonate)(PSS) at the core that can be used as a hyperthermia inducer to improve cancer treatment by using a radiofrequency generator (RF); there is also a layer-by-layer shell with cisplatin (CDDP) and methotrexate-human serum albumin (MTX-HSA) conjugate for lung cancer-specific targeting (Figure 21). CDDP is a chemotherapeutic drug, the HSA coating increases the compatibility and half-life of NPs in the blood while MTX conjugation increases the nanoparticles' ability to target the tumor biomarker and acts as a therapeutic agent.

The obtained nanoparticles showed:

- (a) excellent stability in saline solution

- (b) higher temperature increase rate when exposed to RF with respect to SPIO with APTES NPs
- (c) MTX-HSA coating enhanced the cellular uptake of the NPs and improved the combined effect of hyperthermia with chemotherapy on cancer cells.

These multifunctional nanoparticles were applied during combined chemotherapy-hyperthermia therapy and exhibit a higher anticancer effect than monotherapy, making them powerful candidate for future antitumor therapeutic strategies.

3.3.2 Curcumin-magnetite NPs applications for tumor treatments

Curcumin-loaded MNPs had a significantly improved pharmacokinetics in serum with respect to curcumin alone and, depending on their route of administration and on the type of tumor, their accumulations rate changes. For example, the intratumoral route shows a higher accumulation rate in the liver rather than brain or spleen, while the intraperitoneally route shows a higher accumulation in the spleen [55].

Breast cancer

Amongst different types of cancers, breast cancer is known to be the leading cause of mortality in women with around 450,000 deaths around the world [79]. The majority of breast cancers are referred to as triple-negative breast cancers because they do not over express estrogen receptor, progesterone receptor, or human epidermal growth factor receptor 2. One example of a triple-negative breast cancer cells is MDA-MB-231 which are highly metastatic in nature: *Yallapu et al.* [53] developed a curcumin-loaded MNP assayed against these cancer cells, composed by iron oxide and β -cyclodextrin and coated with Pluronic F68 polymer (polyethylene oxide-co-polypropylene oxide-co-polyethylene oxide) that allows loading of anticancer drugs (curcumin). The results showed that this formulation is extremely valuable in anticancer therapeutics since it exhibits improved uptake in cancer cells, increased loss of mitochondrial membrane potential, and produces higher ROS. Moreover, this formulation proved to be a good imaging agent and the magnetic targeting of MNP-CUR enhanced the delivery of CUR to cancer cells.

Brain tumor

Cui et al. [77] achieved active targeting by combining magnetic guidance and transferrin receptor-binding peptide T7, obtaining a dual targeting structure that is able to cross the blood-brain barrier and to target brain tumor. The magnetic PLGA nanoparticulate system was prepared with a “one-pot” method by a single-emulsion solvent evaporation method, where the hydrophobic magnetic nanoparticles were entrapped into the PLGA NPs. This system has the capability to co-encapsulate a combination of drugs, such as paclitaxel and curcumin, which allowed to obtain a synergistic effect on the inhibition of tumor growth. The results showed that the MNP/T7-PLGA NPs can efficiently penetrate the BBB and increase the brain delivery efficacy and that, together with the synergistic mechanism of PTX and CUR, it exhibited improved glioma therapy efficacy with reduced adverse toxicities.

Pancreatic cancer

Pancreatic cancer is ranked fourth in causing cancer-related deaths in United States in fact, despite significant progress in the cancer therapeutics, most cases still remain largely untreatable with a poor 5-years survival rate. *Yallapu et al.* [78] reported for the first time the effects of a novel MNP-CUR formulations on human pancreatic cancer cells (HPAF-II and Panc-1 human pancreatic cell lines). The MNP-CUR system was formulated with $\text{Fe}^{3+}:\text{Fe}^{2+}$ salts, cyclodextrin and Pluronic F-12 and then loaded with curcumin. The result showed a dose-dependent uptake of MNP-CUR formulation in both cell lines, obtaining an effective internalization in pancreatic cancer cells, and a dose-dependent inhibition of cell proliferation. Finally, MNP-CUR treatment successfully suppressed tumor growth and it also increased the survival rate of animals in a pancreatic cancer xenograft mouse model.

In table 7, some of the studies present in literature are summarized.

Table 7. Examples of magnetic nanoparticles for tumor application

Tumor type	Treatment type	NP's type	NPs' role	Treatment goal	Targeting method	Ref.
Breast cancer	Drug delivery and MRI (theranostic)	CUR-MNPs	Drug carrier and contrast agent	Targeting, treatment and visualization of triple-negative breast cancer cells (MDA-MB-231)	Magnetic-guidance targeting	[53]
Lung cancer	Hyperthermia (therapy)	MNPs	Heat mediator	Solving the problems of traditional chemotherapy by the synergistic application of local hyperthermia with chemotherapy	SPIONPs with LbL-coating with <u>MTX</u> to target the tumor biomarker	[62]

Brain tumor	MRI (diagnosis)	MNPs	Contrast agent	Visualization of gliomas	MNPs with antibodies against vascular endothelial growth factor (<u>mAbVEGF</u>)	[63]
Brain tumor	Drug delivery (therapy)	CUR-MNPs	Drug carrier	Co-delivery of paclitaxel (PTX) and CUR	Ligand-mediated (human transferrin receptor-binding peptide T7) and magnetic-mediated targeting	[77]
Pancreatic cancer	Drug delivery (therapy)	CUR-MNPs	Drug carrier	Antitumor treatment of MNP-CUR formulation	EPR effect (passive targeting)	[78]
Liver cancer	Drug delivery and hyperthermia (therapy)	M-MSN-CUR	Drug carrier and heat mediator	Targeting and treatment through chemotherapy with hyperthermia	Magnetic-guidance targeting	[82]

3.4 Gold NPs

Gold NPs have been widely used in for the diagnosis and treatment of tumor because of their special fundamental properties such as their large surface-to-volume ration, small size, stability over high temperature and high reactivity to living cells [87]. A number of studies have shown that Au NPs conjugated with antibodies are efficient in targeting and destroying cancerous tissue by conversion of near-infrared irradiation to heat [85]. They can be also used as contrast agents in multimodal imaging, carriers in drug delivery and enhancers in cancer therapy.

Targeting and drug delivery

Active targeting can be formed by Au NPs, like the tumor cell targeting. In these applications, Au NPs are engineered for active binding to specific cells, where the selective binding is obtained by functionalizing NPs' surface with biomolecules that can be recognized by cancerous cells and bind them, such as Lam 67R and GRP human prostate tumors, and CCR5 and HER2 for breast tumors. Moreover, Au NPs can be combined with chemotherapy drugs (such as mitoxantrone MTX, doxorubicin DOX, etc.) through electrostatic adsorption or covalent bonds on the surface, making them the most promising delivery system for tumor targeting [22][86]. Cell-specific targeting molecules can also be attached on the drug-loaded Au NPs complexes in order to deliver the drug to specific tumoral cells, combining active targeting with drug delivery.

Photothermal therapy

Plasmonic photothermal therapy (PPTT) is based on the main property of Au NPs to absorb near-infrared light (NIR) very efficiently and convert light energy into kinetic energy, expressed in the form of heat (photothermal conversion) [22]. This therapy represents a minimally invasive oncological treatment strategy which main goal is to induce cellular *hyperthermia* by using a laser with a spectral range of 650-900 nm for deep tissue penetration. Indeed, NPs are embedded within the tumor and generate heat in response to laser application; consequently, the cancer cells are subject to temperature in the range of 41°C–45°C for tens of minutes are destroyed by the induced hyperthermia. Its selectivity depends on the direction of the incident radiation, the type of laser (pulsed or continuous wave) and the type of administration of nanoparticles. Through laser

exposure and plasmon absorption in the NIR, the PPTT can be used also for the treatment of deep tissue malignancies: indeed, the absorption of NIR radiation in tissues is generally much less than that of visible light, thus NIR radiation results to be optimal for the treatment of deep tissues [84][87][93]. Moreover, PTT can be used in combination with other therapy like radio therapy, in order to reduce the dose of antitumor irradiation needed and enhance therapeutic effects [86].

Photodynamic therapy

Photodynamic therapy (PDT) is based on the use of a light stimulating photosensitive molecules, which absorb the energy of the photons and interact with oxygen; that leads to the formation of reactive species, which increase cytotoxicity, immunostimulation and regulate tumor vascularity, which lead to the destruction of the cancerous area. This is a clinical treatment where tumor cells are killed by the combination of light and a photosensitizer (PS) [86]. The effectiveness of phototherapy against cancer cells depends on different elements such as the photoactive agent, wavelength, time of exposure and the distance to the light. While PTT is independent, PDT is dependent entirely on the oxidative nature of ROS [88]. The combined use of curcumin in photodynamic therapy has been studied, showing an efficient apoptosis-promoting effect as a result of the increased nuclear fragmentation and ROS generation [55].

Imaging

Au NPs have been widely used for tumor diagnosis purposes because of their strong tunable SPR that can be detected using multiple imaging modalities and their ability to passively accumulate on tumor cells. Thanks to their capabilities of producing photoacoustic signal and their optical properties, Au NPs are considered very valuable in medical imaging. Furthermore, they are considered highly attractive contrast agent for X-ray-based computed tomography imaging [87].

3.4.1 Gold NPs applications for tumor treatments

Breast cancer

Stuchinskaya et al. [85] obtained a 4-component antibody-phthalocyanine-polyethylene glycol-gold nanoparticle conjugate for targeted photodynamic cancer therapy. A

hydrophobic photosensitizer (PS) with anti-HER2 monoclonal antibodies were covalently bound to the nanoparticles surface in order to selectively target breast cancer cells that overexpress the HER2 epidermal growth factor surface receptor and then to photodynamically destroy them. The *in vitro* results showed that the targeting capability of the nanoconjugates enhances the efficacy of PDT cell death, demonstrating their great potential for targeted photodynamic therapy.

Liver cancer

Liver cancer has become one of the most common malignancies and a highly fatal disease in the world. Existing chemotherapy is unsatisfactory due to its severe systemic toxicity and intrinsic drug resistance. For this reason, it is urgent to seek new agents for highly efficient and safe treatment of liver cancer. *Li et al.* [89] prepared nanoprobe formed by self-assembly of ultra-small gold NPs coupled with matrix metalloproteinase-2 (MMP2) on the surface and loaded with photosensitive drug IR820 for dual-mode imaging-guided photodynamic/photothermal combination therapy for liver cancer. The results showed that, thanks to the presence of MMP-2, the nanosystems presented excellent tumor-targeting properties in both T₁ MRI and *in vivo* fluorescence imaging modes. They also showed a satisfactory photodynamic/photothermal combination therapy effect, demonstrating a great potential for future clinical application.

3.4.2 Curcumin-gold NPs applications for tumor treatments

Breast cancer

Rahimi-Moghaddam et al. [83] synthesized Au NPs with curcumin (Au-CUR) and reported their therapeutic effects on 4T1 breast cancer cells. Gold nanoparticles were obtained through a chemical method: the conjugation was obtained by dissolving HAuCl₄ in deionized water, while curcumin in polyethylene glycol was added dropwise to the Au solution. Here, curcumin was used as a stabilizer and a reducing agent for Au ions during the Au-CUR NPs synthesis. An 808-nm diode laser at a power density of 1.5 W/cm² was used to irradiate the synthesized nanostructures for photothermal treatment on 4T1 cells and the results revealed that Au-CUR nanoparticles had more cytotoxicity effect on breast cancer cell lines under the laser irradiation: in fact, only the 40% of cells were alive after PTT treatment.

Prostate cancer

Nambiar et al. [90] obtained gold nanoparticles using curcumin as reducing and stabilizing agent in order to evaluate cytotoxicity, uptake, and localization in human prostate cancer PC-3 cultured in cell medium supplemented with and without fetal bovine serum (FBS). Results exhibited a decreased cytotoxicity of Au-CUR NPs in PC-3 cells, hence the therapeutic efficacy of the curcumin coating, in the presence of serum protein due to a lower uptake of nanoparticles; on the contrary, in the absence of serum protein, there was an increased accumulation of Au-CUR NPs on the cell surface.

In table 8, some of the researches present in literature are summarized:

Table 8. Examples of gold nanoparticles for tumor application

Tumor type	Treatment type	NP's type	NPs' role	Treatment goal	Targeting method	Ref.
Breast cancer	Targeted PDT (therapy)	Au NPs	PS carrier	Targeting and treatment of breast cancer cells overexpressing HER2 cell surface receptor	Au NPs covalently bound to anti-HER2 monoclonal antibodies	[85]
Liver cancer	Imaging and targeted PDT (theranostic)	Au NPs	PS carrier	Targeting, visualization and treatment of liver cancer	Au-CUR NPs coated with MMP2	[89]
Breast cancer	PTT (therapy)	Au-CUR NPs	Photo-thermo conversion agent	Treatment of 4T1 breast cancer cells	-	[83]

Prostate cancer	Drug delivery	Au-CUR NPs	Drug carrier	Evaluate Au-CUR NPs cytotoxicity for cancer treatment	-	[90]
-----------------	---------------	-------------------	--------------	---	---	------

3.5 Magnetic-plasmonic nanoparticles

In the past decade, different approaches for designing and synthesizing nanoparticles with multifunctional characteristics have been studied in order to overcome limits in a wide range of technological applications. Indeed, the integration of nanomaterials with different properties (such as magnetization, fluoresce and NIR absorption) into a single object of nanoscale dimension can lead to the development of multifunctional NPs for simultaneous targeting, imaging, and therapy administration.

3.5.1 Synthesis

The main synthesis methods are: (a) heterogeneous crystal growth, (b) co-assembly of different block, and (c) template-based method which involves chemical and/or physical binding [91][92]. Among all the multifunctional NPs, magnetic-plasmonic (MP) NPs have received considerable attention: indeed, they are considered the most suitable MP NPs for biomedical applications because they simultaneously exhibit magnetic and surface-enhanced Raman scattering (SERS) activities [91]. However, it is difficult to synthesize NPs for high performances in bio-applications, thus new strategies need to be found. For example, *Kim et al.* proposed a method for synthesizing plasmonic nanostructures involving the conjugation of a magnetic template with gold seeds via chemical binding and seed-mediated growth. The goal was to obtain plasmonic nanostructures with abundant hotspots on a magnetic template. The method was based on four steps: (a) conjugation of Fe₃O₄-SiO₂ core-shell NPs with Au seeds, (b) seed-mediated growth of Au seeds, (c) functionalization of Raman molecules, and (d) second

growth with Au and/or Ag precursors. Finally, cRGDyK-functionalized MP NP assemblies were used for targeted cancer-cell imaging and cell separation under the external magnetic field [91].

3.5.2 Applications in biomedicine

The SPIO nanoparticles modified with tumor-targeting ligands have been used as *in vivo* MRI contrast agents and to induce cell apoptosis via hyperthermia, while NPs conjugated to cancer targeting agents have been used for site specific delivery and therapeutics [92]. *Kim et al.* reported multifunctional nanoparticles that exhibit both magnetic and optical properties for diagnostic imaging (MRI) and simultaneous treatment (targeted photothermal therapy) in breast cancer treatment. They synthesized magnetic gold nanoshells (Mag-GNS) consisting of gold nanoshells surrounding magnetic Fe_3O_4 nanoparticles and conjugated with a cancer-targeting agent: in this synthesis method, the magnetite nanoparticles and gold seed nanoparticles were assembled on amino-modified silica spheres (Figure 20).

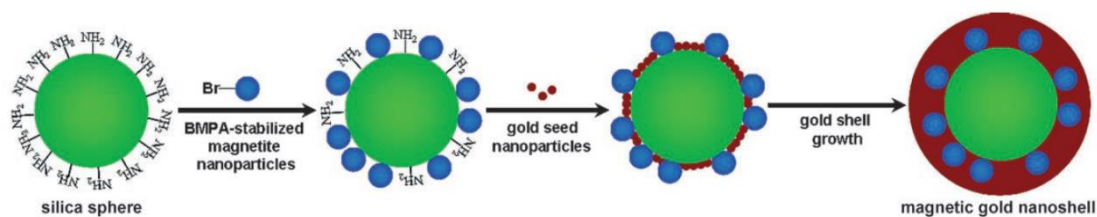


Figure 21. Synthesis of Mag-GNS [93]

For targeted MRI and NIR photothermal therapy, the antibody anti-HER2/*neu* ($\text{Ab}_{\text{HER2}/\text{neu}}$) has been conjugated onto the surface of the Mag-GNS to target HER2/*neu* receptors of the *breast cancer* cells (SKBR3). The final nanosystem was exposed to the NIR laser and cells death was observed. Finally, the cancer cells targeted by these nanostructures was detected by a clinical MRI system and killed as a result of the local heating generated by the absorption of NIR radiation by the Mag-GNS- $\text{Ab}_{\text{HER2}/\text{neu}}$ [93]. Also, *Kirui et al.* reported a novel dumbbell-like nanoparticles having both magnetic and optical properties for targeting, imaging (MRI and fluorescence) and laser photothermal therapy of cancer cells. The hybrid NPs have been conjugated with A33scFv single chain antibody to target A33 antigen that is over-expressed on the surface of SW1222 *colorectal cancer* cells. The results showed that the presence of the targeting antibody facilitated the

cellular particle uptake and that the nanoparticles conjugates can be considered potential multifunctional probes for cancer diagnosis and therapy [92].

In 2015, *Huang et al.* proposed $\gamma\text{Fe}_2\text{O}_3@\text{Au}$ magnetic gold nanoflower-mediated NIR photothermal cancer theragnostic. It exhibited good spatial resolution in MR imaging for precise tumor localization and high-resolution photo acoustics imaging, and it efficiently ablated tumors under NIR irradiation [88][95].

Finally, a multifunctional poly(amino acid)-gold-magnetic complex with self-degradation property has been reported by *Ma et al.*: their goal was to obtain a hybrid nanostructure for multimodal imaging-guided synergistic chemo-photothermal therapy in cancer treatment *via* simple and green chemistry. This complex has shown the ability of multimodal imaging and efficient tumor ablation with the anti-tumor rate of 94%, showing the possibility to use them as a biodegradable nanotherapeutic for clinical applications [94].

Chapter 4

Materials and methods

The engineering and synthesis of nanoparticles with multifunctional characteristics are important for overcoming limits of different biomedical applications. The aim of this study is to develop nanosystems containing both gold and magnetite nanoparticles for tumour treatment, using curcumin biomolecule as a novel reducing and stabilizing agent for the green synthesis. In particular, this chapter describes different synthesis methods tested during the experimental work and the techniques used to characterize the obtained nanoparticles and to evaluate their properties.

4.1 Synthesis and functionalization methods

The main steps that have been explored in this experimental work are:

- Synthesis of gold nanoparticles mediated by curcumin biomolecule
- Functionalization of magnetite nanoparticles with APTES or CA and with curcumin
- Conjugation of gold and magnetite nanoparticles using curcumin biomolecule.

4.1.1 Magnetite nanoparticles

Magnetite nanoparticles (MNPs) have been synthesized through a well-known process present in literature based on the co-precipitation of iron salts in aqueous medium. Then, two functionalization routes have been performed:

- In route 1 the obtained magnetite nanoparticles have been functionalized with the (3-aminopropyl) triethoxysilane (APTES);
- In route 2 magnetite nanoparticles have been functionalized with citric acid (CA).

Finally, both nanoparticles obtained by the two routes were functionalized with curcumin.

Magnetite nanoparticles synthesis. For the synthesis of superparamagnetic iron oxide nanoparticles, the co-precipitation method in aqueous medium of Fe^{2+} and Fe^{3+} salts were used.

1.02 g of $\text{FeCl}_2 \cdot 4\text{H}_2\text{O}$ (0.1 M) and 1.3 g of $\text{FeCl}_3 \cdot 6\text{H}_2\text{O}$ (0.1 M) were dissolved in 50 ml of bi-distilled water, obtaining two different 0.1 M solutions, then magnetic stirring has been performed for each suspension to achieve the complete dissolution of the salts. Afterward, 37.5 ml of the aqueous FeCl_2 solution were added to 50 ml of aqueous FeCl_3 solution, the mixed solution had a pH=1.9. To induce the magnetite formation, the pH value was increased till the achievement of the range 9.5-10 by adding dropwise NH_4OH (ammonia) to the solution keeping it under mechanical stirring; the reaction mixture turned black, indicating the formation of a suspension of iron oxide NPs. During synthesis process, the colour of the iron solution changed from yellow-brown-black (Figure 22). The solution was then sonicated for 20 minutes (SONICA® Ultrasonic Cleaner) and washed two times using bi-distilled water to remove the unreacted compounds. Finally, the MNPs have been resuspended in 100 ml of bi-distilled water. The final solution had a pH value of 8.9 and a nanoparticle averaged concentration of 9 mg/ml.

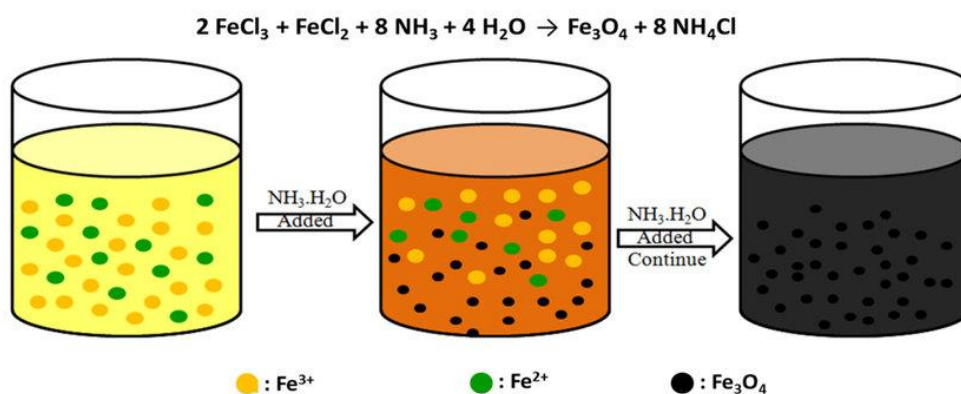


Figure 22. Synthesis of Fe_3O_4 nanoparticles by ex-situ co-precipitation method [96]

Route 1

Functionalization with APTES

The main aim of the functionalization of the MNPs with APTES is to decorate their surface with silanol groups, which allow the binding of curcumin. Furthermore, APTES acts as a stabilizer for nanoparticles in suspension [97].

1110 μl of the SPIONs suspension (9 mg/ml) have been diluted in a solution of 1:1 bi-distilled water and ethanol, obtaining a final volume of 400 ml. The prepared suspension was mixed with a 20 ml of APTES (2% v/v) solution and stirred in thermal bath at 50°C for 24 hours in order to successfully introduce terminal amino ($-\text{NH}_2$) groups on the particles surface. Finally, the solution has been washed two times with ethanol.

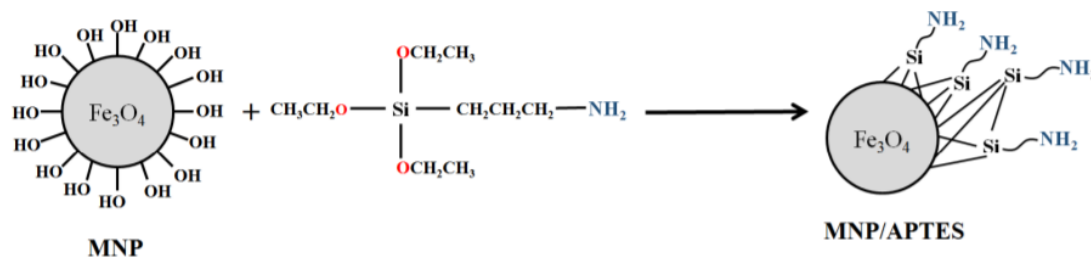


Figure 23. Magnetic nanoparticle (MNPs) functionalization with APTES [98]

This route was repeated one more time with the aim to optimize the results by varying the amount of the SPIONs suspension (5,5 ml) and the quantity of the solvent (1:1 bi-distilled water and ethanol for a final volume of 200 ml).

Only the functionalized nanoparticles obtained through the second approach, by increasing the amount of SPIONs and halving the amount of solvent, had been implemented for the functionalization with curcumin in order to have a higher concentration of NPs into the solution. A schematic resume is reported below.

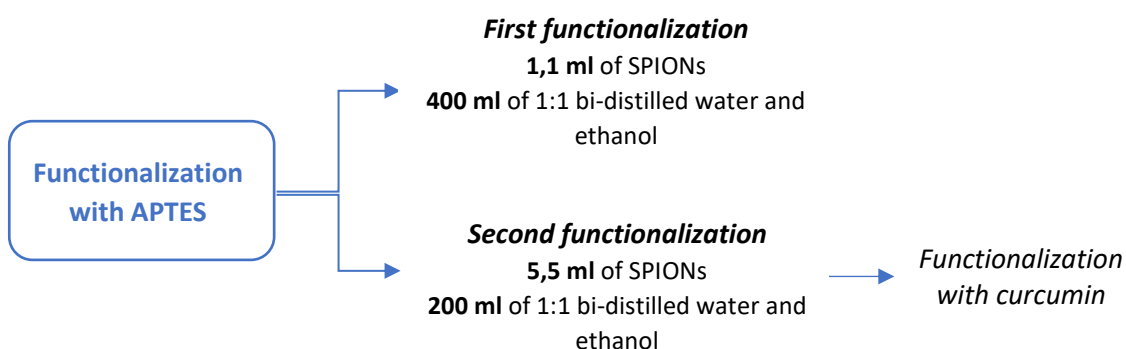


Figure 24. Scheme of the functionalization with APTES of MNPs

Functionalization with curcumin

The second approach for functionalizing MNPs with APTES has been used for the further grafting of the curcumin.

The APTES functionalized MNPs were resuspended in 25 ml of ethanol in order to obtain a particles concentration of 2 mg/ml. Only 20 ml of APTES functionalized MNPs solution has been used for the curcumin functionalization by dissolving 2 mg of curcumin in it. Then it was left under mechanical stirring overnight and finally, the solution has been washed two times with ethanol and resuspended in 10 ml of bi-distilled water. In literature [97] has been reported the reaction mechanism between APTES and curcumin: the APTES terminal NH₂ group binds with the OH group of the curcumin phenolic moiety with the elimination of water (Figure 25).

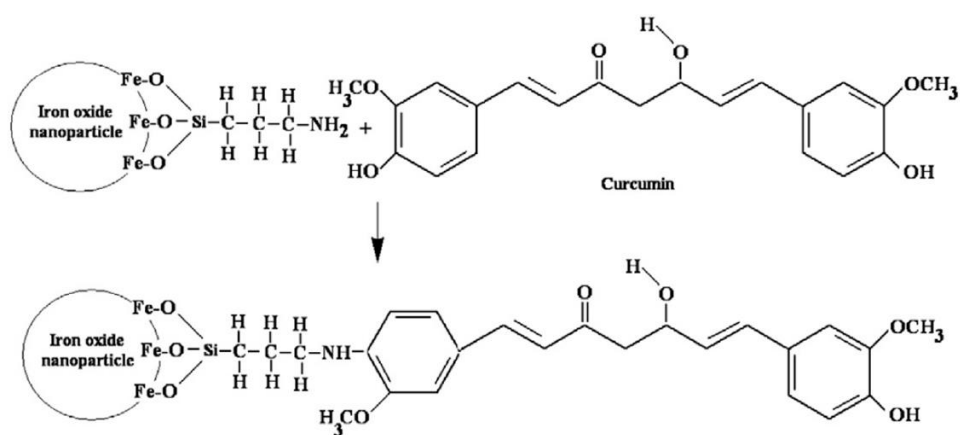


Figure 25. Curcumin binding on APTES coted MNPs [97]

The functionalization with curcumin was performed a second time by changing the amount of curcumin and resuspending the MNPs in two solutions with the aim to optimize the obtained results: the first one contained 12,5 ml of ethanol and the second one 12,5 ml of bi-distilled water. Here the amount of curcumin has been proportionally doubled: 2,5 mg of curcumin were dissolved into each solution. Then the two solutions were left under mechanical stirring overnight and washed two times respectively with water and ethanol.

Both functionalization with curcumin have been used for the next steps. Below is a schematic resume of the main MNPs functionalization steps.

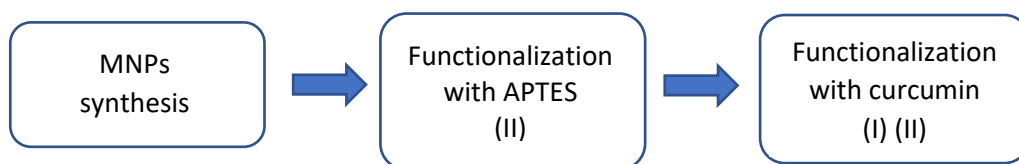


Figure 26. Main magnetic nanoparticle functionalization steps (route 1)

Route 2

Functionalization with citric acid

MNPs functionalized with citric acid were used. In literature [99] it has been shown that the citric acid (CA) is able to improve MNPs suspension stability: higher repulsive interactions between magnetite nanoparticles were achieved, preventing both their aggregation and the formation of clusters. 50 ml of the SPIONs suspension (9 mg/ml) were separated from most of the water by sedimentation using a magnet; then 60 ml of 0,05 M citric acid solution was added, and the pH of the solution was adjusted to about 5,2 by adding NH_4OH dropwise. The suspension was left under mechanical stirring for 90 minutes at the temperature of 80 °C, and afterwards, the obtained functionalized nanoparticles were washed three times with bi-distilled water through an ultrafiltration device. Finally, they were resuspended in 60 ml of water and their pH was adjusted to 10,2 by adding ammonia.

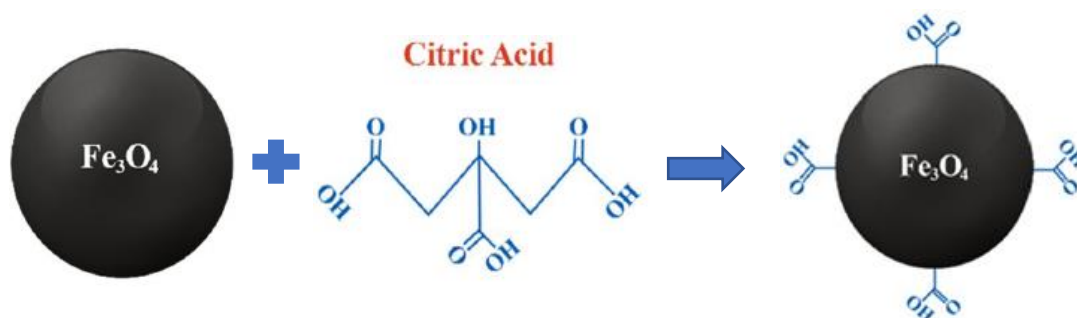


Figure 27. CA functionalization of MNPs [100]

Functionalization with curcumin

6 ml of the CA functionalized MNPs (5,7 mg/ml) suspension have been mixed with a solution made of 2 mg of curcumin dissolved in 12 ml of ethanol. The pH of the obtained solution was 8,9. Then it was left under mechanical stirring overnight. Finally, the solution has been washed with ethanol to remove excess of curcumin and with bi-distilled water to ensure the complete removal of ethanol from the sample and resuspended in 10 ml of bi-distilled water.

Kitture et al. [101] reported the CA conjugation to the curcumin central enol OH group (Figure 28).

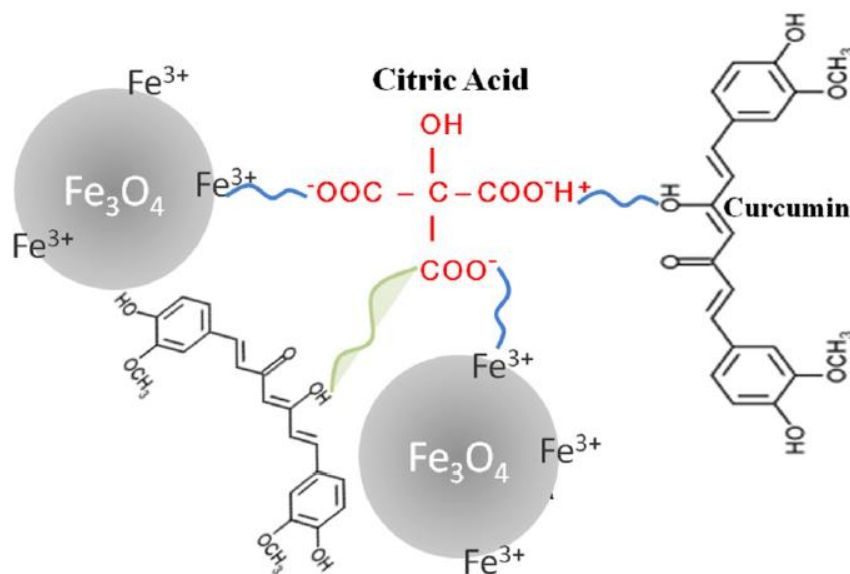


Figure 28. Curcumin binding to CA functionalized MNPs [101]

The functionalization with curcumin has been repeated two more times: the first time the amount of curcumin has been doubled (4 mg); the second time all the quantities have been increased proportionally: the amount of curcumin (10 mg), of ethanol (30 ml) and of CA-MNPs suspension (15 ml).

All the three functionalization have been used then for further functionalization. Below is a schematic resume of the main MNPs functionalization steps.

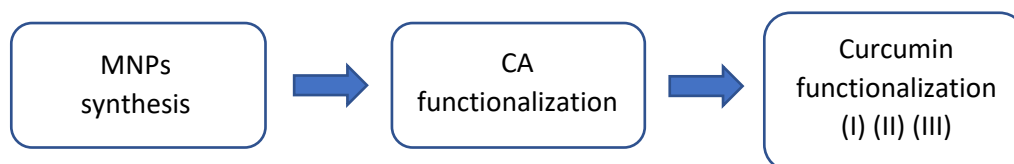


Figure 29. Main magnetic nanoparticle functionalization steps (route 2)

4.1.2 Gold nanoparticles

Gold nanoparticles synthesis. Gold nanoparticles have been obtained by using curcumin biomolecule as a reducing agent for the synthesis.

A solution was prepared by adding 3.68 mg of curcumin to 2 ml of NaOH (10 mM) causing a change in color that turned red. Then the volume was made up to 10 ml with bi-distilled water and the suspension was left under magnetic stirring for few minutes to help curcumin dissolution. Afterwards, 1 ml of the obtained curcumin solution was added

dropwise to the aqueous solution made of 1 ml of H₂AuCl₄ (1 mM) and 8 ml of bi-distilled water. Finally, the solution was left under mechanical stirring for 2 hours.

4.1.3 Gold-magnetite nanoconjugates

The aim of this work is to obtain magnetic-gold nanostructures by using curcumin biomolecule. In the chapter 1, the magnetic-plasmonic heterodimers have been divided in two categories according to their structure: (1) AFNSs and (2) FANSs. Thus, two different synthesis methods have been explored in order to obtain the gold-magnetite conjugation starting from the synthesis of curcumin functionalized MNPs (FANSs) and the curcumin-mediated synthesis of Au NPs (AFNSs).

- **First synthesis (AFNSs):** starting from Au NPs, MNPs (functionalized with CA) were grafted on their surface
- **Second synthesis (FANSs):** starting from MNPs (functionalized with APTES or CA), Au NPs were reduced on their surface.

First synthesis

The curcumin-mediated synthesis of AuNPs was followed by the CA-MNPs (obtained during the first synthesis) grafting on their surface in order to obtain hybrid nanoconjugates composed by a gold core surrounded by a Fe₃O₄ surface coating. Only 5 ml of the previously obtained Au solution was used and mixed with 100 µl of citric acid functionalized MNPs suspension and left under mechanical stirring for 2 hours. Then, the final solution has been divided in two solutions of 2,5 ml. At last, their pH has been modified achieving pH 4 for the first solution and pH 11 for the second solution.



Figure 30. Gold-magnetite nanoparticles: first synthesis steps

Second synthesis

The synthesis of MNPs with curcumin and APTES (route 1), or CA (route 2), was followed by the reduction of AuNPs on their surface in order to obtain hybrid nanoconjugates composed by a Fe₃O₄ core and an Au surface coating.

Gold-magnetite nanoconjugates with APTES

According to the two functionalization with curcumin of the route 1, two syntheses have been tried out:

- (a) 10 ml of APTES-Fe₃O₄ nanoparticles functionalized with curcumin suspension obtained through the first functionalization approach (I) were mixed with a solution containing 4 mg of HAuCl₄ dissolved in 10 ml of bi-distilled water. Then, the obtained solution was left under mechanical stirring for 4 hours and finally washed two times with bi-distilled water.
- (b) Two solutions of 12,5 ml each of APTES-Fe₃O₄ nanoparticles functionalized with curcumin suspended respectively in water and ethanol and obtained through the second functionalization approach (II) are considered. Two solutions made of 4 mg of HAuCl₄ dissolved in 10 ml of bi-distilled water were prepared: one solution was mixed with 12,5 ml of nanoparticles suspension in water and the other solution was mixed with 12,5 ml of nanoparticles suspension in ethanol. The pH of each solution was of ~3 and it has been increased by adding dropwise NH₄OH until reaching a basic pH (~9). Then the solutions were left under mechanical stirring overnight and washed two times respectively with bi-distilled water or ethanol.

A third functionalization approach was then performed without resuspending the nanoparticles suspension in two different solutions but resuspending nanoparticles in 25 ml of water. Only 20 ml of NPs solution was then used for obtained the gold-magnetite nanoparticles by increasing proportionally the quantity of HAuCl₄ and of bi-distilled water and by increasing the pH of the final solution. The obtained nanostructures were used then for the thermal and magnetic characterization.

Gold-magnetite nanoconjugates with citric acid

Considering to the three functionalization with curcumin of route 2, three combinations have been performed:

- (a) 10 ml of CA-Fe₃O₄ nanoparticles functionalized with curcumin suspension obtained through the first functionalization (I) were mixed with a solution made of 4 mg of HAuCl₄ dissolved in 10 ml of bi-distilled water. The final solution was

left under mechanical stirring for 4 hours and then washed two times with ethanol and bi-distilled water. Finally, it was resuspended in water.

- (b) 13 ml of CA-Fe₃O₄ nanoparticles functionalized with curcumin suspended in water and obtained through the second functionalization (II) was mixed with a solution containing 5,2 mg of HAuCl₄ dissolved in 13 ml of bi-distilled water. The pH of the solution was acidic, and it has been increased by adding dropwise NH₄OH until reaching a basic value (~8). In the end, the solution was left under mechanical stirring overnight, washed two times with ethanol and bi-distilled water and resuspended in water.
- (c) 45 ml of the nanoparticles suspension functionalized with curcumin obtained through the third functionalization (III) was mixed with 18 mg of HAuCl₄ dissolved in 45 ml of bi-distilled water. After the pH increase and the mechanical stirring, the final nanoparticles were used for the thermal and magnetic characterization.

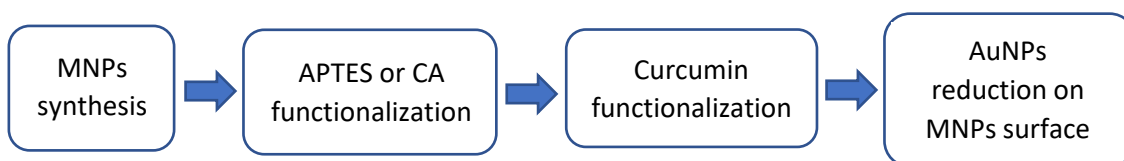


Figure 31. Gold-magnetite nanoparticles: second synthesis steps

4.2 Characterization techniques

Characterization analyses have been performed in order to verify that the nanoparticles synthesis was successful and to investigate their chemical composition, optical and thermal properties and their magnetic behavior. The techniques that have been used are:

- Ultraviolet-visible spectroscopy (UV-vis)
- Fourier transform infrared spectroscopy (FT-IR)
- Energy Dispersive Spectroscopy (EDS)
- Dynamic Light Scattering (DLS)
- Vibrating Sample Magnetometer
- Laser

4.2.1 Ultraviolet-visible Spectroscopy

UV-vis is a technique used to measure the wavelength and the maximum absorbance of a specimen in comparison to a reference. Since it is a light-based technique, the spectrometer contains UV-radiation source that emits a light across a wide range of wavelengths. A monochromator separates light and only one wavelength is allowed to pass through the sample; then a detector is used to convert the light intensity into an electric signal. The UV-vis spectroscopy information is finally presented in a graph of absorbance as a function of wavelength in a range that usually goes from 300 to 800 nm. The sample for this analysis were made of nanoparticles solutions diluted with bi-distilled water (or ethanol), which has been used as reference for the measurements. UV-vis (UV-2600 SHIMADZU) has been used to characterize the optical properties of the following NPs:

- a) Magnetite nanoparticles (M)
- b) Functionalized magnetite nanoparticles (route 1 and route 2) with curcumin
- c) Gold nanoparticles (Au)
- d) Gold-magnetite nanoparticles obtained through the first and second strategy

4.2.2 Fourier Transform Infrared Spectroscopy

FT-IR spectroscopy is a technique used to obtain an infrared spectrum of absorption, or emission, in order to characterize the nanoparticles from a chemical and structural point of view by identifying the organic functional groups present on the samples. When the samples are exposed to the infrared radiation (IR), the specimen absorbs part of radiations at specific frequencies which directly correspond to the vibrational energy levels of the bonds between atoms present in the specimen. Different bonds in a molecule vibrate at different energy levels and thus absorb at different wavelengths of IR. The spectrum of absorption shows all the different adsorption peaks as a function of the wavelength, ranging from 4000 to 450 cm^{-1} ; each peak refers to a specific chemical bond and it makes possible to identify the specific compounds in a complex system.

FT-IR (JASCO 4000 Fourier transform infrared spectroscope) has been used to characterize:

- a) Magnetite nanoparticles (M)
- b) Functionalized magnetite nanoparticles (route 1 and route 2)

- c) Functionalized magnetic nanoparticles (route 1 and route 2) with curcumin

The samples in the form of powder have been prepared by drying the nanoparticles solutions in the incubator at 37 °C until the complete evaporation of the solvent.

4.2.3 Energy Dispersive Spectroscopy

The EDS technique exploits the X-rays emitted by the sample to identify its elemental composition and its chemical characterization: indeed, when the electron beam is focused on the sample, the interaction of electrons with individual atoms causes the excitement of an inner electron, which is displaced in a different energy level. Consequently, the atom is excited and, in order to allow the atom to return to the ground state, another electron from an external shell will occupy the vacancy, and it results in the emission of an X-ray. The EDS detector absorbs the energy of the generated X-rays and converts it into electrical voltages (keV), obtaining a spectrum with different energy peaks corresponding to the various elements in the sample.

One of the two spectroscope that has been used for EDS constitutes a part of the FESEM instrument (Merlin Gemini Zeiss x-ray spectroscope). The nanoparticles that have been characterized through this technique are the gold-magnetite nanoconjugates and the samples have been prepared by drying the nanoparticles solution into an incubator at 37°C until obtaining a powder, which has been then placed on a carbon grid.

4.2.4 Dynamic Light Scattering

DLS is a light scattering method used to study hydrodynamic radius and size distribution of nanoparticles. Nanoparticles are crossed by a laser beam, giving rise to a light scattering phenomenon due to their Brownian motion, which depends on nanoparticles' sizes. By measuring the scattering variations over the time, the diffusion coefficient is calculated, while the hydrodynamic radius is obtained by converting the diffusion coefficient through the Stokes-Einstein equation. The nanoparticles samples were prepared by diluting the nanoparticles solutions with bi-distilled water in appropriate cuvettes. In particular, DLS (Litesizer™ 500 instrument) has been used to characterize:

- a) Magnetite nanoparticles (M)
- b) Functionalized magnetite nanoparticles (route 1 and route 2) with curcumin
- c) Gold-magnetite nanoparticles obtained through the first strategy

The refractive index of magnetite NPs have been settled as 2,34.

4.2.5 Vibrating sample magnetometer (VSM)

The magnetic measurements have been performed to characterize nanoparticles' magnetic behavior. In particular, with this technique it is possible to get information on the magnetization on the sample and its dependence with the strength of the constant magnetic field that is applied during the measurements. The analysed nanoparticles were:

- a) Pure magnetite nanoparticles (M)
- b) Functionalized magnetite nanoparticles (route 1 and route 2)
- c) Gold-magnetite nanoparticles obtained through the first strategy (third synthesis)

The nanoparticles solutions have been dried in the incubator at 37 °C until the complete evaporation of the solvent. The sample were prepared by using the powder and the PVA, and their mass has been measured in order to evaluate the magnetic properties. The results were shown in Am²/kg.

4.2.6 Laser

The laser has been used to verify nanoparticles' ability to increase their temperature under a laser irradiation. The analysed nanoparticles were gold-magnetite nanoparticles with curcumin and APTES, or citric acid, obtained through the first strategy (third synthesis). For preparing the samples, 1 ml of each nanoparticles' solutions have been used to fill two wells of a 12-well plate positioned under a NIR laser beam with a power of 1 W and a wavelength of 808 nm (CNI, model FC-808). The heating of the samples was carried out in steps of 1 minute each for a total of 10 minutes; the temperature recording has been performed at every step by using a thermocouple thermometer.

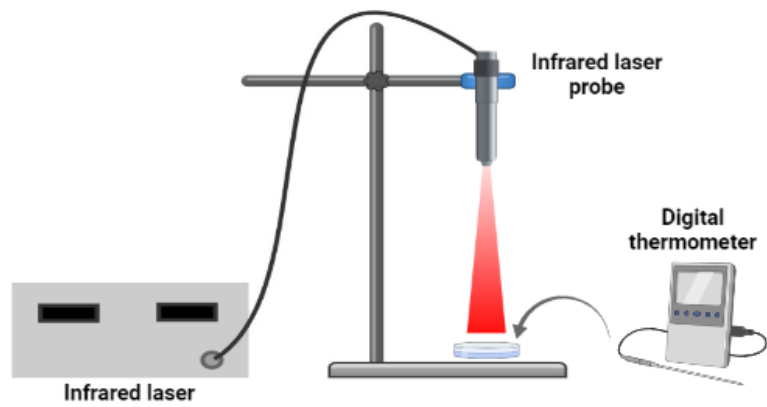


Figure 32. NIR laser and NPs temperature measurement set up [109]

Chapter 5

Results and discussion

This chapter contains the results of the experimental work related to the synthesis and functionalization of the nanoparticles obtained through different strategies. The outcomes of each step will be discussed, highlighting in particular the successful routes. Moreover, when it is possible, the results will be compared to those present in literature.

5.1 Magnetite nanoparticles

In order to prove the successful synthesis of MNPs and their functionalization with APTES or CA, and with curcumin, the FTIR spectrum of pure magnetite nanoparticles and of functionalized magnetite nanoparticles were detected. Thus, FTIR analysis has been conducted at the end of each step of MNPs synthesis and functionalization.

Route 1

Functionalization with APTES

After the synthesis, MNPs have been functionalized with APTES (first approach).

The Figure 33 shows the FTIR spectra of MNPs compared with APTES functionalized MNPs. The peak at 550 cm^{-1} relates to Fe-O group validates the successful formation of MNPs, while the peak at 1000 cm^{-1} refers to the Si-O-Si vibration in the silane layer which confirms the effective functionalization of MNPs with APTES. Additionally, some more peaks verified the introduction of APTES to the surface of MNPs such as the bands around 1030 and 1115 cm^{-1} referring to the SiO-H and Si-O-Si groups, while the absorption bands at 2862 and 2930 cm^{-1} assigned to the stretching vibration of C-H bond of the propyl amine group proved the covalent attachment of aminopropylsilane group.

Table 9. Functional groups related to MNPs synthesis and functionalization with APTES

Functional group	Wavenumber (cm ⁻¹)	Ref.
Fe-O	550	[56]
Si-O-Si vibration	1000	[103]
SiO-H	1030	[108]
Si-O-Si	1115	[108]
-NH ₂ bending	1640	[108]
C-H vibration	2930	[108]
N-H stretching	3445	[108]

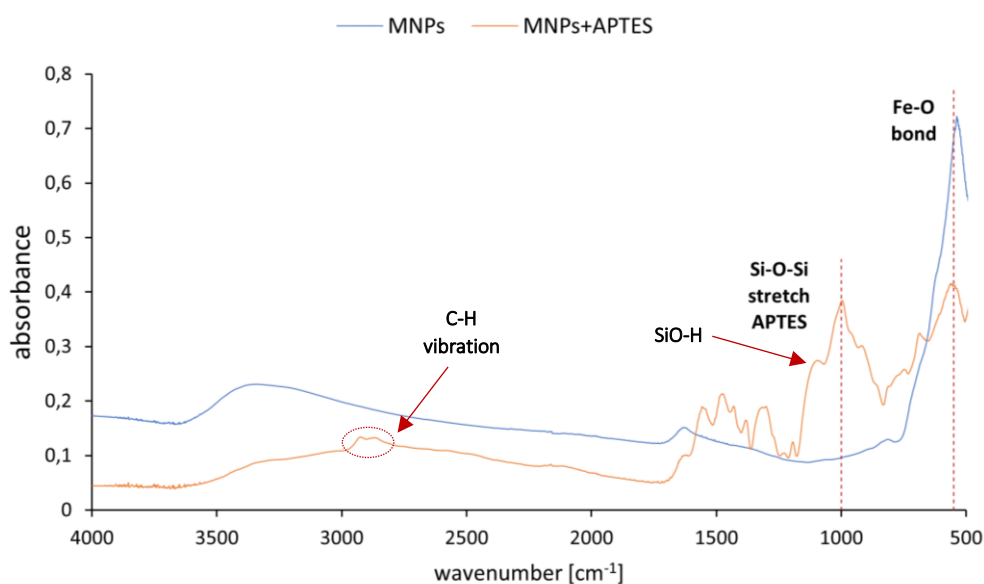


Figure 33. FTIR spectra of MNPs (blue) and APTES functionalized MNPs (red) [First APTES functionalization]

Starting from the MNPs, a second functionalization with APTES was performed by varying the amount of the SPIONs suspension and the quantity of the solvent. The figure 34 shows a comparison between the two FTIR spectra related to the different functionalization with APTES, with an increase in the peak intensity related to the Fe-O, due to the increase of the SPIONs.

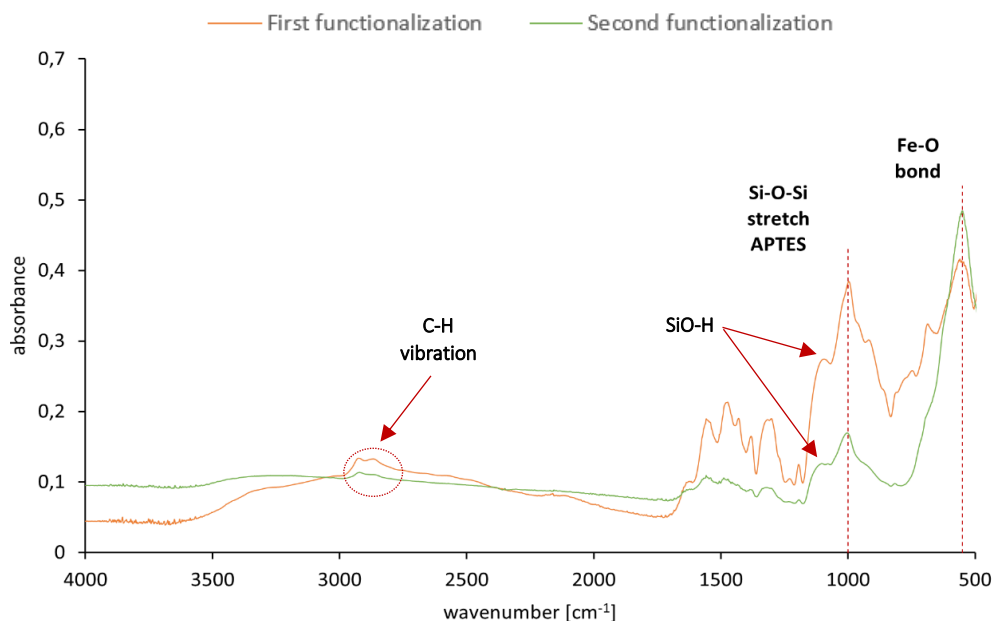


Figure 34. FTIR spectra of APTES functionalized MNPs obtained through the first functionalization (red) and the second functionalization (green)

Functionalization with curcumin

The second functionalization of MNPs with APTES has been used for the further functionalization with curcumin. By observing the FTIR spectrum in Figure 35, it results to be difficult to determine the effective grafting of curcumin on MNPs surface since the main peaks of curcumin, such as the peak at 1500 referred to the aromatic C=C bond, the peak related to the C=O bond at about 1635 cm^{-1} and the peak attributed to the stretching of the phenolic OH group at about 3450 cm^{-1} , are not evident. It may be due to some measurement problems, together with the presence of APTES covering the peaks of curcumin.

Table 10. Functional groups of curcumin detected in FTIR spectrum

Functional group	Wavenumber (cm^{-1})	Ref.
Aromatic C-O stretching	1285	[106][107]
Olefinic C-H bending vibration	1430	[107]
Aromatic C=C vibration	1500	[46][105]
C=O	1635	[105]
Phenolic OH stretching	3200-3500	[46][106]

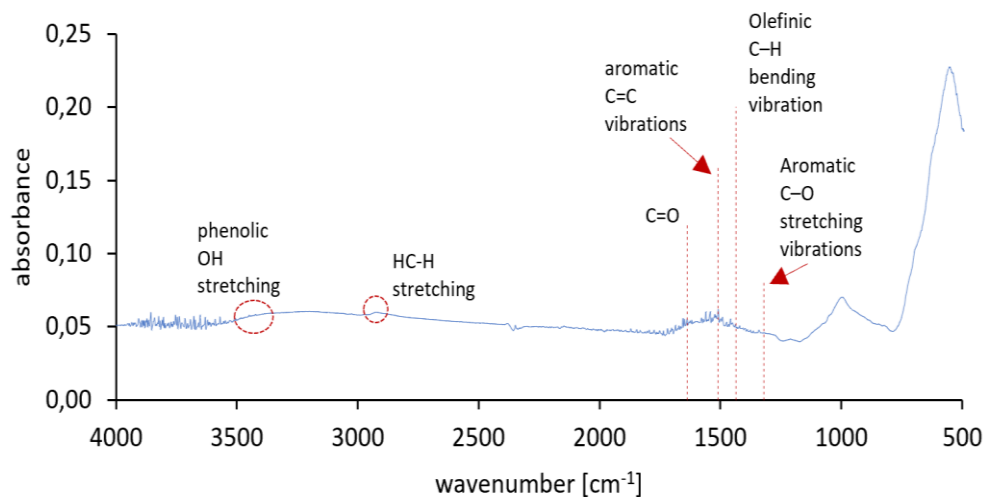


Figure 35. FTIR spectrum of curcumin and APTES functionalized MNPs

In literature [64], it has been showed that the absorption spectrum of curcumin has two strong absorption bands, one in the visible region with maximum ranging from 410 to 430 nm and another band in the UV region with maximum at 265 nm. The UV-vis analysis (Figure 36) presents a broad band going from 350 to 450 nm which may support the hypothesis of the effective functionalization with curcumin of APTES-MNPs.

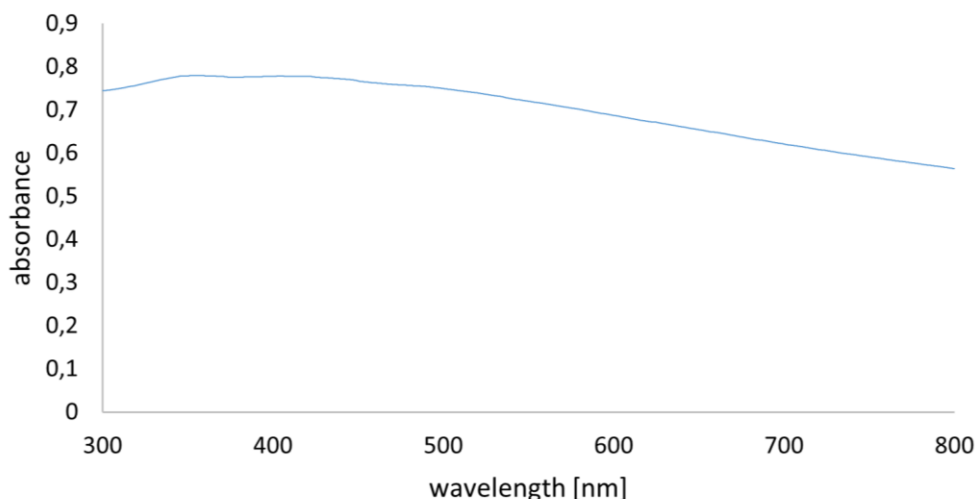


Figure 36. UV-vis of the first functionalization with curcumin of APTES-MNPs

Another approach of functionalization with curcumin was made by varying the amount of curcumin and resuspending the MNPs in two solutions. Curcumin in water has the maximum absorbance band around 435 nm and the weakest absorption band around 268 nm, while in ethanol curcumin has a characteristic absorbance around 300-500 nm with a peak at around 425 nm, a shoulder near 360 and 460 nm, and a weaker absorbance band

around 262 nm. In both cases, the UV-vis spectra (Figure 37) show a broader peak of the curcumin which may confirm the functionalization with curcumin of the APTES-MNPs.

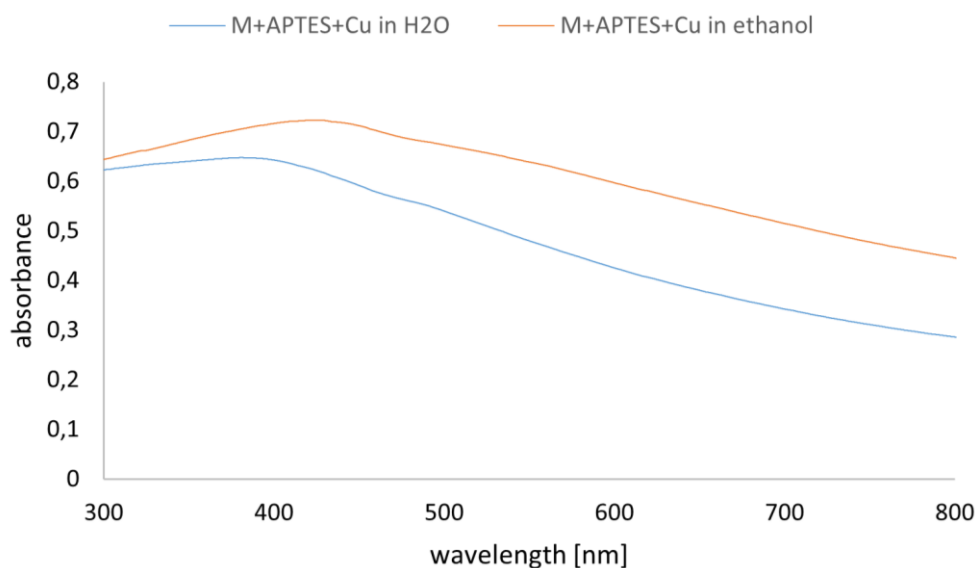


Figure 37. UV-vis of the second functionalization with curcumin of APTES-MNPs

Route 2

Functionalization with citric acid

MNPs have been functionalized with citric acid. In the FTIR spectra of CA functionalized MNPs (Figure 38), there are some peaks showing the successful functionalization of MNPs with the citric acid (Table 11): a peak at about 1330 cm^{-1} can be attributed to the asymmetric stretching of CO from COOH group of citric acid, while the peak at about 1550 cm^{-1} is due to the vibration of C=O of CA-COOH group. At 2660 cm^{-1} is shown the stretching of CH₂.

Table 11. Functional groups related to CA functionalized MNPs

Functional group	Wavenumber (cm^{-1})	Ref.
CO asymmetric stretching	1330	[104]
C=O vibration	1550	[104]
CH₂ stretching	2660	[99]

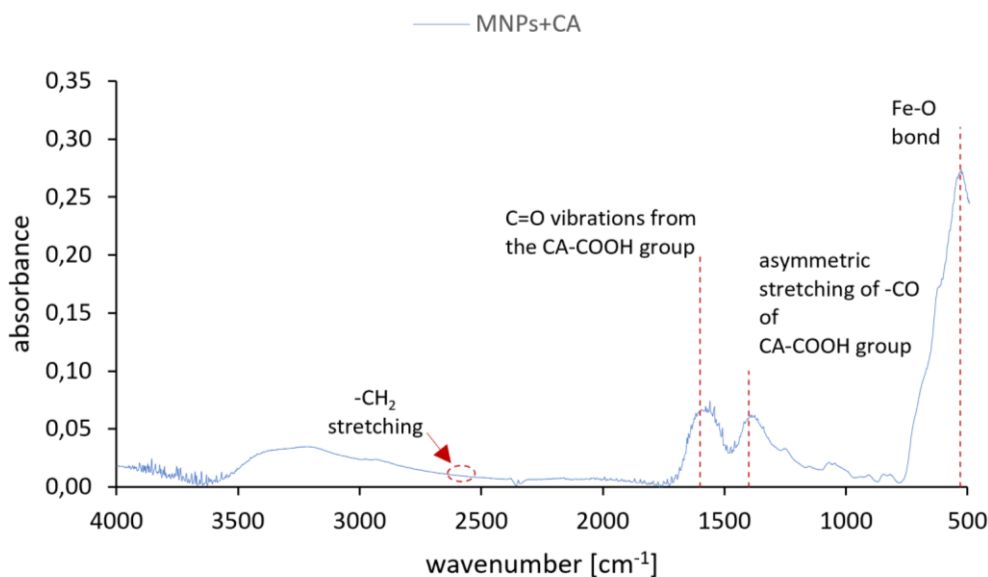


Figure 38. FTIR spectrum of CA functionalized MNPs

Functionalization with curcumin

The MNPs with CA has been used for the next functionalization with curcumin. As for the APTES, also the FTIR spectrum (Figure 39) of MNPs functionalized with citric acid and curcumin does not show clearly the main peaks of curcumin, such as the peak around 1500 cm^{-1} referring to the aromatic C=C bond, at about 1635 cm^{-1} attributed to the C=O bond and around 3450 cm^{-1} assigned to the stretching of the phenolic OH group.

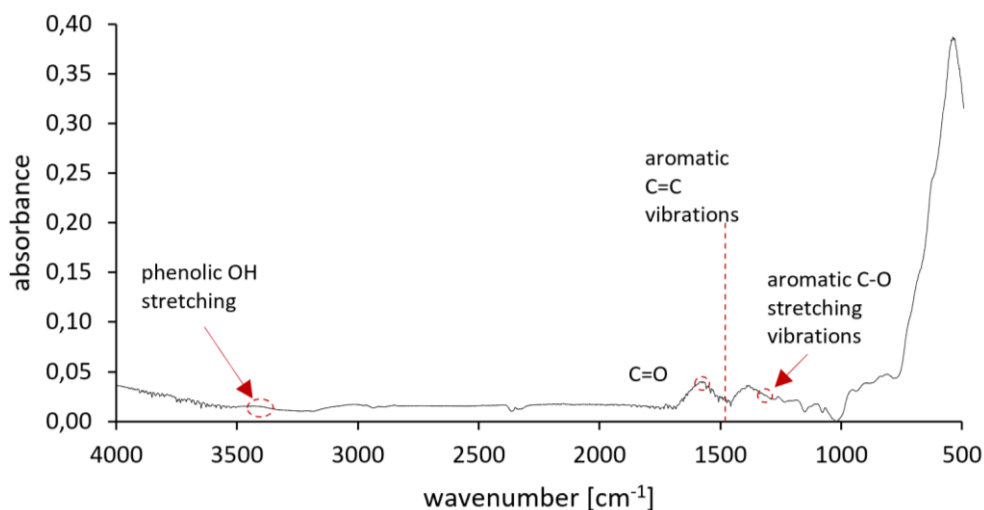


Figure 39. FTIR spectrum of curcumin and CA functionalized MNPs

As shown in previous studies [99], the CA capped MNPs without curcumin does not reveal any light absorption peak, while the UV-vis spectrum in Figure 40a shows a small shoulder around 400 nm which can be due to the curcumin on the CA-MNPs' surface.

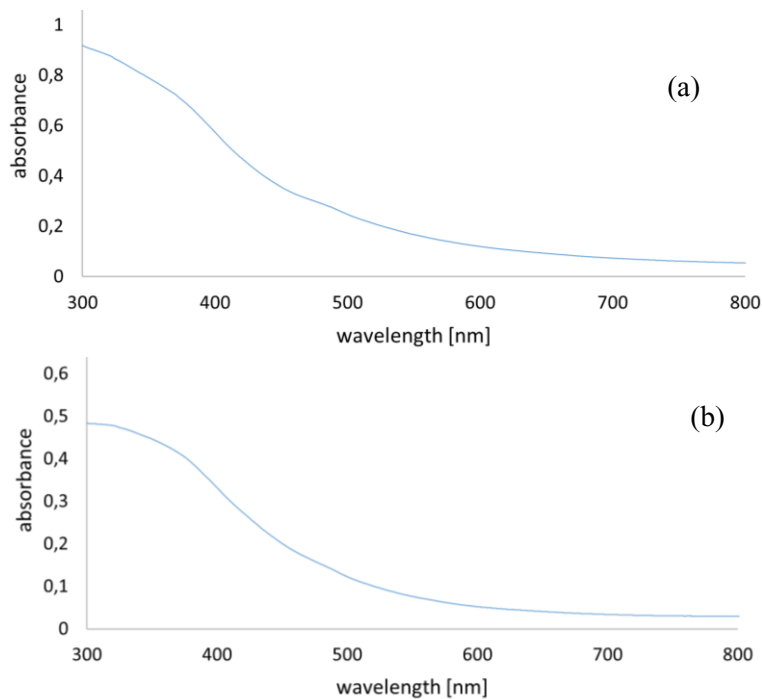


Figure 40. UV-vis of the CA-MNPs with curcumin (a) first functionalization, (b) second functionalization)

The functionalization with curcumin has been repeated another time by changing the amount of curcumin, and the obtained UV-vis spectrum (Figure 40b) results to be similar to the one obtained through the first curcumin functionalization approach, with only a slightly increased absorbance at about 400 nm.

5.2 Gold nanoparticles

El Kurdi *et al* [48] obtained AuNPs using curcumin as a reducing and stabilizing agent in acidic media and this synthesis has been repeated during the experimental work with the main aim to subsequently graft MNPs on their surface. The UV-vis spectrum below (Figure 41) confirms that the curcumin-mediated gold nanoparticles synthesis has been successfully achieved since it shows the gold absorbing peak at 550 nm. Indeed, a SPR band was obtained with a remarkable increase in the intensity, meaning that the Au^{3+} to Au^0 reduction was obtained [83]. According to the literature [104], in fact, the typical gold absorbing window is usually between 500 nm and 600 nm.

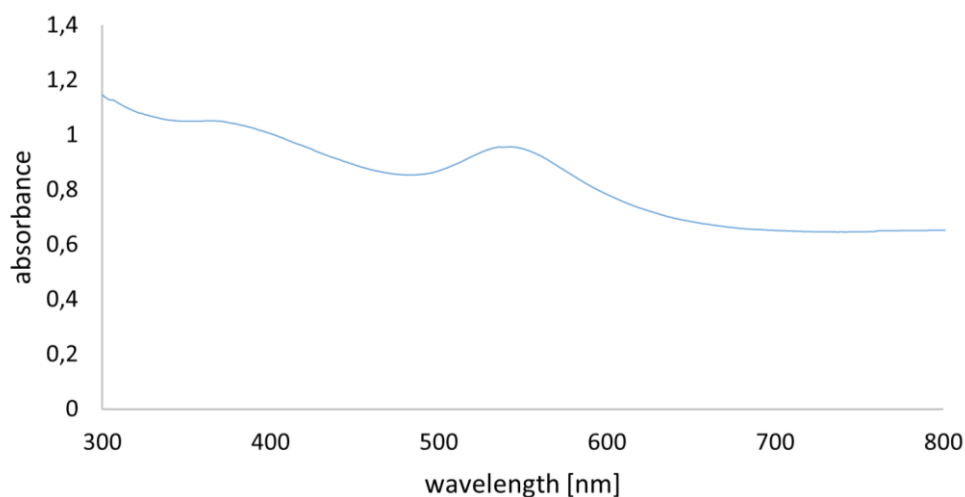


Figure 41. UV-vis of curcumin-gold nanoparticles

5.3 Gold-magnetite nanoparticles

Further analyses have been presented in order to assess the role of curcumin as a linking agent for the formation of the multifunctional gold-magnetite nanostructures. Two different synthesis methods have been performed, as described in Chapter 4, for obtaining the nanoconjugates starting from the curcumin-mediated AuNPs (first synthesis) or from the curcumin-functionalized MNPs (second synthesis).

5.3.1 First synthesis method

The first synthesis method for obtaining the gold-magnetite nanostructures is based on the use of curcumin-mediated synthesized AuNPs, which represent the core, and a surface coating made of CA-MNPs grafted on gold nanoparticles' surface. The obtained nanostructures have been analysed through UV-vis. The spectra below (Figure 42a) show the results of the UV-vis analysis of the two obtained nanoparticles solutions at different pH (acidic and basic) compared with AuNPs spectrum: as reported in literature [48], it has been found that at high pH, curcumin usually reacts totally since the absorption peak is absent and only a peak around 550 nm is present, which refers to the Au NPs; while at acidic and neutral pH, an absorption peak of curcumin around 425 nm should be slightly visible. In this case, no evident peak related to curcumin is revealed, probably because of the presence of citric acid, as the previous UV-vis spectra of curcumin functionalized CA-MNPs have shown. In Figure 42b, the spectrum of the CA-MNPs with curcumin is

compared to the UV-vis spectrum of the nanoparticles obtained through this second synthesis method at pH 4: a peak of weak intensity can be seen in the second case at around 550 nm, which may confirm the presence of gold. However, these results were unsatisfactory and only the second synthesis was chosen for further studies.

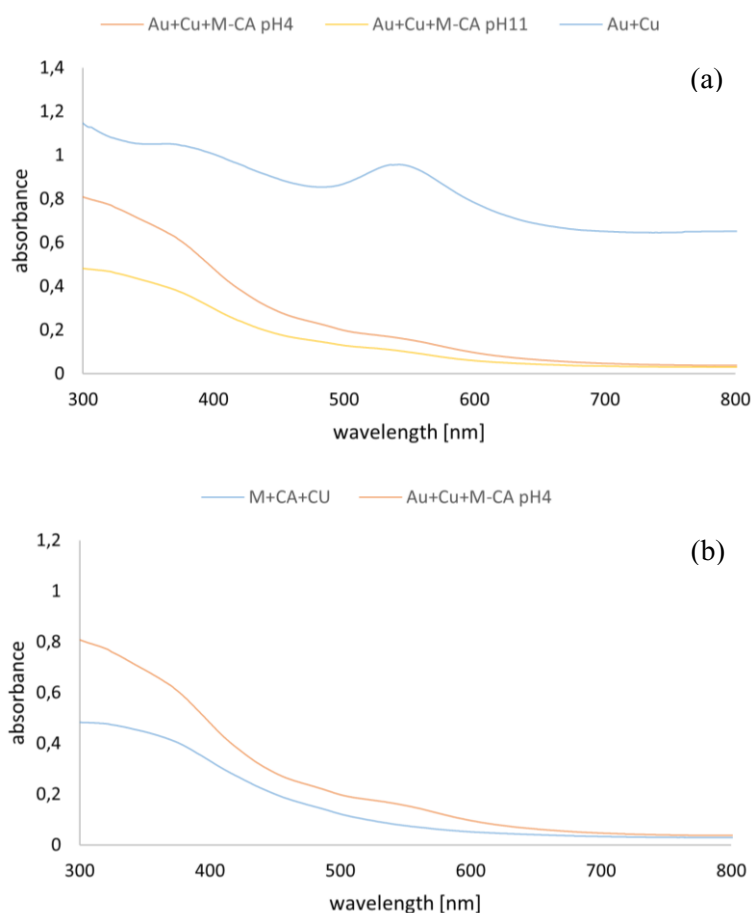


Figure 42. UV-vis spectra of (a) gold-magnetite nanostructures at acidic and basic pH compared to AuNPs, (b) gold-magnetite nanostructures at acidic pH compared to M+CA+CU NPs

5.3.2 Second synthesis method

The second synthesis method for obtaining the gold-magnetite nanoconjugates is based on the use of curcumin functionalized APTES- or CA-, MNPs as a core, followed by the reduction of gold nanoparticles on their surface. The nanostructures have been analysed through UV-vis, EDS, DLS, magnetic analysis and thermal analysis.

Route 1

In this first route, the APTES-MNPs functionalized with curcumin have been used as a core, followed by the gold seed growth on the surface. The UV-vis spectra reported below (Figure 43) show a comparison between the APTES-MNPs functionalized with gold and without gold. No noticeable peak is evident; thus a second approach was carried out with the aim to improve the obtained results by modifying the curcumin functionalization of APTES-MNPs strategy: in particular, the nanoparticles solution was divided in two solutions and resuspended in water and ethanol, while the quantity of curcumin was proportionally doubled.

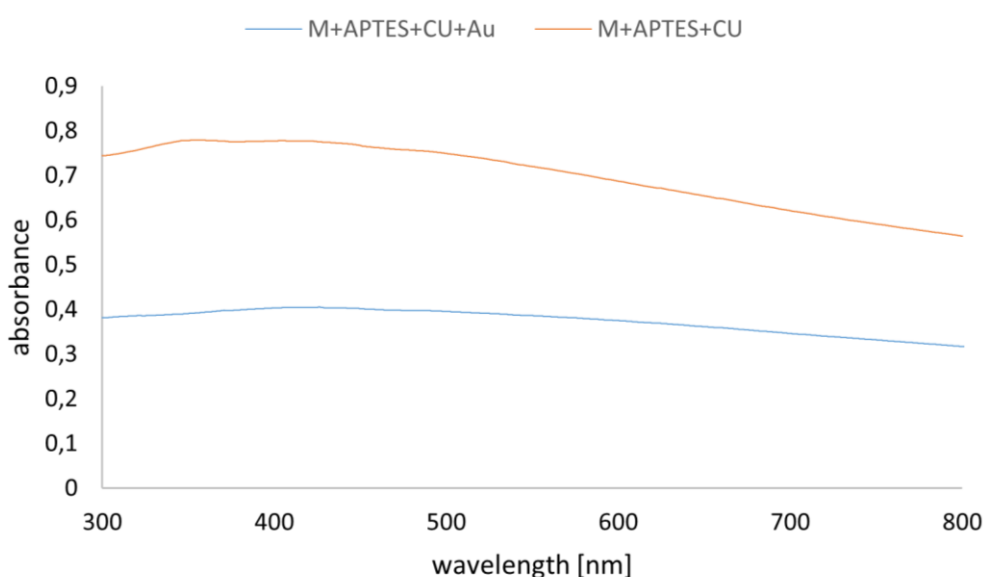


Figure 43. UV-vis spectra of APTES-MNPs with curcumin compared to the same structure functionalized with gold (first curcumin functionalization)

Starting from the second curcumin functionalization, a second synthesis of the gold-magnetite nanostructures was achieved. The two hybrid nanostructures solutions were suspended in water and ethanol and their pH has been increased until reaching a basic value. The results have been analysed with UV-vis, EDS, DLS, VSM and by using a laser.

UV-vis. Figure 44 shows the UV-vis spectra of the obtained nanoconjugates suspended in water and ethanol. A slightly different spectrum is obtained with respect the first synthesis, but no evident peak is present. The hypothesis is that the, since curcumin absorption band is between 350 and 500 nm, while the SPR window of gold is between

500 and 600 nm, the obtained wider band going from 350 to 550 nm can be related to the presence of both curcumin and gold nanoparticles.

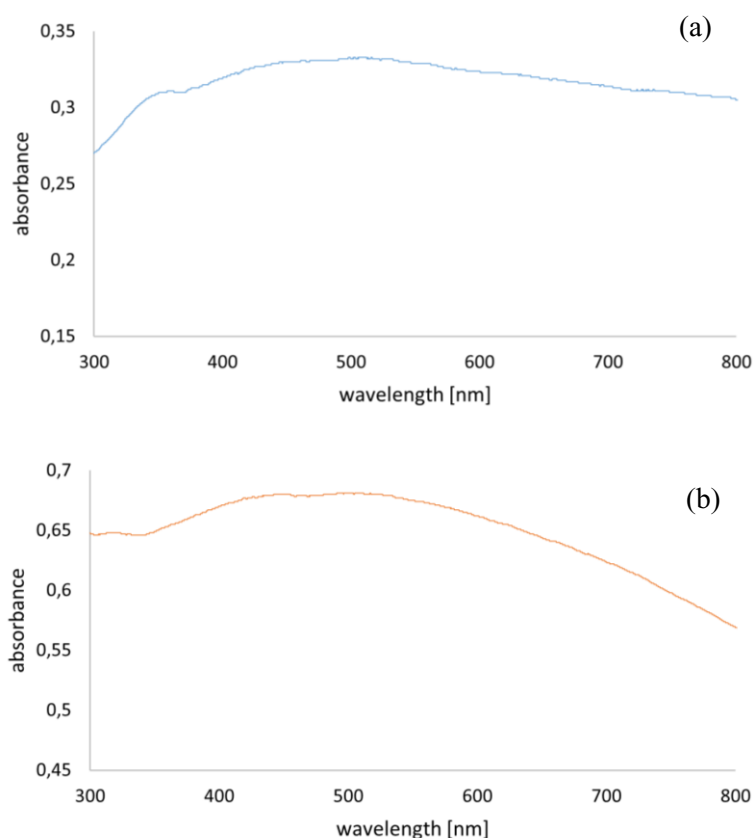


Figure 44. UV-vis spectra of gold-magnetite nanostructures with APTES and curcumin (second curcumin functionalization): (a) suspended in water, (b) suspended in ethanol

EDS and FESEM. This hypothesis is confirmed for both magnetite nanoparticles suspended in water and ethanol by the chemical composition analysis since the presence of gold has been detected in the EDS spectrum (Figure 45), together with the components of magnetite, iron and oxygen, the silicon peak because of the MNPs functionalized with APTES, and the carbon peak due to the grid used for preparing the samples. The SEM images show the structure of the obtained nanocojugates (Figure 46). Big aggregates of magnetic nanoparticles are present, while the white spots represent the gold nanoparticles of about 100 nm.

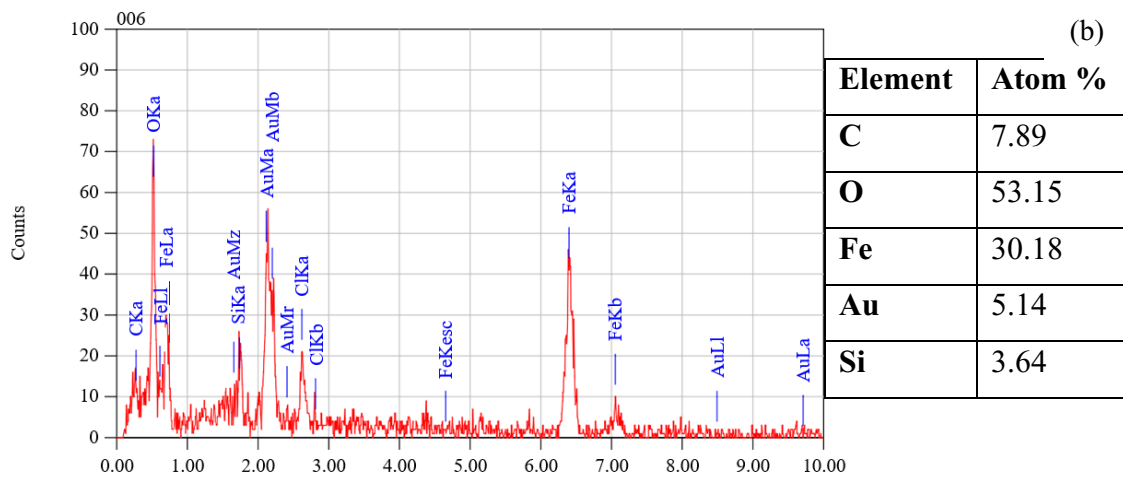
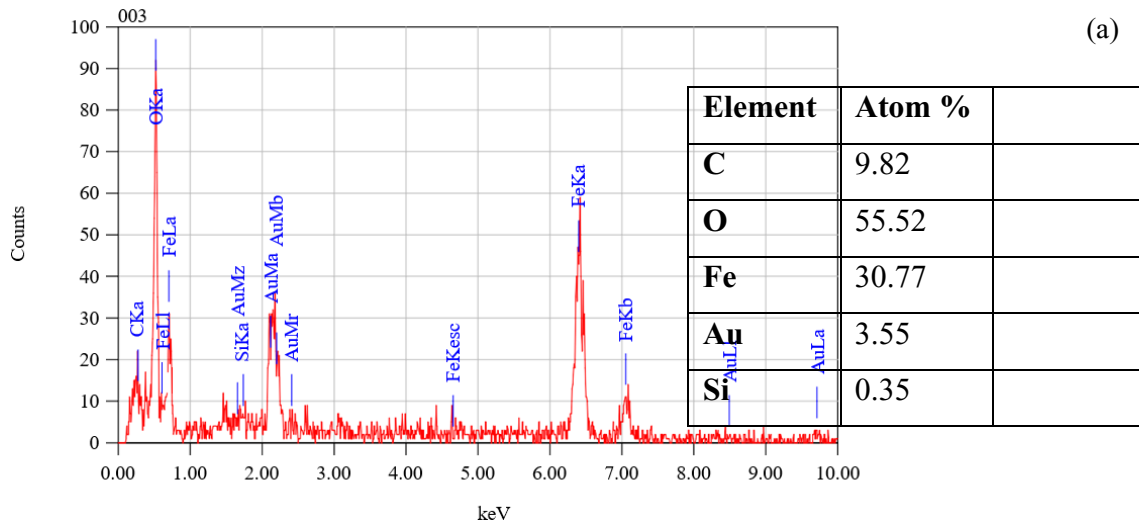
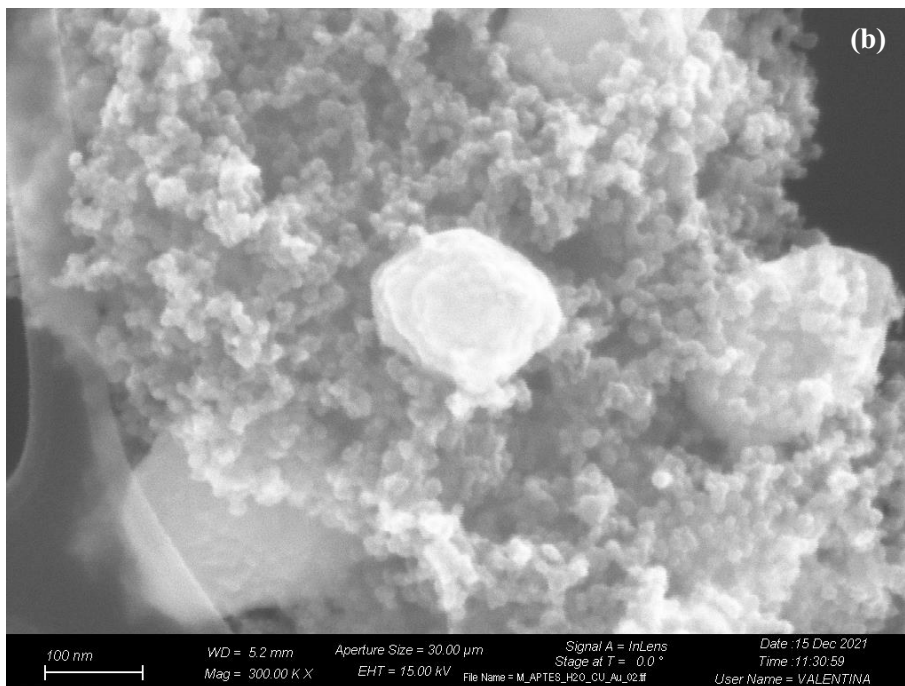
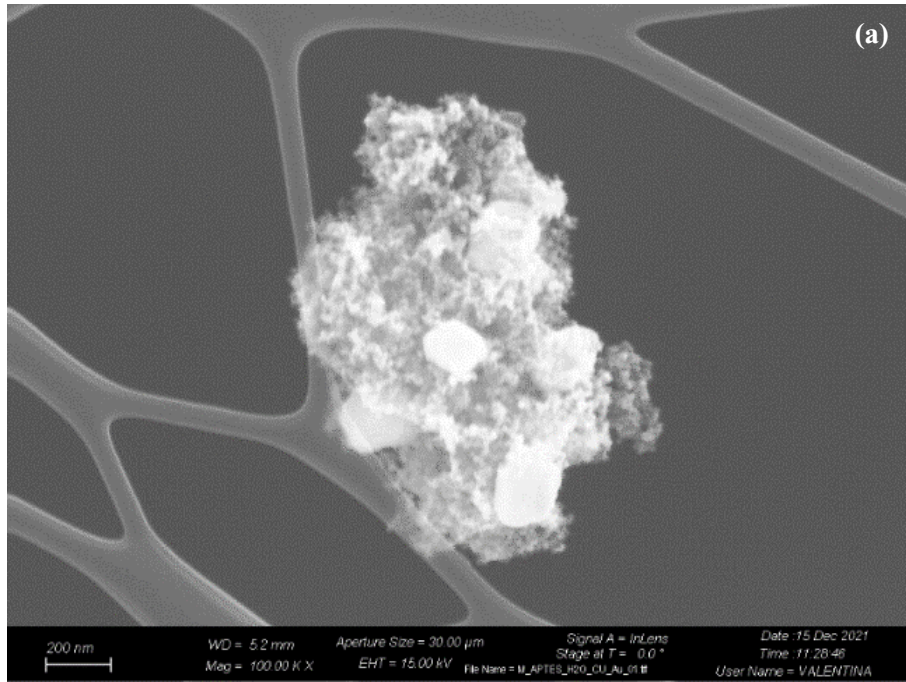


Figure 45. EDS analysis of gold-magnetite nanostructures (second curcumin functionalization):
 (a) suspended in water, (b) suspended in ethanol



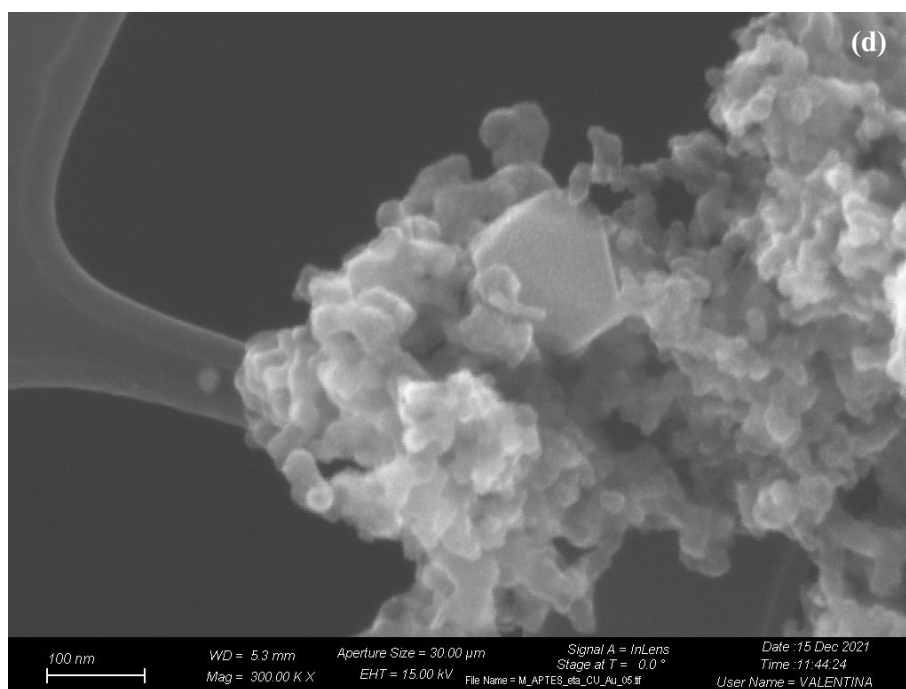
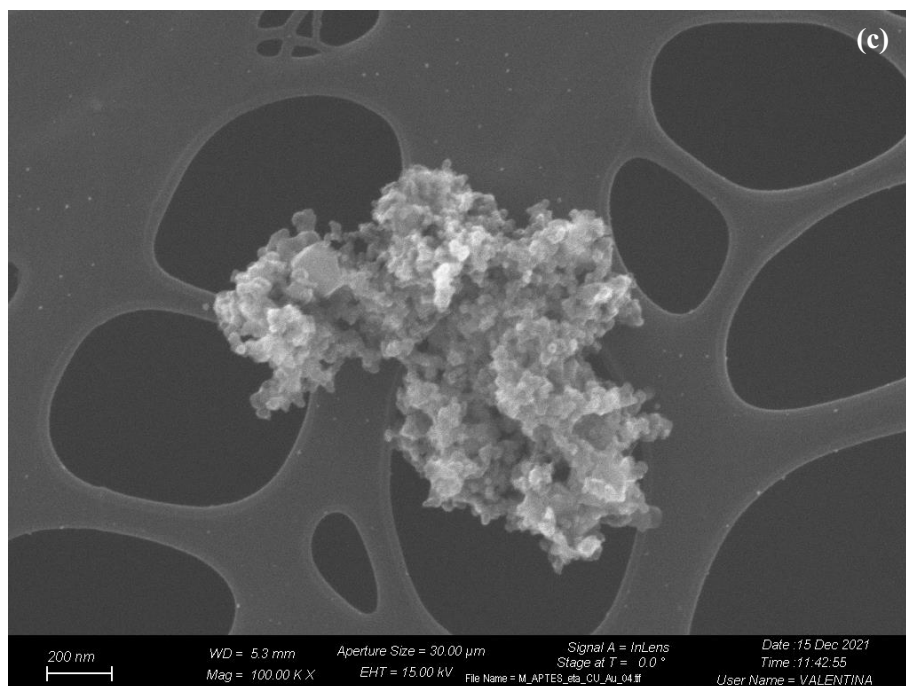


Figure 46. SEM images of gold-magnetite nanostructures with APTES (second curcumin functionalization): (a-b) suspended in water, (c-d) suspended in ethanol

DLS. DLS analysis was performed to determine the hydrodynamic diameter and the polydispersity index (PDI) of gold-magnetite nanoparticles functionalized with APTES and curcumin, compared with the pure magnetite nanoparticles. PDI represents a measure

of the heterogeneity of a sample based on size, while the hydrodynamic diameter measurements include the electric dipole layer that adheres to its surface: thus, the obtained diameter is bigger than the real nanoparticles' one.

The measurements have been reported as “mean ± standard deviation” in Table 12.

Table 12. DLS results gold-magnetite NPs (route 1)

	Hydrodynamic diameter	PDI
Pure magnetite NPs	1270±44 nm	32,3±25,6 %
Gold-magnetite NPs	1302±72 nm	56,5±24,1 %

The average hydrodynamic diameter of the gold-magnetite nanoparticles functionalized with APTES and curcumin is bigger than the pure magnetite NPs' one, as well as the PDI indicating that this sample is less monodisperse than the other.

A third synthesis of the gold-magnetite nanostructures was finally performed without dividing the nanoparticles solution and by resuspending nanoparticles only in water; the amount of H_{Au}Cl₄ and bi-distilled water was proportionally increased, as well as the pH of the final solution. The obtained nanoconjugates were used then for the thermal and magnetic characterization.

Laser. A NIR laser and a thermocouple thermometer were used to assess the nanoparticles property to increase their temperature under a laser irradiation. The laser was activated for 10 minutes in steps of 1 minute each. The Figure 47 shows the time-dependent temperature of the gold-magnetite heterodimers with APTES starting from the room temperature, with an increase of 16 °C. These results make the obtained nanoconjugates suitable tools for the hyperthermia therapy for the tumor cells ablation.

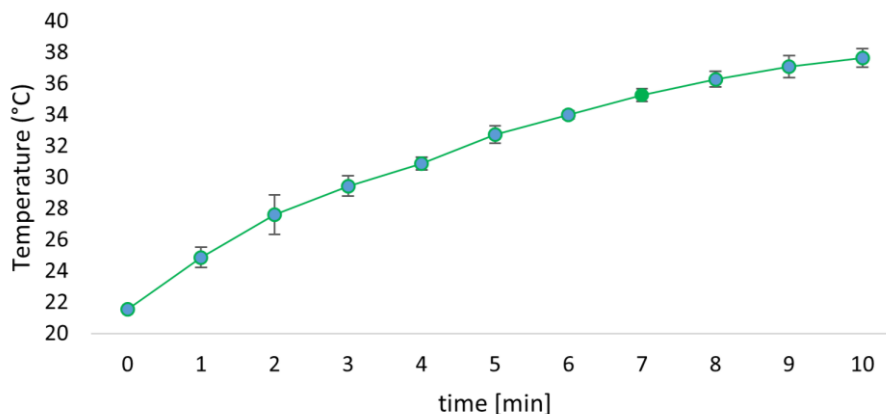


Figure 47. Time dependent temperature measurements of gold-magnetite heterodimers with curcumin and APTES

Vibrating sample magnetometer (VSM). The magnetic properties of the APTES-MNPs with and without curcumin and AuNPs functionalization were evaluated by VSM at room temperature. Each sample has been compared to the curve of the pure magnetite nanoparticles. In Figure 48, the magnetization saturation (Am^2/kg) as a function of the applied magnetic field (kA/m) is reported. In both cases, the nanoparticles showed no hysteresis (no remanence nor coercivity), which is consistent with the superparamagnetic behavior of pure SPIONs. As shown in literature [103], relatively small or negligible reduction in the saturation magnetization value of MNPs was observed after the functionalization with APTES and then with curcumin and gold nanoparticle; the results suggest that this reduction occurred after the functionalization because of the monolayer coverage of APTES on MNPs' surface and because of the further coating with curcumin. However, the use of a direct functionalization strategy for the APTES prevented high loss in the magnetization of MNPs. Moreover, the presence of gold nanoparticles may be responsible for an additional decrease of saturation magnetization of the final multifunctional nanostructures.

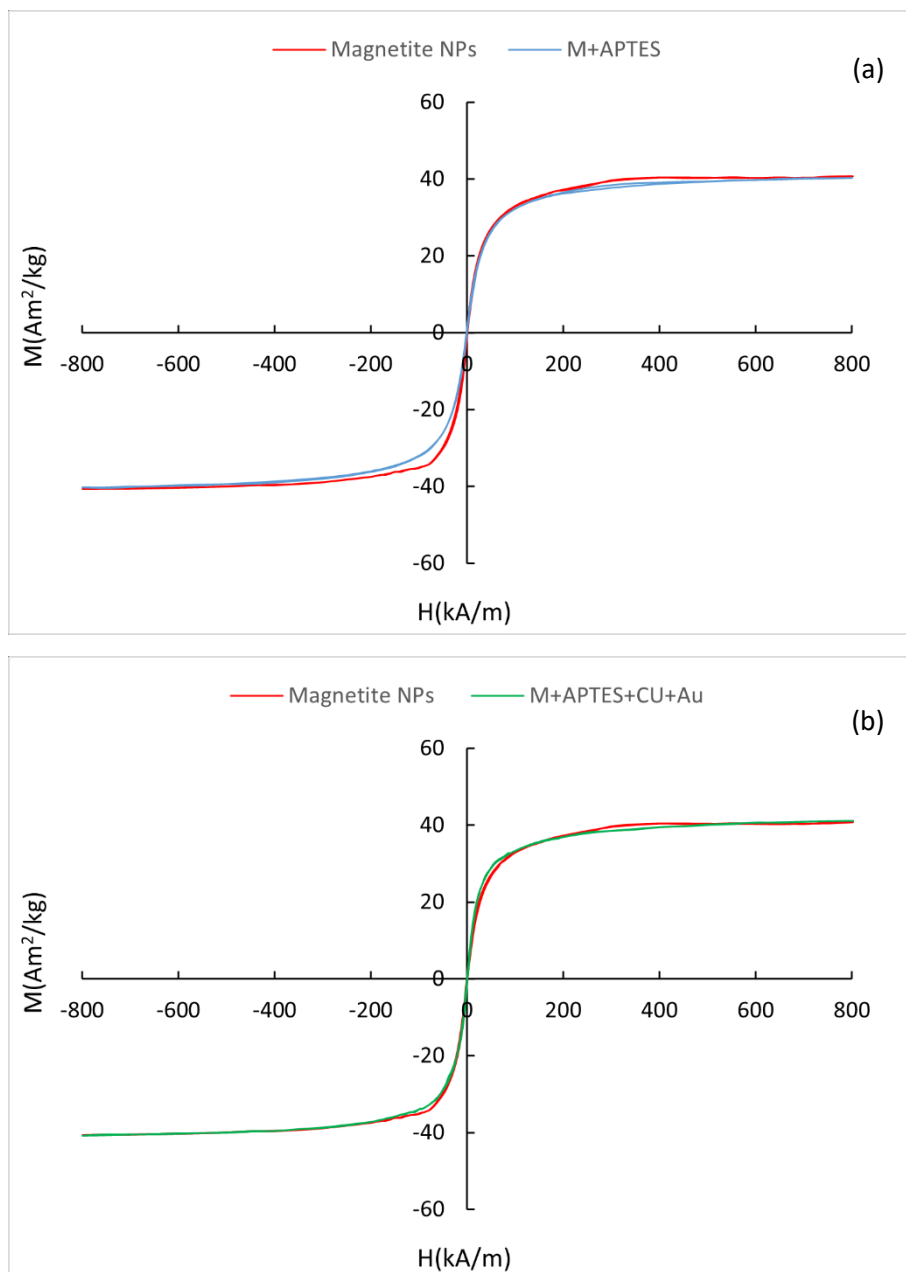


Figure 48. Magnetization curve of pure MNPs compared with: (a) APTES-MNPs and (b) APTES-MNPs functionalized with curcumin and AuNPs

Route 2

In the second route, the CA-MNPs functionalized with curcumin have been used as a core, followed by the gold growth on the surface. The spectra of UV-vis analysis (Figure 49) show a comparison between the CA-MNPs functionalized with gold and without gold. Considering the spectrum of the gold-magnetite nanostructures, a broad band centred at 400 nm is present, which can be due to the presence of the curcumin, while a

small shoulder, probably due to the gold, at 500 nm is visible. However, a second synthesis has been performed with the aim to improve the obtained results.

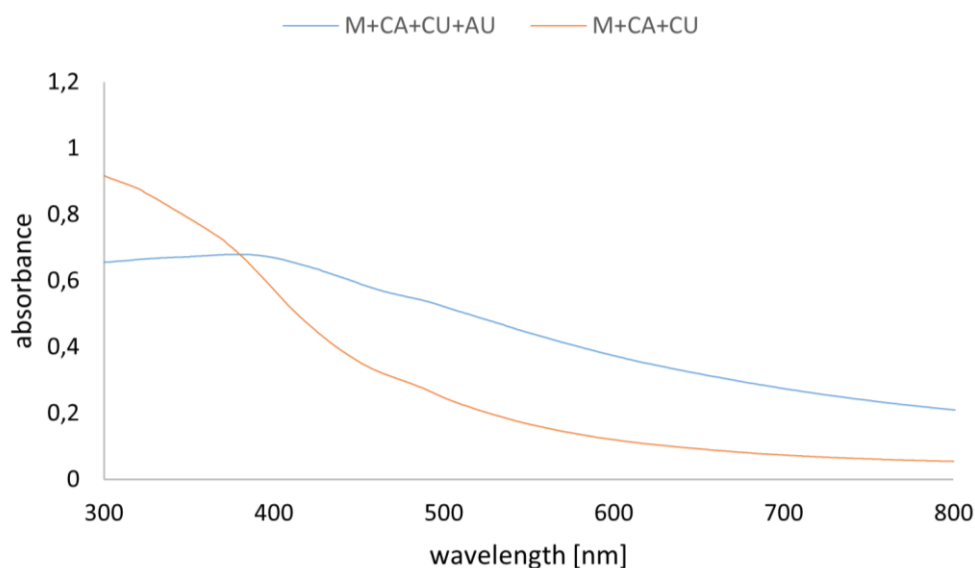


Figure 49. UV-vis spectra of CA-MNPs with curcumin compared to the same structure functionalized with gold (first curcumin functionalization)

Following the second curcumin functionalization of CA-MNPs, a second synthesis of the gold-magnetite nanostructures was achieved. The gold-magnetite nanostructures solution is suspended in water and its pH has been increased until reaching a pH of about 8. The results have been analysed with UV-vis, EDS, DLS, VSM and by using a laser.

UV-vis. The UV-vis analysis has been performed again for nanostructures obtained through the second synthesis and compared to the spectrum of CA-MNPs without gold, but no evident peaks related to gold or curcumin are present in the UV-vis spectra. In Figure 50, it is possible to see an increase in the slope between 350 and 500 nm of the UV-vis spectrum of CA-MNPs with gold, which can be due to the presence of gold nanoparticles.

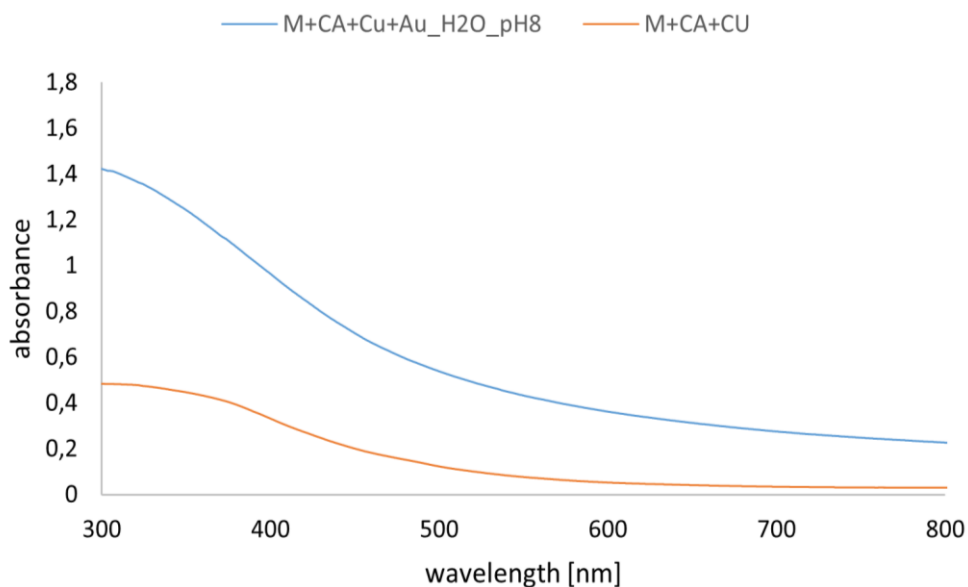


Figure 50. UV-vis spectra of gold-magnetite nanostructures with CA and curcumin (second curcumin functionalization)

EDS e FESEM. In the EDS spectrum, the presence of gold has been detected (Figure 51), which may confirm the successful reduction of gold nanoparticles on the CA-MNPs' surface. The iron and oxygen peaks of the magnetite nanoparticles and the carbon peak of the grid have been also detected. The obtained nanocojugates in the SEM images result to be more monodispersed with respect the ones functionalized with the APTES, confirming the ability of the citric acid to stabilize the solution by creating repulsive forces between the nanoparticles. Different nanostructures with diameters going from 50 to 190 nm were obtained (Figure 52a-c).

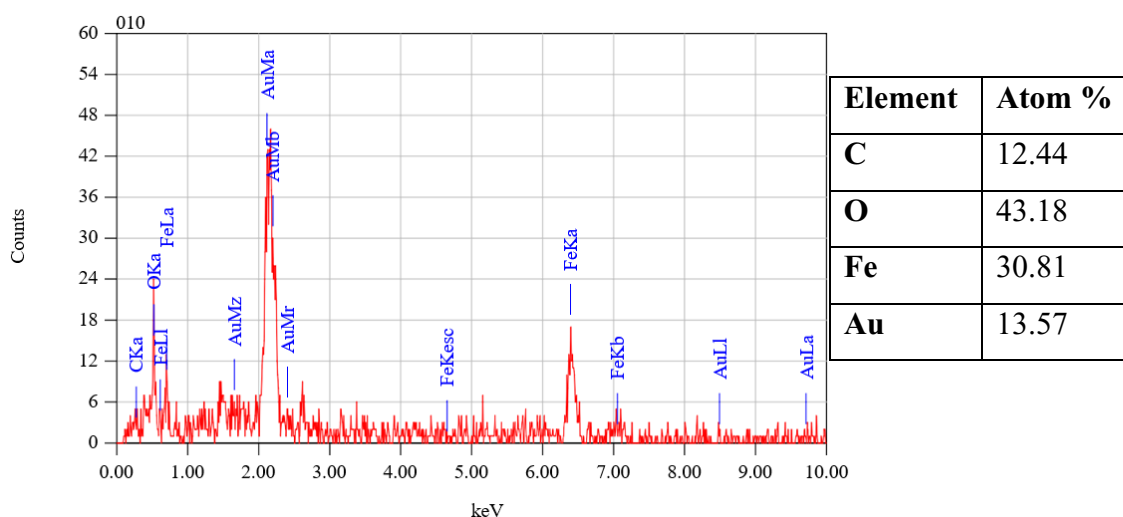
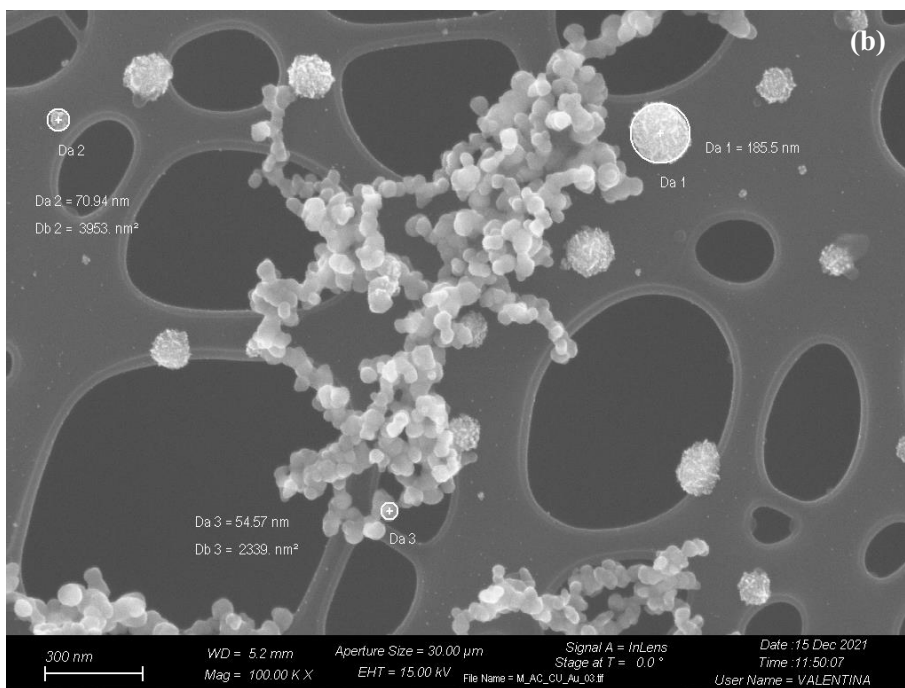
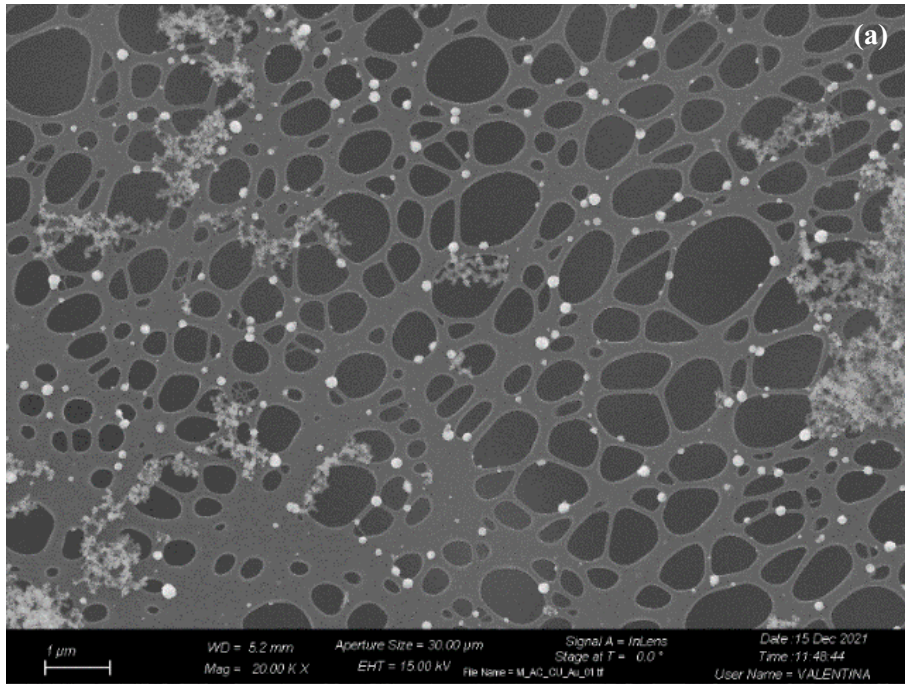


Figure 51. EDS analysis of gold-magnetite nanostructures (second curcumin functionalization): (a) suspended in water



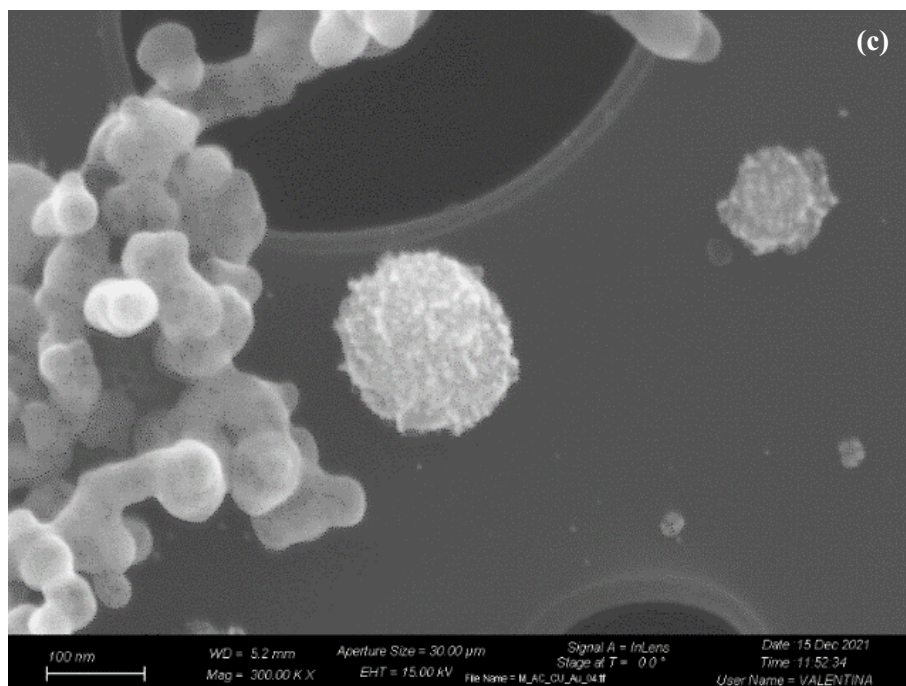


Figure 52. (a-c) SEM images of gold-magnetite nanostructures with CA (second curcumin functionalization)

DLS. The hydrodynamic diameter and the polydispersity index (PDI) of gold-magnetite nanoparticles functionalized with citric acid and curcumin, compared with the pure magnetite nanoparticles and the magnetite nanoparticles functionalized with APTES only was obtained through DLS analysis. The measurements have been reported as “mean \pm standard deviation” in Table 13.

Table 13. DLS results gold-magnetite NPs (route 2)

	Hydrodynamic diameter	PDI
Pure magnetite NPs	1270 \pm 44 nm	30 \pm 18 %
CA-magnetite NPs	339 \pm 58,7 nm	27,5 \pm 2,9 %
Gold-magnetite NPs	1178 \pm 153,6 nm	46,55 \pm 8 %

The average hydrodynamic diameter of the MNPs functionalized with citric acid is lower than the pure magnetite NP's one, as well as the PDI, indicating the effective role of CA as a stabilizing agent which allow to obtain smaller and more monodispersed nanostructures. In the case of the gold-magnetite nanoparticles functionalized with citric acid and curcumin, the average hydrodynamic diameter results to be slightly bigger with respect the MNPs functionalized with citric acid, as well as the PDI, probably because of

the further functionalization with gold leading to an increase of the diameter and the formation of more aggregations.

In Chapter 4, a third approach for the curcumin functionalization of the magnetite nanoparticles with citric acid has been presented. Starting from this functionalization, a third synthesis of gold-magnetite nanostructures was performed and used for the thermal and magnetic characterization.

Laser. Gold-magnetite nanostructures with citric acid were tested by using a NIR laser irradiation to assess their capability to increase their temperature. The Figure 53 shows the time-dependent temperature of the gold-magnetite heterodimers with CA starting from the room temperature, with an increase of 13 °C. Considering the standard heating presented in literature [101] which is necessary for the tumor cells to ablate (around 50 °C), this nanosystem should work good for hyperthermia therapy.

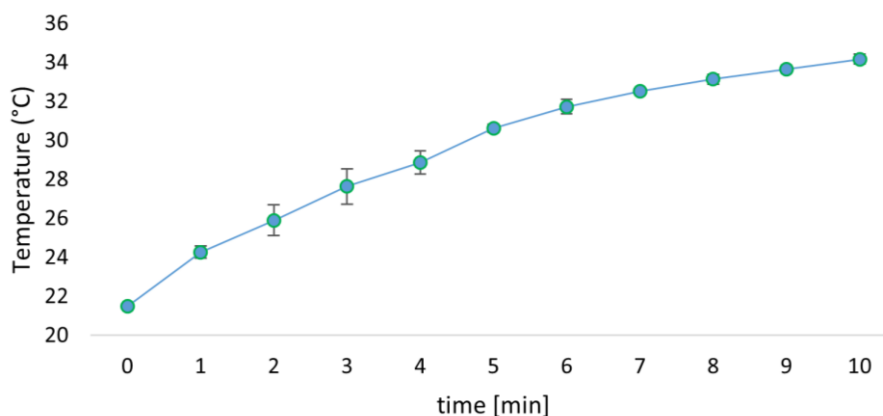


Figure 53. Time dependent temperature measurements of gold-magnetite heterodimers with curcumin and with CA

Vibrating sample magnetometer (VSM). Figure 54 reports the curves in the plane M-H of the CA-MNPs with and without the curcumin and AuNPs functionalization. The magnetization saturation (Am^2/kg) as a function of the applied magnetic field (kA/m) is reported. All the curves show a superparamagnetic behavior, with no coercivity and remanence. Specifically, the magnetization curve of CA-MNPs shows a magnetic saturation of about $58,6 \text{ Am}^2/\text{kg}$. The curve of CA-MNPs with curcumin and AuNPs shows a lower magnetization with respect the CA-MNPs. These results suggest that the functionalization with curcumin and AuNPs influenced the magnetic properties of the

CA-MNPs, particularly the presence of gold nanoparticles led to a decrease of saturation magnetization of the multifunctional nanostructures.

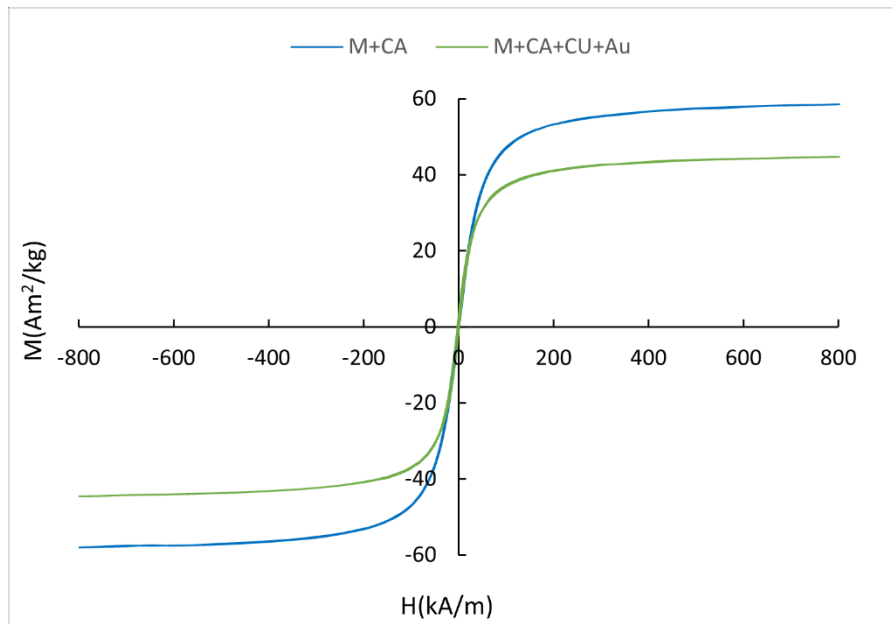


Figure 54. Magnetization curve of CA-MNPs (blue) compared with CA-MNPs functionalized with curcumin and AuNPs (green)

Chapter 6

Conclusions

This work reports the development of a simple and eco-friendly synthesis process of multifunctional gold-magnetite nanostructures for potential cancer treatment applications, by using curcumin as novel reducing agent for gold nanoparticles on magnetite nanoparticles' surface. Magnetite and gold nanoparticles have been chosen for obtaining multifunctional nanoconjugates because of the possibility to combine magnetic and plasmonic properties in one nanocomposite. The role of curcumin as linker and, as a reducing and stabilizing agent has been studied.

The co-precipitation method was used to synthesize the superparamagnetic iron oxide nanoparticles and then, two different routes were applied for functionalizing the obtained nanoparticles. The first route employed the use of APTES as a coating and stabilizing agent; two approaches were performed for the APTES functionalization and only the second one was used for the further grafting of curcumin on NPs' surface. The successful APTES-MNPs formation was assessed by FTIR analysis. Afterwards, two different curcumin functionalization paths were followed and, in both cases, FTIR analysis showed the main curcumin peaks, while the UV-vis spectra detected the curcumin absorption peak, suggesting that an effective graft of curcumin on nanoparticles' surface occurred. The second route was based on the use of citric acid on bare SPIONs' surface, acting as a stabilizing agent. The effective functionalization was proven by some characteristic peaks of CA detected by FTIR analysis. By changing the amount of curcumin, different approaches were tried to optimize the curcumin grafting on CA-MNPs. The obtained nanoparticles were analysed through FTIR spectrum, which showed the characteristic peaks of curcumin and citric acid, confirming the correct functionalization of CA-MNPs with curcumin. The UV-vis spectra showed the curcumin absorbance band between 350 and 450 nm, which confirmed the results obtained through FTIR analysis.

A rapid single step methods for the curcumin-mediated synthesis of AuNPs was successfully carried out, confirming the role of curcumin as reducing and stabilizing agent. The UV-vis analysis ascertained the optical properties of curcumin gold

nanoparticles: it showed the presence of the surface plasmon resonance related peak at 550 nm.

In conclusion, two synthesis methods have been explored to obtain the gold-magnetite heterodimers starting from the curcumin-mediated AuNPs followed by the CA-MNPs grafting on their surface, or from the curcumin functionalized MNPs followed by the reduction of AuNPs on their surface. In the first synthesis, the grafting of the magnetite nanoparticles with citric acid on AuNPs' surface was analysed through UV-vis spectroscopy; however, the obtained results were unsatisfactory since it was not possible to graft magnetite NPs onto AuNPs' surface and only the second synthesis was chosen for further studies. In the second synthesis, the presence of AuNPs on MNPs' surface was confirmed by the peaks of gold detected in the EDS spectra, showing the effective action of curcumin as reducing agent and as a linker between the magnetite and gold nanoparticles. SEM images showed highly aggregated M-APTES-CU NPs, decorated with gold nanoparticles of a higher dimension, represented by the white spots, while a more monodispersed nanostructures were shown in the SEM images of M-CA-CU NPs, which confirms the ability of the citric acid to stabilize the solution by creating repulsive forces between the nanoparticles. The magnetic properties were analysed through a VSM and the results showed that the gold-magnetite nanostructures with APTES, or citric acid, presented no hysteresis, according to the superparamagnetic behavior. Moreover, MNPs functionalization does not highly influence the magnetic properties of the pure magnetite. The measurements with a NIR laser and a thermocouple thermometer were performed to assess the nanoparticles property to increase their temperature under a laser irradiation. The results showed an increase of temperature of 16 °C for the nanoparticles with APTES and of 13 °C for the ones with citric acid. These results make the obtained nanoconjugates suitable tools for hyperthermia therapy for the tumor cells.

Additional improvements are needed to be developed to obtain multifunctional nanostructures that can be used as theranostic devices for cancer treatment. In particular, the next steps should aim to optimize the morphological structure of the nanoconjugates, increasing their monodispersity. Moreover, the active targeting of the tumor cells can be accomplished by implementing further surface functionalization with targeting moiety (such as ligand, antibody, peptide) which are able to target specific changes in cancer cell biology. Finally, the magnetic properties of SPIONs can be utilized not only as guidance

system of nanoparticles to the tumor site, but also for the magnetic hyperthermia. In this way, the hyperthermia therapy can be performed by exploiting, in a synergistic way, the optical and magnetic properties of the obtained nanoconjugates in order to reach deeper tumor tissues.

References

- [1] Nene A., Xuefeng Y., Poonam K., Hongrong L., Prakash S., Seeram R., “Magnetic Iron Oxide Nanoparticle (IONP) Synthesis to Applications: Present and Future”. *Materials*, vol. 13, pp. 4644, 2020; doi:10.3390/ma13204644.
- [2] Nguyen Hoan Nam, Nguyen Hoang Luong, “Nanoparticles: Synthesis and applications”. *Materials for Biomedical Engineering - Inorganic Micro and Nanostructures*, ch. 7, pp. 211-240, 2019; doi: <https://doi.org/10.1016/B978-0-08-102814-8.00008-1>.
- [3] Sanvicens N., Marco M.P., “Multifunctional nanoparticles – properties and prospects for their use in human medicine”. *Applied Molecular Receptors Group*, vol. 26, Issue 8, pp. 425-433, 2008; doi:10.1016/j.tibtech.2008.04.005.
- [4] Wu. W, Wu Z., Yu T., Jiang C., Kim W., “Recent progress on magnetic iron oxide nanoparticles: synthesis. Surface functional strategies and biomedical applications”. *Sci. Technol. Adv. Mater.*, vol. 16, 023501 (43pp), 2015; doi:10.1088/1468-6996/16/2/023501.
- [5] Gupta A.K., Gupta M., “Synthesis and surface engineering of iron oxide nanoparticles for biomedical applications”. *Biomaterials*, vol. 26, no. 18, pp. 3995–4021, 2005; doi: 10.1016/j.biomaterials.2004.10.012.
- [6] D. Portet, B. Denizot, E. Rump, J.-J. Lejeune, P. Jallet. J., “Nonpolymeric Coating of Iron Oxide Colloids for Biological Use as Magnetic Resonance Imaging Contrast Agents”. *Colloid Interface Sci.*, vol. 238, pp. 37-42, 2001; doi: <https://doi.org/10.1006/jcis.2001.7500>.
- [7] Dyal A., Loos K., Noto M., et al., “Activity of *Candida rugosa* lipase immobilized on gamma-Fe₂O₃ magnetic nanoparticles”. *J Am Chem Soc.*, vol. 125: 1684-5, 2003; doi: 10.1021/ja021223n.
- [8] Cai, L., Wang, W., Yang X.Y., Zhou, P., Tang, H.W., Rao, J., et al., “Preparation of fluorescent-magnetic silica nanoprobe for recognition and separation of human lung cancer cells”. *Austin J. Anal. Pharm. Chem.*, vol. 1, pp. 1027, 2014.
- [9] Ilovitsh T., Danan Y., Meir R., Meiri A., Zalevsky Z., “Cellular imaging using temporally flickering nanoparticles”. *Sci. Rep.*, vol. 5, pp. 8244, 2015; doi: 10.1038/srep08244.

- [10] Giani G., Fedi S., Barbucci R., “Hybrid magnetic hydrogel: a potential system for controlled drug delivery by means of alternating magnetic field”. *Polymers*, vol. 4, pp. 1157-1169, 2012; doi: <https://doi.org/10.3390/polym4021157>.
- [11] Hola K., et al, “Tailored functionalization of iron oxide nanoparticles for MRI, drug delivery, magnetic separation and immobilization of biosubsta”. *Biotechnol Adv*, 2015; doi: <http://dx.doi.org/10.1016/j.biotechadv.2015.02.003>.
- [12] Srivastava P., Sharma P.K., Muheem A., Warsi M.H., “Magnetic Nanoparticles: A Review on Stratagems of Fabrication and its Biomedical Applications”. *Drug Delivery & Formulation*, vol. 11, 2017; doi: 10.2174/1872211311666170328150747.
- [13] Berry C.C., “Progress in functionalization of magnetic nanoparticles for applications I biomedicine”. *J. Phys. D: Appl. Phys.*, vol. 42, (9pp), 2009; doi:10.1088/0022-3727/42/22/224003.
- [14] Mohammed, L., et al., “Magnetic nanoparticles for environmental and biomedical applications: A review”. *Particuology*, 2016; doi: <http://dx.doi.org/10.1016/j.partic.2016.06.001>.
- [15] Gul S., Khan B.S., Rehman I.U., Khan M.A., Khan M.I., “A Comprehensive Review of Magnetic Nanomaterials Modern Day Theranostics”. *Frontiers in Materials*, 2019; doi: 10.3389/fmats.2019.00179.
- [16] Mohaptra J., Xing M, Liu J.P., “Inductive Thermal Effect of Ferrite Magnetic Nanoparticles”. *Materials*, 2019; doi:10.3390/ma12193208.
- [17] Salunkhe A.B., Khot V.M, Pawar S.H., “Magnetic Hyperthermia with Magnetic Nanoparticles: A Status Review”. *Medical Chemistry*, vol. 14, 2014; doi: 10.2174/1568026614666140118203550.
- [18] Jiang Q.L., Zheng S.W., Hong R.Y., Deng S.M., Guo L., Hu R.L., Gao B., Huang M., Cheng L.F., Liu G.H., Wang Y.Q., “Folic acid-conjugated Fe₃O₄ magnetic nanoparticles for hyperthermia and MRI in vitro and in vivo”. *Applied Surface Science*, vol. 34, pp. 224-233, 2014; doi: <http://dx.doi.org/10.1016/j.apsusc.2014.04.018>.
- [19] Jordan A., Scholz R., Maier-HauffK., Johannsen M., Wust P, Nadobny J., Schirra H., Schmidt H., Deger S., Loening S., Lanksch W., Felix R., “Presentation of a new magnetic field therapy system for the treatment of human solid tumors with magneticfluid hyperthermia”. *J Magn Magn Mater* 2001;225:118–26.

- [20] Chatterjee J., Haik Y., Chen C-J., “Size dependent magnetic properties of iron oxide nanoparticles”. *J Magn Magn Mater* 2003;257(1):113–8.
- [21] Sengani M., Grumezescu A. M., Raejeswari V. D., “Recent trends and methodologies in gold nanoparticle synthesis – A prospective review on drug delivery aspect”. *OpenNano*, vol. 2, pp. 37–46, 2017; doi: <http://dx.doi.org/10.1016/j.onano.2017.07.001>.
- [22] Bai X., Wang Y., Song Z., Feng Y., Chen Y., Zhang D., Feng L., “The Basic Properties of Gold Nanoparticles and their Applications in Tumor Diagnosis and Treatment”. *International Journal of Molecular Sciences*, vol. 21, pp. 2480, 2020; doi:10.3390/ijms21072480.
- [23] Kim M., Lee J.H., Nam J.M., “Plasmonic Photothermal Nanoparticles for Biomedical Applications”. *Adv. Sci.*, vol. 6, 1900471, 2019; doi: 10.1002/advs.201900471.
- [24] De Souza C.D., Nogueira B.R., Rostelato M.E., “Review of the methodologies used in the synthesis gold nanoparticles by chemical reduction”. *Journal of Alloys and Compounds*, vol. 798, pp. 714-740, 2019; doi: <https://doi.org/10.1016/j.jallcom.2019.05.153>.
- [25] Vilches C., Quidant R., “Targeted hyperthermia with plasmonic nanoparticles”. *Frontiers of Nanoscience*, vol. 16, pp. 307-352, 2020; doi: <https://doi.org/10.1016/B978-0-08-102828-5.00012-7>.
- [26] Yi G., Hong S.H., Son J., Yoo J., Park C., Choi Y., Koo H., “Recent advances in nanoparticle carriers for photodynamic therapy”. *Quant Imaging Med Surg*, vol. 8, pp. 433-443, 2018; doi: 10.21037/qims.2018.05.04.
- [27] Shams S.F., Ghazanfari M.R., Schmitz-Antoniak C., “Magnetic-Plasmonic Heterodimer Nanoparticles: Designing Contemporarily Features for Emerging Biomedical Diagnosis and Treatments”. *Nanomaterial*, vol. 9, 2018; doi: 10.3390/nano9010097.
- [28] Stafford S., Garcia Serrano R., Gun’ko Y.K., “Multimodal Magnetic-Plasmonic Nanoparticles for Biomedical Applications”. *Appl. Sci.*, vol. 8, 2018; doi:10.3390/app8010097.
- [29] Temelie M., Popescu R.C., Cocioaba D., Vasile B.S., Savu D., “Biocompatibility study of magnetite nanoparticles synthesized using green method”. *Romanian Journal of Physics*, vol. 63, 703, 2018; doi: https://rjp.nipne.ro/2018_63_7-8/RomJPhys.63.703.pdf.

- [30] Pin Yew Y., Shameli K., Miyake M., Khairuidin Ahmad N.B., Mohamad S.E., Naiki T., Xin Lee K., “Green biosynthesis of superparamagnetic magnetite Fe₃O₄ nanoparticles and biomedical applications in targeted anticancer drug delivery system: A review”. *Arabian Journal of Chemistry*, vol. 13, pp. 2287-2308, 2020; doi: <https://doi.org/10.1016/j.arabjc.2018.04.013>.
- [31] Hannoyer B., Enoki T., Prasad B.L.V., Shouche Y.S., Ogale S., Sastry M., “Bacteria-mediated precursor dependent biosynthesis of superparamagnetic iron oxide and iron sulfide nanoparticles”. *Langmuir*, vol. 24, pp. 5787–5794, 2008; doi: 10.1021/la704019p.
- [32] Alagu Sundaram P., Augustine R., Kannan M., “Extracellular biosynthesis of iron oxide nanoparticles by *Bacillus subtilis* strains isolated from rhizosphere soil”. *Biotechnology and Bioprocess Engineering*, vol. 17, pp. 835-840, 2012; doi: 10.1007/s12257-011-0582-9.
- [33] Ngernipimai S., Thomas C., Maensiri S., Siri S., “Stability and cytotoxicity of well-dispersed magnetite nanoparticles prepared by hydrothermal method”. *Advanced Materials Research*, vol. 506, pp. 122-125, 2012; doi: 10.4028/www.scientific.net/AMR.506.122.
- [34] Phumying S., Labuayai S., Thomas C., Amornkitbamrung V., “Aloe vera plant-extracted solution hydrothermal synthesis and magnetic properties of magnetite (Fe₃O₄) nanoparticles”. *Applied Physics*, vol. 111, pp. 1187-1193, 2013; doi: 10.1007/s00339-012-7340-5.
- [35] Ahmed S., Annu S., Ikram S., Yudha S., “Biosynthesis of gold nanoparticles: A green approach”. *Journal of Photochemistry & Photobiology, B: Biology*, vol. 161, pp. 141-153, 2016; doi: <http://dx.doi.org/10.1016/j.jphotobiol.2016.04.034>.
- [36] De Matteis V., Rizzello L., Cascione M., Liatsi-Douvitsa E., Apriceno A., Rinaldi R., “Green Plasmonic Nanoparticles and Bio-Inspired Stimuli-Responsive vesicles in cancer therapy application”. *Nanomaterials*, vol. 10, 2020; doi: 10.3390/nano10061083.
- [37] Menon S., Rajeshkumar S., Venkat Kumar S., “A review on biogenic synthesis of gold nanoparticles, characterization, and its applications”. *Resource-Efficient Technologies*, vol. 3, pp. 516-527, 2017; doi: <http://dx.doi.org/10.1016/j.refit.2017.08.002.4>.

- [38] Kumavat S.D, Chaudhari Y.S., Borole P., Mishra P., Shenghani K., Duvvuri P., “Degradation studies of curcumin”. *International Journal of Pharmacy Review & Research*, vol. 3, pp. 50-55, 2013.
- [39] Priyadarsini I.K., “The Chemistry of Curcumin: from extraction to therapeutic agent”. *Molecules*, vol. 19, pp. 20091-20112, 2015; doi: 0.3390/molecules191220091.
- [40] Nandiyanto A.B.D., Wiryani A.S., Rusli A., Purnamasari A., Abdullah A.G., Ana, Widiaty I., Hurriyati R., “Extraction of curcumin pigment from Indonesian local turmeric with its infrared spectra and thermal decomposition properties”. *IOP Conf. Ser.: Mater. Sci. Eng.*, vol. 180, 2018; doi: 10.1088/1757-899X/180/1/012136.
- [41] Lee W.H., Loo C.Y., Bebawy M., Luk F., Mason R.S., Rohanizadeh R., “Curcumin and its derivatives: their Application in Neuropharmacology and Neuroscience in the 21st century”. *Current Neuropharmacology*, vol. 11., pp. 338-378, 2013; doi: 10.2174/1570159X11311040002.
- [42] Nasery M.M., Abadi B., Poormoghadam D., Zarrabi A., Keyhanvar P., Khanbabaei H., Ashrafizadeh M., Mohammadinejad R., Tavakol S., Sethi G., “Curcumin Delivery Mediated by Bio-Base Nanoparticles: A Review”. *Molecules*, vol. 25, 2020; doi: 10.3390/molecules25030689.
- [43] Tønnesen H.H., Másson M., Loftsson T., “Studies of curcumin and curcuminoids. XXVII. Cyclodextrin complexation: solubility, chemical and photochemical stability”. *International Journal of Pharmaceutics*, vol. 244, pp. 127-135, 2002; doi: 10.1016/S0378-5173(02)00323-X.
- [44] Salehi B., Calina D., Docea A.O., Koirala N., Aryal S., Lombardo D., Pasqua L., Taheri Y., Salgado Castillo C.M., Martorell M., Martins N., Iriti M., Rasul Suleria H.A., Sharifi-Rad J., “Curcumin’s Nanomedicine Formulations for Therapeutic Application in Neurological Diseases”. *Journal of Clinical Medicine*, vol. 430, 2020; doi: 10.3390/jcm9020430.
- [45] Hadisoewignyo L., Hartono S.B., Kresnamurti A., Soeliono I., Nataline Y., Prakoso G.A., Aulia Elok D.A.R., “Evaluation of anti-inflammatory activity and biocompatibility of curcumin loaded mesoporous silica nanoparticles as an oral drug delivery”. *Adv. Nat. Sci.: Nanosci. Nanotechnol.*, vol. 9, 2018; doi: 10.1088/2043-6254/aad5d5.
- [46] Ismail E.H., Sabry D.Y., Mahdy H., Khalil M.M.H., “Synthesis and Characterization of some Ternary metal Complexes of Curcumin with 1,10-

- phenanthroline and their Anticancer Applications”. *Journal of scientific research*, vol. 6, pp. 509-519, 2014; doi: <http://dx.doi.org/10.3329/jsr.v6i3.18750>.
- [47] Kadasala N.R., Lin L., Gilpin C., Wei A., “Eco-friendly (green) synthesis of magnetically active gold nanoclusters”. *Science and Technology of Advanced Materials*, vol. 18, pp. 210-218, 2017; doi: 10.1080/14686996.2017.1290492.
- [48] Patra D., El Kurdi R., “Curcumin as a novel reducing and stabilizing agent for the green synthesis of metallic nanoparticles”. *Green chemistry letters and review*, vol. 14, pp. 474-487, 2021; doi: 10.1080/17518253.2021.1941306.
- [49] Rahimnia R., Salehi Z., Ardestani M.S., Doosthoseini H., “SPION Conjugated Curcumin Nano-Imaging Probe: Synthesis and Bio-Physical Evaluation”. *Iranian Journal of Pharmaceutical Research*, vol. 18, pp. 183-197, 2017.
- [50] Sreelakshmi Ch., Goel N., Addlagatta A., Datta K.K.R., Ummanni R., Subba Reddy B.V., “Green Synthesis of Curcumin Capped Gold Nanoparticles and Evaluation of Their Cytotoxicity”. *Nanoscience and Nanotechnology letters*, vol. 5, pp. 1-8, 2013; doi: 10.1166/nnl.2013.1678.
- [51] Prabhu S.N., “Green route synthesis of stable isotropic gold nanoparticles using leaf extract of *Curcuma longa* and their characterization”. *Advances in Applied Science Research*, vol. 6, pp. 167-179, 2015.
- [52] Abdulwahab F., Henari F.Z., Cassidy S., Winsor K., “Synthesis of Au, Ag, Curcumin Au/Ag, and Au-Ag Nanoparticles and Their Nonlinear Refractive Index Properties”. *Journal of Nanomaterials*, vol. 1, pp. 1-5, 2016; doi: 10.1155/2016/5356404.
- [53] Yallapu M.M., Othman S.F., Curtis E.T., Bauer N.A., Chauhan N., Kumar D., Jaggi M., Chauhan S.C., “Curcumin-loaded magnetic nanoparticles for breast cancer therapeutics and imaging applications”. *International Journal of Nanomedicine*, vol. 7, pp. 1761-1779, 2012; doi: 10.2147/IJN.S29290.
- [54] Ashkbar A., Rezaei F., Attari F., Ashkevarian S., “Treatment of breast cancer in vivo by dual photodynamic and photothermal approaches with the aid of curcumin photosensitizer and magnetic nanoparticles”. *Scientific reports*, vol. 10, 2020; doi: 10.1038/s41598-020-78241-1.
- [55] Araya-Sibaja A.M., Salazar-López N.J., Romero K.W., Vega-Baudrit J.R., Dominguez-Avila J.A., Velázquez Contreras C.A., Robles-Zepeda R.E., Navarro-Hoyos M., González-Aguilar A.G., “Use of nanosystems to improve the

- anticancer effects of curcumin”. *Beilstein J. Nanotechnol.*, vol. 12, pp. 1047-1062, 2021; doi.org/10.3762/bjnano.12.78.
- [56] Nosrati H., Sefidi N., Sharafi A., Danafar H., Manjili H.K., “Bovine Serum Albumin (BSA) coated iron oxide magnetic nanoparticles as biocompatible carriers for curcumin-anticancer drug”. *Bioorganic Chemistry*, vol. 76, pp. 501-509, 2018; doi: 10.1016/j.bioorg.2017.12.033.
- [57] Cheng K.K., Chan P.S., Fan S., Kwan S.M., Yeung K.L., Wang Y.J., Chow A.H.L., Wu E.X., Baum L., “Curcumin-conjugated magnetic nanoparticles for detecting amyloid plaques in Alzheimer's disease mice using magnetic resonance imaging (MRI)”. *Biomaterials*, vol. 44, pp. 155-172, 2015; doi: 10.1016/j.biomaterials.2014.12.005.
- [58] Mancarella S., Greco V., Baldassarre F., Vergara D., Maffia M., Leporatti S., “Polymer-Coated Magnetic Nanoparticles for Curcumin Delivery to Cancer Cells”. *Macromol. Biosci.*, vol. 15, pp. 1365-1374, 2015; doi: 10.1002/mabi.201500142.
- [59] Bhandari R., Gupta P., Dziubla T., Hilt J.Z., “Single Step Synthesis, Characterization and Applications of Curcumin Functionalized Iron Oxide Magnetic Nanoparticles”. *Mater Sci Eng C Mater Biol Appl.*, vol. 67, pp. 59-64, 2016; doi: 10.1016/j.msec.2016.04.093.
- [60] Sindhy K., Rajaram A., Sreeram K.J., Rajaram R., “Curcumin conjugated gold nanoparticles synthesis and its biocompatibility”. *RSC Adv.*, vol. 4, pp. 1808-1818, 2014; doi: 10.1039/c3ra45345f.
- [61] Singh D.K., Jagannathan R., Khandelwal P., Abraham P.M., Poddar P., “In situ synthesis and surface functionalization of gold nanoparticles with curcumin and their antioxidant properties: an experimental and density functional theory investigation”. *Nanoscale*, vol. 5, pp. 1882-1893, 2013; doi: 10.1039/c2nr33776b.
- [62] Yang S., Huang C., Wang C., Shieh M., Chen K., “The synergistic effect of Hyperthermia and Chemotherapy in Magnetite Nanomedicine-Based Lung Cancer Treatment”. *International Journal of Nanomedicine*, vol. 15, pp. 10331-10347, 2020; doi: 10.2147/IJN.S281029.
- [63] Abakumov M.A., Nukolova N., Sokolsky-Papkov M., “VEGF-targeted magnetic nanoparticles for MRI visualization of brain tumor”. *Nanomedicine: Nanotechnology, Biology, and Medicine*, vol. 11, pp. 825-833, 2015; doi: 10.1016/j.nano.2014.12.011.

- [64] Stylianopoulos T., “EPR-effect: utilizing size-dependent nanoparticle delivery to solid tumors”. *Therapeutic delivery*, vol. 4, pp. 421-423, 2013; doi: 10.4155/tde.13.8.
- [65] Goddard Z.R., Marín M.J., Russell D.A., Searcey M., “Active targeting of gold nanoparticles as cancer therapeutics”. *Chemical Society Reviews*, vol. 49, pp. 8774-8789, 2020; doi: 10.1039/d0cs01121e.
- [66] Cheng A.L., Hsu C.H., Lin J.K., Hsu M.M., Ho Y.F., Shen T.S., Ko J.Y., Lin J.T., Lin B.R., Ming-Shiang W., Yu H.S., Jee S.H., Chen G.S., Chen T.M., Chen C.A., Lai M.K., Pu Y.S., Pan M.H., Wang Y.J., Tsai C.C., Hsieh C.Y., “Phase I clinical trial of curcumin, a chemopreventive agent, in patients with high-risk or pre-malignant lesions”. *Anticancer Res.*, vol. 21, pp. 2895-2900, 2001.
- [67] Saghatelian T., Tananyan A., Janoyan N., Tadevosyan A., Petrosyan H., Hovhannisyanyan A., Hayrapetyan L., Arustamyan M., Arnhold J., Rotmann A.R., Hovhannisyanyan A., Panossian A., “Efficacy and safety of curcumin in combination with paclitaxel in patients with advanced, metastatic breast cancer: A comparative, randomized, double-blind, placebo-controlled clinical trial”. *Phytomedicine*, vol. 70, 2020; doi: 0.1016/j.phymed.2020.153218.
- [68] Bayet-Robert M., Kwiatowski F., Leheurteur M., Gachon F., Planchat E., Abrial C., Mouret-Reynier M.A., Durando X., Barthomeuf C., Chollet P., “Phase I dose escalation trial of docetaxel plus curcumin in patients with advanced and metastatic breast cancer”. *Cancer Biol. Ther.*, vol. 9, pp. 8-14, 2010; doi: 10.4161/cbt.9.1.10392.
- [69] Garcea G., Berry D.P., Jones D.J.L., Singh R., Dennison A.R., Farmer P.B., Sharma R.A., Steward W.P., Gescher A.J., “Phase I Clinical Trial of Oral Curcumin: Biomarkers of Systemic Activity and Compliance”. *Cancer Epidemiol. Biomarkers Prev.*, vol. 14, pp. 120–125, 2005.
- [70] Carroll R.E., Benya R.V., Turgeon D.K., Vareed S., Neuman M., Rodriguez L., Kakarala M., Carpenter P.M., McLaren C., Meyskens F.L. Jr., Brenner D.E., “Phase IIA Clinical Trial of Curcumin for the Prevention of Colorectal Neoplasia”. *Cancer Prev. Res.*, vol. 4, pp. 354–364, 2011; doi: 10.1158/1940-6207.capr-10-0098.
- [71] Sharma R.A., Euden S.A., Platton S.L., Cooke D.N., Shafayat A., Hewitt H.R., Marczylo T.H., Morgan B., Hemingway D., Plummer S.M., Pirmohamed M., Gescher A.J., Steward W.P., “Phase I Clinical Trial of Oral Curcumin”. *Clin. Cancer Res.*, vol. 10, pp. 6847–6854, 2004; doi: 10.1158/1078-0432.ccr-04-0744.

- [72] Dhillon N., Aggarwal B.B., Newman R.A., Wolff R.A., Kunnumakkara A.B., Abbruzzese J.L., Ng C. S., Badmaev V., Kurzrock R., “Phase II Trial of Curcumin in Patients with Advanced Pancreatic Cancer”. *Clin. Cancer Res.*, 14, 4491–4499, 2008; doi: 10.1158/1078-0432.ccr-08-0024.
- [73] Ide H., Tokiwa S., Sakamaki K., Nishio K., Isotani S., Muto S., Hama T., Masuda H., Horie S., “Combined inhibitory effects of soy isoflavones and curcumin on the production of prostate-specific antigen”. *Prostate*, vol. 70, pp. 1127–1133, 2010; doi: 10.1002/pros.21147.
- [74] Zou J.Y., Su C.H., Luo H.H., Lei Y.Y., Zeng B., Zhu H.S., Chen Z.G.J., “Curcumin converts Foxp3⁺ regulatory T cells to T helper 1 cells in patients with lung cancer”. *Cell. Biochem.*, vol. 119, pp. 1420–1428, 2018; doi: 10.1002/jcb.26302.
- [75] Vadhan-Raj S., Weber D.M., Wang M., Giralto S.A., Thomas S.K., Alexanian R., Zhou X., Patel P., Bueso-Ramos C.E., Newman R.A., Aggarwal B., “Curcumin Downregulates NF-kB and Related Genes in Patients with Multiple Myeloma Results of a Phase III Study”. *B. Blood*, vol. 110, pp. 1177, 2007; doi: 10.1182/blood.v110.11.1177.1177.
- [76] Golombick T., Diamond T.H., Manoharan A., Ramakrishna R., “Monoclonal gammopathy of undetermined significance, smoldering multiple myeloma, and curcumin: A randomized, double-blind placebo-controlled cross-over 4g study and an open-label 8g extension study”. *Am. J. Hematol.*, vol. 87, pp. 455–460, 2012; doi: 10.1002/ajh.23159.
- [77] Cui Y., Zhang M., Zeng F., Jin H., Xu Q., Huang Y., “Dual-Targeting Magnetic PLGA Nanoparticles for Codelivery of Paclitaxel and Curcumin for Brain Tumor Therapy”. *ACS Appl. Mater. Interfaces*, vol. 8, pp. 32159–32169, 2016; doi: 10.1021/acsami.6b10175.
- [78] Yallapu1 M.M., Ebeling M.C., Khan S., Chauhan N., Gupta B.K., Puumala S.E., Jaggi M., Chauhan S.C., “Novel Curcumin-Loaded Magnetic Nanoparticles for Pancreatic Cancer Treatment”. *Mol Cancer Ther*, vol. 12, pp. 1471–80, 2013; doi: 10.1158/1535-7163.MCT-12-1227.
- [79] Kumari M., Sharma N., Manchanda R., Gupta N., Syed A., Bahkali A.H., Nimesh S., “PGMD/curcumin nanoparticles for the treatment of breast cancer”. *Scientific Reports*, vol. 11, 2021; doi: 10.1038/s41598-021-81701-x.
- [80] Ombredane A.S, Silva V.R.P., Andrade L.R., Pinheiro W.O., Simonelly M., Oliveira J.V., Pinheiro A.C., Goncalves G.F., Felice G.J., Garcia M.P., Campos

- P.M., Luz G.V.S., Joanitti G.A., “In Vivo Efficacy and Toxicity of Curcumin Nanoparticles in Breast Cancer Treatment: A Systematic Review”. *Front Oncol.*, vol. 11, 2021; doi: 10.3389/fonc.2021.612903.
- [81] Matloubi Z., Hassan Z., “HSA-curcumin nanoparticles: a promising substitution for Curcumin as a Cancer chemoprevention and therapy”. *DARU Journal of Pharmaceutical Sciences*, vol. 28, pp. 209-219; doi: 10.1007/s40199-020-00331-2.
- [82] Xing H., Wang Z., Shao D., Chang Z., Ge M., Li L., Wu M., Yan Z., Dong W., “Janus nanocarriers for magnetically targeted and hyperthermia-enhanced curcumin therapy of liver cancer”. *RSC Adv.*, vol. 8, pp. 30448-30454, 2018; doi: 10.1039/c8ra05694c.
- [83] “Gold-Curcumin Nanostructure in Photothermal Therapy on Breast Cancer Cell Line: 650 and 808 nm Diode Lasers as Light Sources”. *J Biomed Phys Eng.*, vol. 9, pp. 473-482, 2019; doi: 10.31661/jbpe.v0i0.906.
- [84] Dickerson E.B., Dreaden E.C., Huangb X., El-Sayed I.H., Chub H., Pushpanketh S., McDonald J.F., El-Sayedb M.A., “Gold nanorod assisted near-infrared plasmonic photothermal therapy (PPTT) of squamous cell carcinoma in mice”. *Cancer Lett.*, vol. 269, pp. 57–66, 2008; doi: 10.1016/j.canlet.2008.04.026.
- [85] Stuchinskaya T., Moreno M., Cook M.J., Edwards D.R., Russell D.A., “Targeted photodynamic therapy of breast cancer cells using antibody–phthalocyanine–gold nanoparticle conjugates”. *Photochem. Photobiol. Sci.*, vol. 10, pp. 822-831, 2011; doi: 10.1039/c1pp05014a.
- [86] D’Acunto M., Cioni P., Gabellieri E., Presciuttini G., “Exploiting gold nanoparticles for diagnosis and cancer treatments”. *Nanotechnology*, vol. 32, 2021; doi: 10.1088/1361-6528/abe1ed.
- [87] Siddique S., Chow J.C.L., “Gold Nanoparticles for Drug Delivery and Cancer Therapy”. *Appl. Sci.*, vol. 10, 2020; doi: 10.3390/app10113824.
- [88] Kang M.S., Lee S.Y., Kim K.S., Han D.W., “State of the Art Biocompatible Gold Nanoparticles for Cancer Theragnosis”. *Pharmaceutics*, vol. 12, 2020; doi: 10.3390/pharmaceutics12080701.
- [89] Li B., Sun L., Li T., Zhang Y., Niu X., Xiec M., You Z., “Ultra-small gold nanoparticles self-assembled by gadolinium ions for enhanced photothermal/photodynamic liver cancer therapy”. *J. Mater. Chem. B*, vol. 9, pp. 1138-1150, 2021; doi: 10.1039/d0tb02410d.

- [90] Nambiar S., Osei E., Fleck A., Darko J., Mutsaers A.J., Wettig S., “Synthesis of curcumin-functionalized gold nanoparticles and cytotoxicity studies in human prostate cancer cell line”. *Applied Nanoscience*, vol.8, pp. 347-357, 2018; doi: 10.1007/s13204-018-0728-6.
- [91] Kim M.S., Park B.C., Kim Y.J., Lee J.H., Koo T.M., Ko M.J., Kim Y.K., “Design of Magnetic-Plasmonic Nanoparticle Assemblies via Interface Engineering of Plasmonic Shells for Targeted Cancer Cell Imaging and Separation”. *Department of Materials Science and Engineering*, vol. 16, 2020; doi: 10.1002/sml.202001103.
- [92] Kirui D.K., Rey D.A., Batt C.A., “Gold hybrid nanoparticles for targeted phototherapy and cancer imaging”. *Nanotechnology*, vol. 21, 2010; doi: 10.1088/0957-4484/21/10/105105.
- [93] Kim J., Park S., Lee J.E., Jin S.M., Lee J.H., Lee I.S., Yang I., Kim J.S., Kim S.K., Cho M.H., Hyeon T., “Designed Fabrication of Multifunctional Magnetic Gold Nanoshells and Their Application to Magnetic Resonance Imaging and Photothermal Therapy”. *Angew. Chem. Int. Ed.*, vol. 45, pp.7754 –7758, 2006; doi: 10.1002/anie.200602471.
- [94] Ma J., Li P., Wang W., Wang S., Pan X., Zhang F., Li S., Liu S., Wang H., Gao G., Xu B., Yuan Q., Shen H., Liu H., “Biodegradable Poly(amino acid)-Gold-Magnetic Complex with Efficient Endocytosis for Multimodal Imaging-Guided Chemo-Photothermal Therapy”. *ACS Nano*, vol. 12, pp. 9022–9032, 2018; doi: 10.1021/acsnano.8b02750.
- [95] Huang J., Guo M., Ke H., Zong C., Ren B., Liu G., Shen H., Ma Y., Wang X., Zhang H., Deng Z., Chen H., Zhang Z., “Rational Design and Synthesis of γ Fe₂O₃@Au Magnetic Gold Nanoflowers for Efficient Cancer Theranostics”. *Advanced Materials*, vol. 27, pp. 5049–5056, 2015; doi: 10.1002/adma.201501942.
- [96] Wulandari I.K., Santjojo D., Shobirin A.R., Sabarudin A., “Characteristics and Magnetic Properties of Chitosan-coated Fe₃O₄ Nanoparticles prepared by Ex-situ Co-precipitation Method”. *Rasayan Journal of Chemistry*, vol. 10, pp. 1348-1358, 2017; doi: 10.7324/RJC.2017.1041907.
- [97] Sundar S., Mariappan R., Piraman S., “Synthesis and characterization of amine modified magnetite nanoparticles as carriers of curcumin-anticancer drug”. *Powder Technology*, vol. 266, pp. 321-328, 2014; doi: 10.1016/j.powtec.2014.06.033.

- [98] Costa V.M., De Souza M.C.M., Fechine P.B.A., Macedo A.C., Goncalves L.R.B., “Nanobiocatalytic systems based on lipase-Fe₃O₄ and conventional systems for isoniazid synthesis: a comparative study”. *Brazilian Journal of Chemical Engineering*, vol. 33, pp. 661-673, 2016; doi: 10.1590/0104-6632.20160333s20150137.
- [99] Miola M., Ferraris S., Pirani F., Multari C., Bertone E., Rožman K.Z., Kostevšek N., Verné E., “Reductant-free synthesis of magnetoplasmonic iron oxide-gold nanoparticles”. *Ceramics International*, vol. 43, pp. 15258-15265, 2017; doi: 10.1016/j.ceramint.2017.08.063.
- [100] Dheyab M.A., Aziz A.A., Jameel M.S., Noqta O.A., Khaniabadi P.M., Mehrdel B., “Simple rapid stabilization method through citric acid modification for magnetite nanoparticles”. *Scientific report*, vol. 10, 2020; doi: 10.1038/s41598-020-67869-8.
- [101] Kitture R., Ghosh S., Kulkarni P., Liu X.L., Maity D., et al., “Fe₃O₄-citrate-curcumin: Promising conjugates for superoxide scavenging, tumor suppression and cancer hyperthermia”. *Journal of Applied Physics*, vo. 111, 2012; doi: 10.1063/1.3696001.
- [102] Nguyen T.T., Mammeri F., Ammar S., “Iron Oxide and Gold Based Magneto-Plasmonic Nanostructures for Medical Applications: A Review”. *Nanomaterials*, vol. 8, 2018; doi: 10.3390/nano8030149.
- [103] Karade V.C., Sharma A., Dhavale R.P., Dhavale R.P., Shingte S.R., Patil P.S., J.H., Zahn D.R.T., Chougale A.D., Salvan G., Patil P.B., “APTES monolayer coverage on self-assembled magnetic nanospheres for controlled release of anticancer drug Nintedanib”. *Scientific Reports*, vol. 11, 2021; doi: 10.1038/s41598-021-84770-0.
- [104] Miola M., Multari C., Debellis D., Laviano F., Gerbaldo R., Vernè E., “Magneto-plasmonic heterodimers: Evaluation of different synthesis approaches”. *J Am Ceram Soc.*, vol. 105, pp. 1276–1285, 2022; doi: 10.1111/jace.18190.
- [105] A. Rohman, Sudjadi, Devi, D. Ramadhani and A. Nugroho, “Analysis of curcumin in curcuma longa and Curcuma xanthorriza using FTIR spectroscopy and chemometrics”. *Research Journal of Medicinal Plant*, vol. 4, pp. 179-186, 2015; doi: 10.3923/rjmp.2015.179.186.

- [106] Mazyed E.A., Zakaria S., “Enhancement of dissolution characteristics of clopidogrel bisulphate by proniosomes”. *Int J Appl Pharm*, vol. 11, pp. 77-85, 2019; doi: 10.22159/ijap.2019v11i2.30575.
- [107] Nandiyanto A.B.D., Wiryani A.S., Rusli A., Purnamasari A., Abdullah A.G., Ana, Widiaty I, Hurriyati R., “Extraction of Curcumin Pigment from Indonesian Local Turmeric with Its Infrared Spectra and Thermal Decomposition Properties”. *IOP Conf. Ser.: Mater. Sci. Eng.*, vol. 180, 2017; doi: 10.1088/1757-899X/180/1/012136.
- [108] Poursaberi T., Karimi M., Hassanisadi M., Sereshti H., “Magnetic removal of nitrate ions from aqueous solution using amino-silica coated magnetic nanoparticles modified by oxovanadium(IV) porphyrin”. *Journal of Porphyrins and Phthalocyanines*, vol. 17, pp. 359-366, 2013; doi: 10.1142/S108842461350048X.
- [109] “Figure 27. NIR laser and NPs and NPs temperature measurement set up”: image Created with **BioRender.com** and with **Chemix** (<https://chemix.org>).